Master Thesis in Geosciences

Plio-Pleistocene glacial outbuilding of the mid-Norwegian continental shelf: seismic sequence stratigraphy of the Naust Formation

By

Rabia Talat

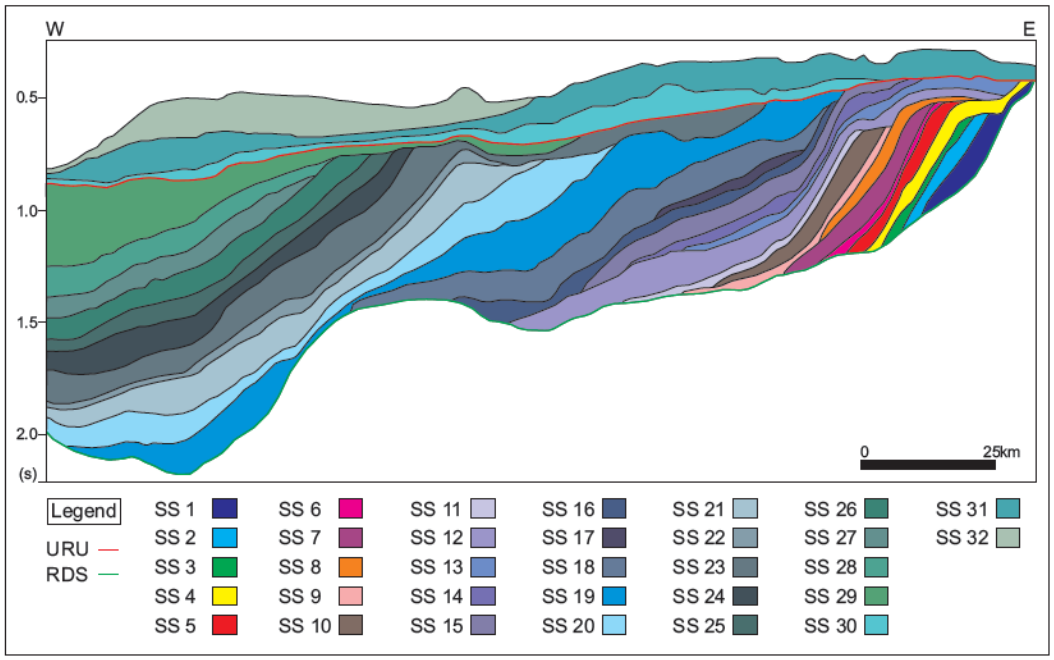

UNIVERSITY OF OSLO

FACULTY OF MATHEMATICS AND NATURAL SCIENCES

Plio-Pleistocene glacial outbuilding of the mid-Norwegian continental shelf: seismic sequence stratigraphy of the Naust Formation

By

Rabia Talat

Master Thesis in Geosciences

Discipline: Petroleum Geology and Petroleum Geophysics

Department of Geosciences

Faculty of Mathematics and Natural Sciences

UNIVERSITY OF OSLO

[June 2012]

Acknowledgement

First and foremost I would like to express my sincere gratitude to Allah who blessed me for successful accomplishment of this thesis.

This thesis has been carried out under the supervision of Professor Johan Petter Nystuen and Professor Jan Inge Faleide at the Department of Geosciences, in the University of Oslo. I owe a special thank to Professor Johan Petter Nystuen for his constant support, admirable guidance, inspiring ideas, encouragement and valuable suggestions. I am gratified to Professor Jan Inge Faleide for perceptive comments, valuable guidance and aspiring suggestions.

I am also very grateful to Dr. Michael Heeremans for his continuous collaboration, co-operation and technical support for Petrel Software.

Fugro and TGS-Nopec are acknowledged for contributing to the seismic database. At the same time I acknowledge Schlumberger for providing software for seismic interpretation.

I would like to thank my husband who has been a source of motivation for me and has been giving me full support. And in the end, I am obliged to my parents for their invaluable encouragement, endless efforts and great affection. They accompanied me to go through stages of my life and due to whom I learnt to dream my goals and with their friendliness I got confidence to achieve those goals.

Rabia Talat

Oslo, June, 2012

Abstract

Late Cenozoic outbuilding of the mid-Norwegian continental shelf (62º N-69º 30'N) demonstrates strong relationship between uplift, erosion, subsidence, variations in relative sea level, basin infill, glacial dynamics and climate. During Late Cenozoic clastic wedges prograded NW making toplap truncations with the URU (Upper Regional Unconformity). Sequences above the URU demonstrate aggradation and progradation at smaller scale.

The purpose of this study has been to get better understanding of the Plio-Pleistocene source-to-sink relationships, influence of glacial-interglacial cyclicity, variation in accommodation space as function of basin subsidence and glacioeustacy, and glacial dynamics and sedimentation. The present project includes seismic stratigraphic interpretation of 45 multi-channel 2D regional high resolution seismic lines of the mid-Norwegian continental shelf followed by seismic sequence analysis and seismic facies analysis. 32 sequences developed during 32 glacial-interglacial cycles which were initiated about 2.8 m.y. ago. The seismic sequences have been grouped and mapped into four megasequences.

Megasequence-1 is comprised of steeper clinothems whereas megasequence-2 and megasequence-3 have gentler clinothems. Moreover, seismic sequences associated with megasequence-2 and megasequence-3 have great extension in mid-Norwegian continental shelf. Ages of seismic sequences have been interpolated partly from previous studies. Glacial-interglacial cyclicity is about 70 000 years in megasequence-1, 80 000 years in megasequence- 2, 115 000 years in megasequence-3 and c. 70 000 years in megasequence-4. Relative sea level fluctuations have been determined with trajectory analysis. Glaciations of Iceland and Svalbard margin have been correlated with glaciations of the mid-Norwegian continental shelf.

Depositional environments have been determined using seismic facies. Furthermore, four seismic facies are interpreted with in the Naust Formation which correspond to glacigenic debris flows, glacimarine sediments, slide debrites and hemipelagic/contouritic sediments.

Contents

1. Introduction

The mid-Norwegian continental shelf (62 º N and 69 º 30'N) has a long structural and sedimentological history dating back to late Palaeozoic time. The present morphology and bathymetry of this part of the Norwegian continental shelf (NCS) were completed during the latest Cenozoic with the development of a thick prograding shelf succession (Fig. 1.1). This succession, being of Plio-Pleistocene age and represented by the Naust Formation (Dalland et al., 1988), is the result of an enormous production of siliciclastic detritus in mainland-Norway, transported and deposited during several cycles of glaciations (Dahlgren et al., 2002a, b; Hjelstuen et al., 2004a; Rise et al., 2005, 2010; Ottesen et al., 2009; Hafeez, 2011; Faleide et al., 2012).

It is generally considered that the onset and internal stratigraphy of the large-scale outbuilding of the sedimentary shelf was related to Late Neogene uplift of Scandinavia, accompanied by climatic deterioration and establishment of large Pleistocene ice caps in northern Europe (e.g. Vorren and Mangerud, 2008). The Pleistocene clastic wedge of the mid-Norwegian shelf thus represents an archive of the Late Cenozoic climatic history, but also reflects fluctuations in accommodation space caused by subsidence created by tectonics and compaction, and glacio-eustacy. In addition, geometry and architectural style of the progradational succession are also the result of repeated cycles of glaciation and deglaciation, dimension and extent of ice sheets in Scandinavia, glacial dynamics and glaciomarine processes. The mid-Norwegian Plio-Pleistocene continental shelf succession was developed with high sedimentation rate and consists of glacigenic debris flows, glacimarine sediments, slide debrites and till units. Thus, the stratigraphic and sedimentological architecture of the Plio-Pleistocene mid-Norwegian clastic shelf succession is the product of the interaction of a series of external and internal physical factors.

The main objective of this Master Thesis project has been to improve the understanding of the Plio-Pleistocene development of the mid-Norwegian continental shelf, as manifested by the progradational Naust Formation. Particular attention has been paid to the sequence stratigraphy of the Naust Formation, with identification of regional significant sequence stratigraphic surfaces, formed as unconformities and conformities, mapping and recognition of their regional attributes and interpretation of their origin. Depositional processes have been

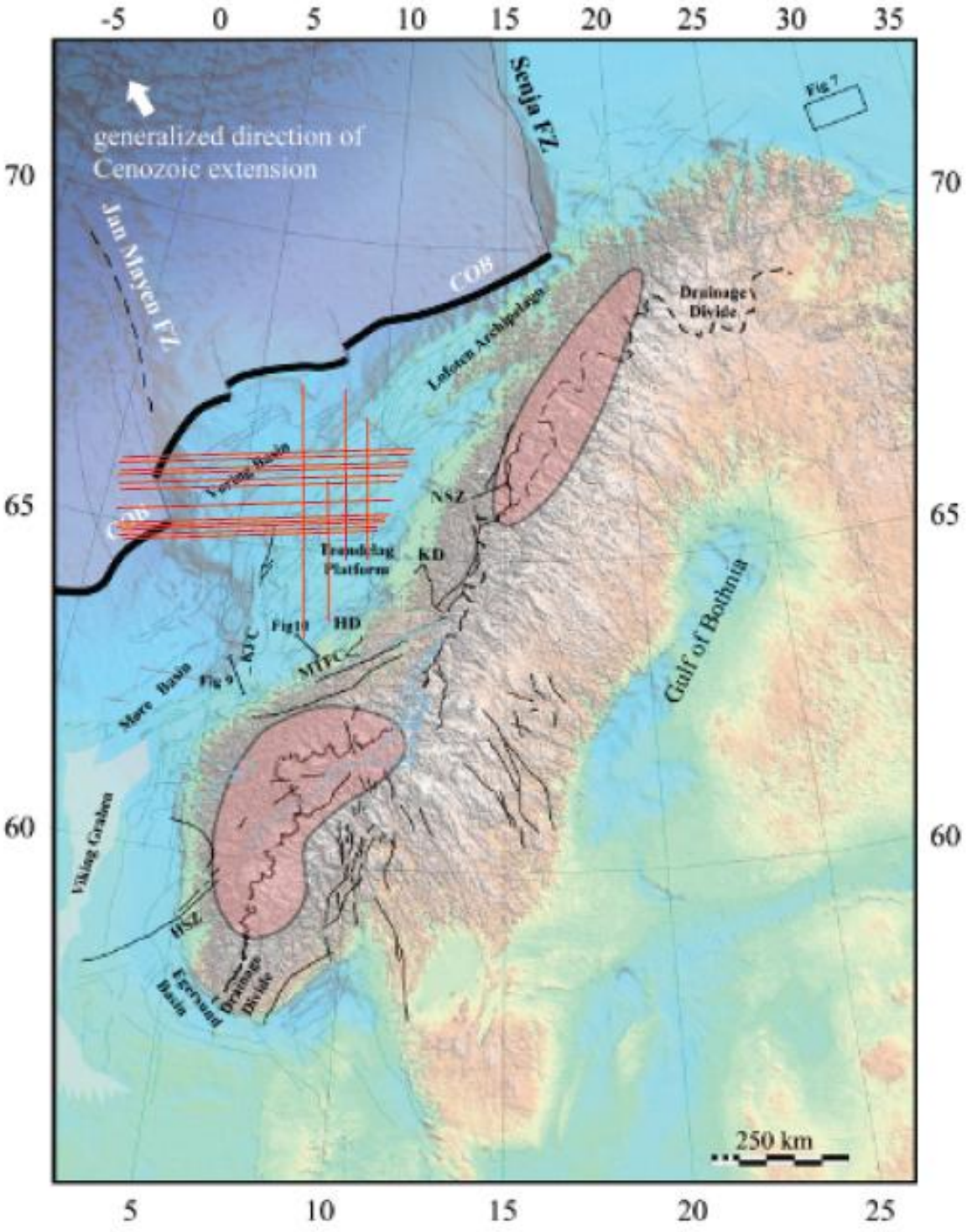

Figure 1.1 Location map showing the Norwegian Sea margin with some of its principal offshore and onshore structures and rift basins with the dataset of the study (Modified after Redfield et al., 2005, from Smelror et al., 2007).

interpreted from seismic facies, changes in relative sea level from offlap breaks and erosional and depositional relationships from seismic reflection terminations.

An overall goal of the study has been to define and correlate depositional sequences that may be interpreted as the product of separate glacial-interglacial cycles. In this respect the master project represents a continuation and further progress of the project on the Plio-Pleistocene shelf development at the University of Oslo, as also included the Master Thesis project by Hafeez (2011) and the preliminary report by Faleide et al. (2012).

2. Geological framework of the Pliocene-Pleistocene glacial succession on the mid-Norwegian continental shelf

2.1 Main stages of development

The Pliocene-Pleistocene glacial Naust Formation is located on the mid-Norwegian shelf. The shelf developed on a passive continental margin that formed by the break up of the Eurasia-North American continental plate and opening of the Norwegian-Greenland Sea in early Eocene time (e.g. Blystad et al. 1995). Before the rifting and sea-floor spreading, there were several periods of stretching, thinning and subsidence during Carboniferous, Permian-Early Triassic and Late Jurassic times (Fig. 2.1). All rift phases and subsequent post-rift thermal cooling phases were characterized by subsidence and deposition of sediments, mostly marine sand and mud, but also continental facies. Basin inversions also took place along rotated fault blocks and structural highs (Fig. 2.1). The Caledonian basement underlies most of the mid-Norwegian margin, and weak zones inherited from the Caledonian orogeny played a major role in later evolution of the continental margin off mid-Norway with formation of sub-basins, structural highs and lineaments (e.g. Brekke et al., 2001; Smelror et al., 2007; Faleide et al., 2010, and references therein) (Figs. 2.1 and 2.2).

The Cenozoic continental breakup and related basaltic sea-floor spreading was associated with uplift of the rifted margins on both side of the evolving sea-way and sediment infill of the shelfal and continental margin areas, as well as the new oceanic basin (e.g. Doré et al., 1999; Brekke et al., 2001; Faleide et al., 2010).

The Norwegian Sea margin experienced two main phases of compression during Middle Eocene/Early Oligocene and in Middle Miocene (Doré and Lundin, 1996; Lundin and Doré, 2002; Smelror et al., 2007). Middle to Late Miocene compressional tectonics generated numerous reverse faults and inversion domes, like the prominent Helland-Hansen Arch, onto which Pliocene-Pleistocene successions onlaps and downlaps. The compressional phases also gave rise to unconformities and hiatuses in the Cenozoic sedimentary succession.

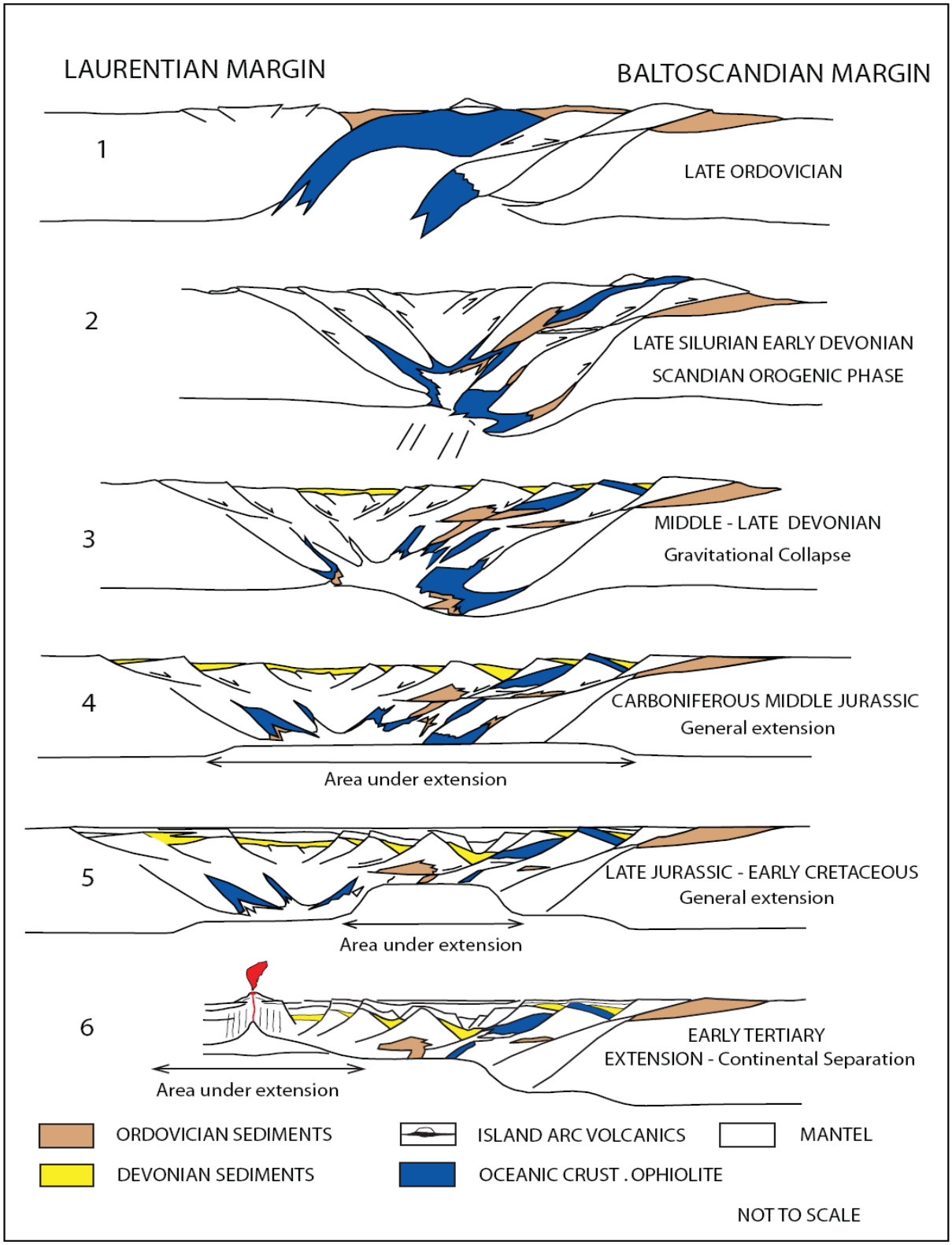

Figure 2.1 Diagram demonstrating the tectonic development of the Norwegian Continental Margin (after Skogseid et al., 1992).

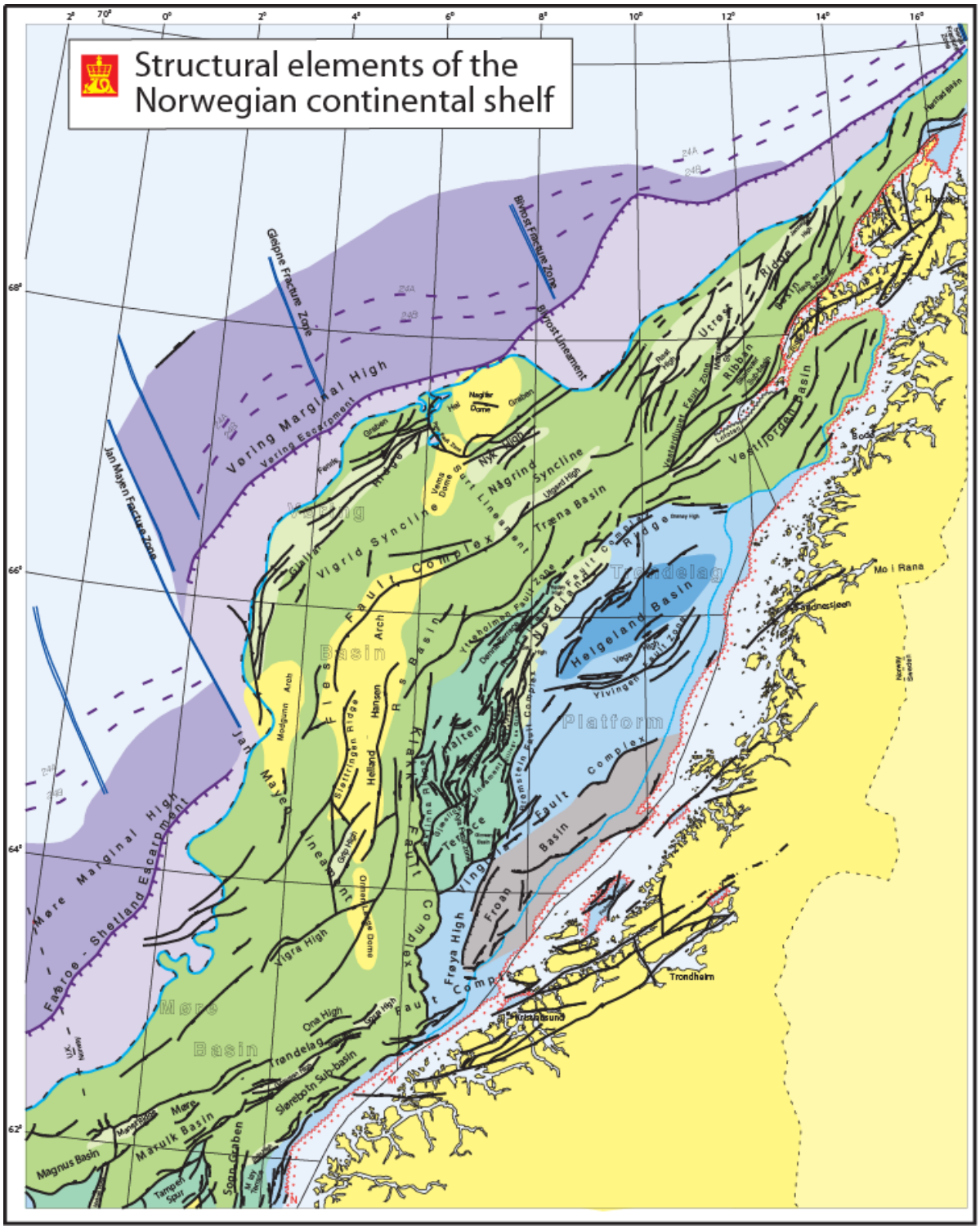

Figure 2.2 Structural map of the mid-Norwegian continental shelf (After Blystad et al., 1995)

2.2 Cenozoic sedimentation

The Cenozoic sedimentation on the mid-Norwegian margin was introduced by the Paleocene to Lower Eocene *Rogaland Group*, following the Upper Cretaceous shale dominated Shetland Group. The Rogaland Group consists of argillaceous marine sediments with clastic sand wedges in the east. The depositional environment was relatively deep marine with some submarine fans building out from the southeast. In the northern North Sea submarine fans were deposited from the west (Dalland et al., 1988; Isaksen et al., 1989).

In the Eocene-Oligocene *Hordaland Group* (Fig. 2.3), with the Brygge Formation, marine mud depositions continued and include smectitic clays formed from volcanic ash spread from subaerial eruptions. The group also includes claystone, sandstone with thin limestone and dolomite streaks. At the basin margins the Hordaland Group is incomplete owing to erosion or non-deposition (Dalland et al., 1988; Isaksen et al., 1989; Eidvin et al., 2001, 2007; Faleide et al., 2010).

The *Nordland Group*, of Middle Miocene to Recent age (Dalland et al., 1988; Isaksen et al., 1989; Eidvin et al., 1989, 1993, 2001, 2007; Rundberg and Eidvin, 2005), overlies an mid-Miocene hiatus, shifting from shales and clays in the Hordaland Group to more massive and blocky claystones in lower part of the Nordland Group (Dalland et al., 1988; Isaken et al., 1989; Løseth and Henriksen 2005). On the mid-Norwegian shelf the Nordland Group consists of the Kai, Molo and Naust formations (Fig. 2.3).

The *Kai Formation* was deposited in marine environment with variable water depth. It consists of claystone, siltstone and thin sandstone beds with stringers of limestone with glauconite, pyrite and shell fragments commonly. It is aged from Early Miocene to Late Pliocene (Dalland et al., 1988; Eidvin et al., 2007) (Fig. 2.3). The Kai Formation makes the most basinward wedge-out of all the Cenozoic successions (Martinsen et al., 1999; Løseth and Henriksen 2005).

The *Molo Formation* consists of a prograding system with steep clinoforms. The absence of top set beds is interpreted as the result of later erosion. The lithology has variations throughout its distribution. However, it contains sand with well rounded and rust-tinted

pebbles. In the distal parts it consists of glauconitic sand, silt and clay. The Molo Formation was deposited in a coastal shallow marine to prograding deltaic environment which might

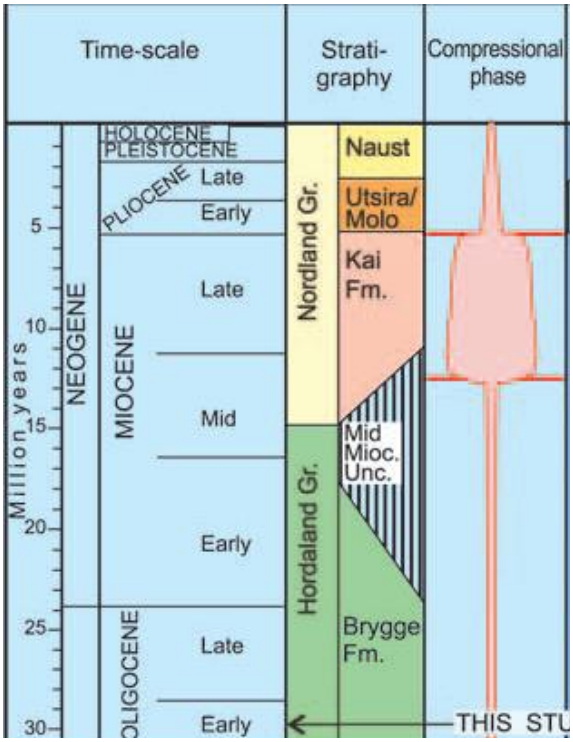

Figure 2.3 The Late Cenozoic stratigraphy in the northern North Sea and the mid-Norwegian continental shelf (modified from Løseth and Henriksen 2005).

have been wave-dominated with extensive long-shore drift. The age of the Molo Formation is from Late Miocene to Early Pliocene (Eidvin et al., 2007), and the formation is correlated with parts of the Utsira Formation in the North Sea area (Isaksen et al., 1989; Eidvin et al., 2001, 2007) (Fig. 2.3).

The Molo Formation is terminated on top by a regional surface on top of which the Naust Formation is downlapping and prograding. This surface is the Regional downlap surface (RDS) on the mid-Norwegian continental shelf.

2.3 Naust Formation and glacial sedimentation

The Upper Pliocene to Recent *Naust Formation* is present across the mid-Norwegian Shelf and consists of interbedded claystone, siltstone and sand with very coarse clastic sediments

in the upper part at some locations. The depositional environment is generally marine to glaciomarine (Dalland et al., 1988) (Fig. 2.3).

Naust Formation consists of clay rich diamictons with few intervals of sandy diamictons on the shelf margin (Eidvin et al., 2000). Muddy sediments along with ice-rafted debris are accumulated on more distal areas (Eldholm et al., 1987).

Seismic facies

Seismic facies of the Naust Formation demonstrate complex sigmoid-oblique clinoform configuration with a gentle (1-2°) angle of dip. Seismic facies show a repetitive pattern of unconformity bounded and lensoid sequences (Henriksen and Vorren, 1996). On the inner shelf the topset beds are missing due to erosion. However on the outer shelf the sequences reveal better preservation. On the Vøring plateau, the Naust Formation exhibits a parallel-laminated interval acoustic facies.

On the Møre Basin lower part of the Naust Formation below regional angular unconformity (URU: Upper Regional Unconformity) reveals low angle sigmoid-oblique clinoforms dipping towards NNW. Above URU, the Naust Formation is characterized by subparallel, sub-horizontal reflections having moderate to good continuity (King et al., 1996).

Lower and Upper Boundaries

The lower boundary of the Naust Formation is RDS (Regional Downlap Surface). The upper boundary of the Naust Formation is the present-day sea bed which reveals present bathymetric expressions of the Mid-Norwegian margin and adjoining Norwegian Basin.

The change in style of progradation from the Molo Formation to the Naust Formation signifies a marked change in sedimentary environment from peri-glacial to glacial regime in the late Pliocene to early Pleistocene. Late Pliocene-Pleistocene deposition depicts a gradual climatic deterioration. Major ice sheets approached the coastal areas of mid-Norway and finally advanced across the continental shelf and deposited large amounts of sediments. The direction of ice movements is deduced from pattern of glacial striations or flutes which show that ice streams partly followed the bedrock boundaries and structural features in subsurface

(Henriksen et al., 2005). The progradation of thick clastic wedges prevailed in response of uplift and glacial erosion of source areas in mainland Norway in Late Pliocene (Faleide et al., 2010). During the last 2.8 Ma tremendous amounts of sediments were supplied to the mid-Norwegian continental margin as a result of increased erosion due to combination of mainland uplift and onset of extensive glaciations (Henriksen and Vorren, 1996; Hjelstuen et al., 2004a; Rise et al., 2005, 2010; Stoker et al., 2005; Dowdeswell et al., 2010).

Below the Pleistocene unconformity, the Upper regional unconformity (URU), the complete Cenozoic succession is tilted, having strong angular relationship, thus revealing Late Pliocene uplift (Faleide et al., 2010). It is supposed that glaciers might have entered the shelf locally in restricted periods from 1.5-0.5 Ma, whereas the amount of Ice Rafted Detritus (IRD) increased in the Norwegian Sea at 1.1 Ma (Jansen et al., 2000; Smelror et al., 2007). These data may possibly reflect the first ice-stream expansion to the shelf edge through the Norwegian Channel (Sejrup et al., 1995; Smelror et al., 2007).

The sediments in the Naust Formation are partly glacial and partly marine. The latter facies may represent reworked glacial sediments and are typically poorly sorted. Such type of sediments compact readily; the load of grounded ice sheets may have caused the compaction. The ice sheets reached several times out onto the shelf and deposited much debris load at or close to shelf edge that was displaced further out into the basin during succeeding ice ages

The continuation of ice flows along the south coast of Norway caused erosion and reworking of Cenozoic and Mesozoic fine-grained sediments, resulting into thick Pleistocene sedimentary fans deposited at the slope in front of bathymetric troughs, as the North Sea Fan. The Late Cenozoic sedimentation rate was relatively high and the clayey sediments did not compact properly to reduce their water so they have plastic folding and diapir structures (Faleide et al., 2010).

The Pleistocene deposits show cyclic sedimentation with till deposits alternating with galciomarine sediments (Sejrup et al., 1995; Martinsen et al., 1999). Large volumes of Pleistocene sediments have likely been eroded by the erosion of grounded ice sheets during many periods (Sejrup et al., 1995, 1996; Martinsen et al., 1999). Also huge amounts of sediments were removed by the Storegga Slide in the Møre Basin about 7000 years BP

(Bugge et al., 1987; Martinsen et al., 1999). The mass wasting through debris flows, slumping and sliding became the mechanisms of transporting sediments from the North Sea, parts of the Møre Basin area and the mid-Norwegian shelf westwards into the Norwegian Sea (Sejrup et al., 1996; Martinsen et al., 1999).

During peak glaciations the last 0.5 Ma the mid-Norwegian shelf was thoroughly covered by ice sheets (Butt et al., 2002; Bugge et al., 2004; Ottesen et al., 2005; Rise et al., 2005; Smelror et al., 2007). The clastic shelf prograded rapidly. Nearly 180,000 km^3 of sediments were deposited off mid-Norway during the past 2.7 Ma (Rise et al., 2005; Ottesen et al., 2005; Smelror et al., 2007).

Erosion and transportation of sediments to the shelf edge by regional ice streams caused a large scale exhumation of Norway during the last 600,000 years (Smelror et al., 2007). Ice streams flowed towards the southwest from the deep trough of Vestfjorden, crossed the outer Trænabanken and terminated in the Skjoldryggen area during the Elsterian and Saalian (third & second last glacial periods). After the Saalian the direction of ice flow changed significantly and the dominant ice flow went through Vestfjorden before turning into Trænadjupet and even extended approximately 100 km to shelf edge during the Weichselain (last glaciation) (Dowdeswell et al., 2006; Smelror et al., 2007).

3. Data and Methods

Data and methods chapter is comprised of the details of seismic data which were provided for seismic sequence analysis and a brief detail of the tools, analysis methods and drawbacks.

3.1 Data

The data available for interpretation is part of the multichannel 2D seismic reflection survey which is named as MNR (Mid Norway Regional) survey. This survey was acquired since 2004 and survey programme was extended till 2011 with a total of 90,000 line kilometers and contributed to understand the regional geology. This survey was executed by Fugro Multi Client Services AS and TGS-NOPEC. Most of the available lines were interpreted during this study and 33 reflectors were picked including sequence boundaries, seabed, an upper regional unconformity (URU) and a regional downlap surface (RDS). Petrel software was used for interpretation of seismic horizons and correlating them on dip and strike lines.

12 seismic key lines were selected to be displayed in a regional map of the study area (Fig. 3.1) and their interpretation and description will be given in chapter 4. The dip lines trend east-west and cover a maximum distance of 448 km (in dip lines), extending from the Trøndelag Platform in the east to the Lava Front in the west. However, strike lines running north-south cover a maximum distance in one of the strike lines of 495 km, extending from the Vøring Marginal High in the north to the Froan Basin in the south. Vetrical distance of up to 2-2.5 seconds TWT was focused for interpretation of the Naust Formation.

The time thickness maps utilizing milliseconds of two-way travel time (TWT) have been generated using Petrel after interpretation of reflectors. The seismic lines had high resolution and good data coverage. Dip lines had better data coverage as compared with the strike lines. However, the coverage in west of the Helland-Hansen Arch was rather poor. Sequence boundaries were easy to pick because of high acoustic impedance contrast with other reflectors.

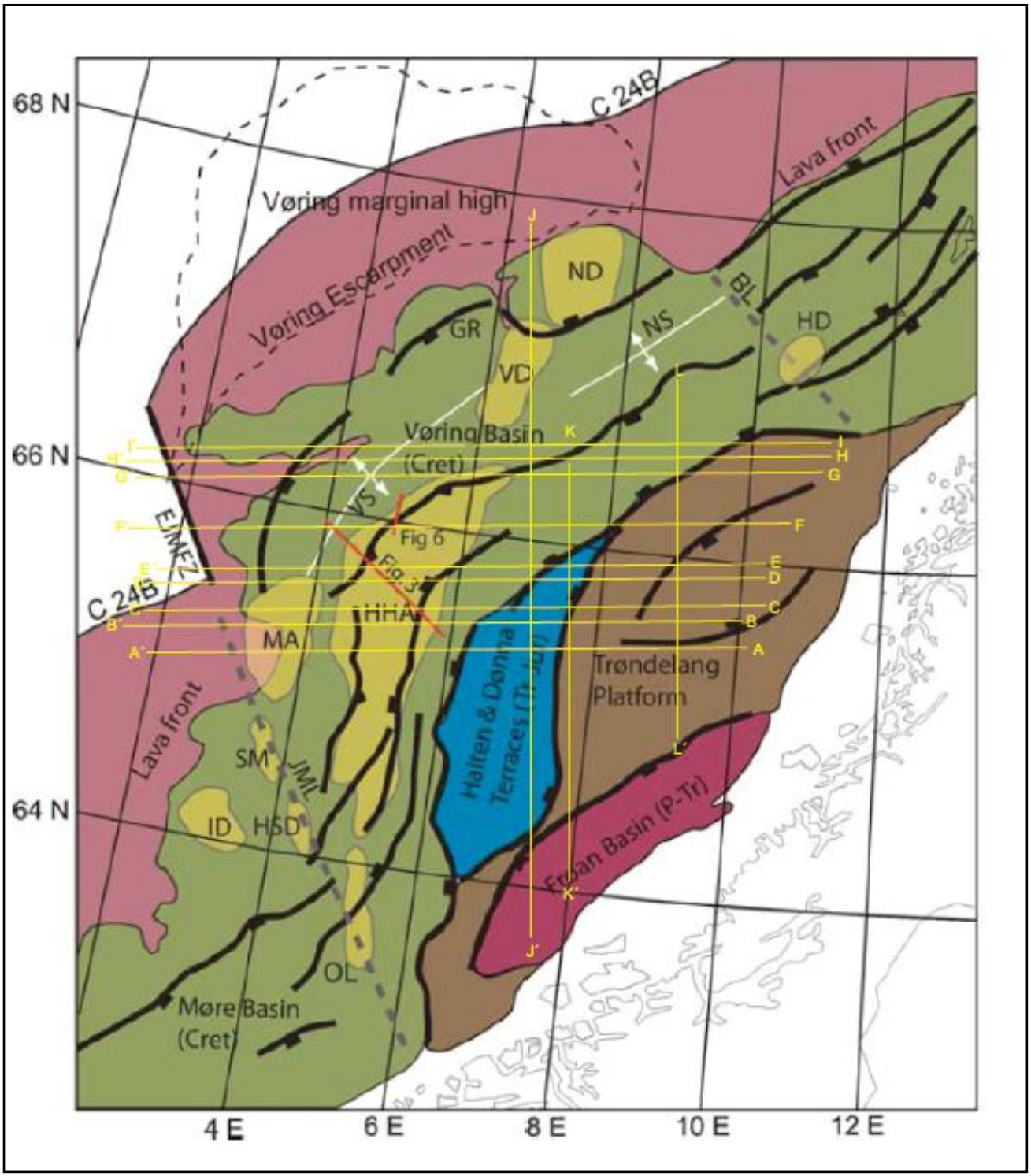

Figure 3.1 The structural map of the Mid-Norwegian margin with the dataset of the study area illustrating the main structural provinces and structures. BL: Bivrost Lineament, EJMFZ: East Jan Mayen Fracture Zone, GR: Gjallar Ridge, HD: Hedda Dome, HHA: Helland-Hansen Arch, HSD: Havsule Dome, ID: Isak Dome, JML: Jan Mayen Lineament, MA: Modgunn Arch, ND: Naglfar Dome, NS: Någrind Syncline, OL: Ormen Lange Dome, SM: Southern Modgunn Arch, VD: Vema Dome and VS: Vigrid Syncline (Modified from Doré et al., 2008).

3.2 Sequence Stratigraphy

Sequence stratigraphy is used as well-established tool for investigating rock successions. Sequence stratigraphy has become advanced since it was defined and its roots can be traced back to 18th century (Nystuen, 1998). Sequence stratigraphy deals with analyzing changes in facies and geometric nature of strata and recognition of key surfaces to establish the chronological order of basin filling and erosional activity (Catuneanu et al., 2009).

Sequence stratigraphy is a sub-discipline of stratigraphy, whereas stratigraphy is historical geology of stratified rocks. Various definitions of sequence stratigraphy have been published (Fig. 3.2) In its simplest way sequence stratigraphy can be defined as 'the sub-division of sedimentary basin fills into genetic packages bounded by unconformities and their correlative conformities' (Emery, 1996, p. 3). Sequence stratigraphy gives a chronostratigraphic framework for correlation and mapping of sedimentary facies and stratigraphic prediction. Numerous geological disciplines are utilized in sequence stratigraphic study such as seismic stratigraphy, chronostratigraphy, biostratigraphy and sedimentology (Emery, 1996).
Furthermore, the interaction of rate of eustacy, subsidence and sediment supply result into the formation of sequences and their stratal patterns (Van Wagoner et al., 1988a).

3.3 Seismic sequence stratigraphy

Seismic sequence stratigraphy is a very beneficial tool for continuous subsurface imaging of, structural trends, lapout relationships, imaging of depositional features, stratal stacking patterns, geomorphology and stratal geometries (Catuneanu, 2006; Catuneanu et al., 2009).

Seismic sequence stratigraphy is analyzed using seismic data; therefore depositional trends are detected referring to aggradation versus erosion and progradation versus retrogradation. In addition, seismic sequence stratigraphy is also a method in analysing variations in the interaction of sedimentation and base level control on depositional trends (Catuneanu et al., 2002).

3.3.1 Sequence boundaries and unconformities

A sequence is a relatively conformable succession of genetically related strata bounded by unconformities and their correlative conformities (Mitchum, 1977; Catuneanu et al., 2009). Whereas, sequence boundaries are defined as unconformities or their correlative conformities (Hampson et al., 1999).

Sequence stratigraphy (Posamentier et al., 1988; Van Wagoner, 1995): the study of rock relationships within a time-stratigraphic framework of repetitive, genetically related strata bounded by surfaces of erosion or nondeposition, or their correlative conformities.

Sequence stratigraphy (Galloway, 1989): the analysis of repetitive genetically related depositional units bounded in part by surfaces of nondeposition or erosion.

Sequence stratigraphy (Posamentier and Allen, 1999): the analysis of cyclic sedimentation patterns that are present in stratigraphic successions, as they develop in response to variations in sediment supply and space available for sediment to accumulate.

Sequence stratigraphy (Embry, 2001b): the recognition and correlation of stratigraphic surfaces which represent changes in depositional trends in sedimentary rocks. Such changes were generated by the interplay of sedimentation, erosion and oscillating base level and are now determined by sedimentological analysis and geometric relationships.

Note that sedimentation is separated from base level changes. Also note important keywords:
- *"cyclicity": a sequence is a cyclothem, i.e. it corresponds to a stratigraphic cycle;*
- *"time framework": in the early days of sequence stratigraphy, the bounding surfaces were taken as time lines, in the view of the global-eustasy model. Today, independent time control is necessary for large scale correlations;*
- *"genetically related strata": no major hiatuses are assumed within a sequence.*

Figure 3.2 illustrating various definitions of sequence stratigraphy (after Catuneanu, 2002).

However an unconformity is a surface which separates younger strata from older strata and along which subaerial erosional truncation, or subaerial exposure with a considerable hiatus exists. A conformity is a bedding surface that separates younger from older strata and along which there is no erosion, non-deposition or hiatus indicated (Wagoner et al., 1988b).

3.3.2 Stratal terminations

Stratal stacking patterns are result of the interaction of variations in rates of sedimentation and base level and reveal combinations of depositional trends together with progradation, aggradation, retrogradation and downcutting. Stratal stacking pattern results into distinguished genetic type of deposit such as transgressive, normal regressive and forced regressive (Hunt and Tucker, 1992; Posamentier and Morris, 2000) with a discrete geometry and facies preservation style. Various types of stratal terminations are given in Figs. 3.3 and 3.4.

3.4 Clinoforms

Clinoforms are identified through break-in-slope and their migration patterns. The term clinoform is used for depositional profile with the complete sigmoidal topset-foreset-bottomset (Steel and Olsen, 2002). However according to Rich, (1951) the clinoform is referred to as the sloping constituent of a sigmoidal surface. Shelf slope basin clinoforms demonstrate advancement of a shelf margin having several hundreds of meters of height (Emery, 1981), whereas shoreline clinothems reveal progradation of deltas, strand plains and barrier-island shorelines which might be few tens of meters in height (Helland-Hansen & Hampson, 2009).

Topset beds much close to adjacent reflectors were difficult to be interpreted laterally due to tuning effect and destructive interference as shown in (Fig. 3.5). Shelf margin scale clinoforms and their trajectories have been interpreted on seismic sections in the present study. The seismic resolution of seismic sections was good to determine palaeo-shelf edge through trajectory analysis in present study. However, trajectory analysis is dependent upon preservation of offlap breaks of clinoforms (Helland-Hansen & Hampson, 2009; Helland-Hansen et al., 2012).

Truncation: termination of strata against an overlying erosional surface. *Toplap* may develop into truncation, but truncation is more extreme than toplap, and implies either the development of erosional relief or the development of an angular unconformity.

Toplap: termination of inclined strata (clinoforms) against an overlying lower angle surface, mainly as a result of nondeposition (sediment bypass), ± minor erosion. Strata lap out in a landward direction at the top of the unit, but the successive terminations lie progressively seaward. The toplap surface represents the proximal depositional limit of the sedimentary unit. In seismic stratigraphy, the *topset* of a deltaic system (delta plain deposits) may be too thin to be "seen" on the seismic profiles as a separate unit (thickness below the seismic resolution). In this case, the topset may be confused with toplap

Onlap: termination of low-angle strata against a steeper stratigraphic surface. Onlap may also be referred to as *lapout*, and marks the lateral termination of a sedimentary unit at its depositional limit. Onlap type of stratal terminations may develop in marine, coastal, and nonmarine settings:

- marine onlap: develops on continental slopes, mainly during transgressions (*slope aprons*; Galloway, 1989) and forced regressions (*regressive slope onlap surfaces*; Embry, 2001), as a result of gravity flow processes.

- coastal onlap: refers to lower shoreface strata onlapping onto the ravinement surface during the shoreline transgression

- fluvial onlap: refers to the landward shift of the upstream end of the aggradation area within a fluvial system during base level rise (transgression or normal regression).

Downlap: termination of inclined strata against a lower-angle surface. Downlap may also be referred to as *baselap*, and marks the base of a sedimentary unit at its depositional limit. Downlap is commonly seen at the base of prograding clinoforms, either in shallow marine or deep marine environments. It is uncommon to generate downlap in nonmarine settings, excepting for lacustrine environments. Downlap therefore represents a change from marine (or lacustrine) slope deposition to marine (or lacustrine) condensation or nondeposition.

Offlap: the progressive offshore shift of the updip terminations of the sedimentary units within a conformable sequence of rocks in which each successively younger unit leaves exposed a portion of the older unit on which it lies. Offlap is the product of base level fall, so it is diagnostic for forced regressions.

Figure 3.3 depicting types of stratal terminations (definitions from Mitchum, 1977) modified from Emery, 1996, after Catuneanu, 2002.

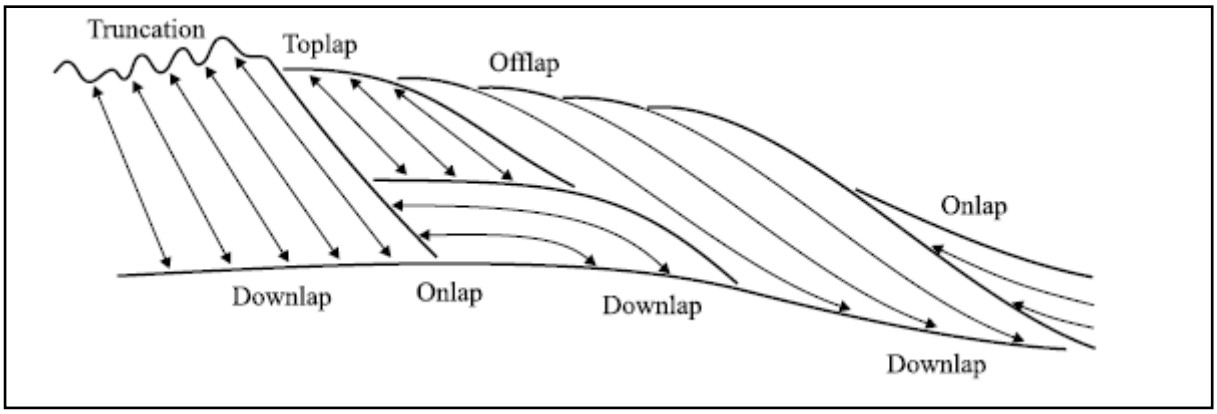

Figure 3.4 demonstrating types of stratal terminations, there may probably be confusion between onlap and downlap due to variation in ratio between dip of strata and dip of stratigraphic surface against which they terminate (modified from Emery 1996; after Catuneanu, 2002).

Topset beds are the proximal part of a clinoform. They are usually horizontal. The topset beds were mostly eroded in present study however wherever they were preserved, trajectory analysis was carried out where offlap breaks of clinoforms were retained.

Foreset beds are the inclined element of clinoforms and reveal sediment deposition along slopes. Foreset beds were mostly preserved during progradation of clinoforms in the study area. Foreset beds were making comparatively higher angles in lower part of formation and dipping angles became gentler in upper parts.

Bottomset beds are the lateral component of clinoforms. Bottomset beds were making downlaps with RDS and were composed of largely fine grained sediments.

3.5 Parasequences and stacking patterns

'A parasequence set is a succession of genetically related parasequences which form a distinctive stacking pattern that is bounded , in many cases, by major marine-flooding surfaces and their correlative surfaces'(Van Wagoner et al., 1988a, p.39).

Moreover, a marine flooding surface is a surface along which younger strata are separated from older strata and across which sudden increase in water depth is evident. This deepening is usually associated with minor submarine erosion and non-deposition, thus may reveal a small hiatus along marine ravinement surfaces.

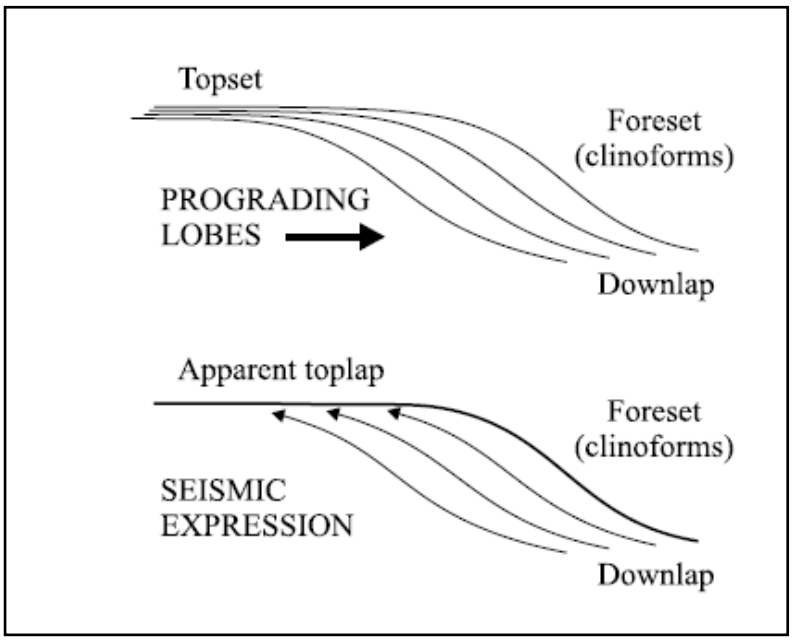

Figure 3.5 illustrating seismic expression of a topset package which is thinner as compared with the seismic resolution. The topset seems to be toplap due to interference being closer and tuning effect (after Catuneanu, 2002).

Maximum flooding surface (Frazier, 1974; Posamentier et al., 1988; Van Wagoner et al., 1988a; Galloway, 1989) is a surface through which variation in shoreline trajectory from transgression to high stand normal regression occurs. This is usually a downlap surface in shallow water regime where highstand coastlines prograde on top of transgressive condensed sections (Catuneanu et al., 2009).

In addition, parasequence set boundaries separating individual parasequence stacking patterns, may coincide with sequence boundaries and may be downlap surfaces and boundaries of system tracts. The outcome of ratio between depositional rates and accommodation rates are stacking patterns of parasequences in parasequence sets which may be progradational, retrogradational or aggradational. These stacking patterns within a sequence might be predictable (Van Wagoner et al., 1988a).

Progradational stacking pattern

A progradational stacking pattern is referred to the architecture of a vertical succession of parasequences. In a progradational stacking pattern facies at top of each consecutive paraseqence becomes gradually more basinwards (Myers and Milton, 1996). This stacking pattern is constructed due to high ratio between rate of sedimentation and rate of accommodation (Van Wagoner et al., 1988a). The progradational stacking pattern was largely found in the present study, moreover with help of stacking patterns of clinoforms variations in relative sea level were predicted.

Aggradational stacking pattern

Aggradational stacking pattern is formed provided with more or less equal rates of accommodation and sedimentation (Van Wagoner et al., 1988a). There is no net movement of the shoreline and no shift of facies in aggradational stacking pattern (Myers and Milton, 1996). There was found aggradational stacking pattern in few places in seismic sections in this study.

Retrogradational stacking pattern

In a retrogradational stacking pattern facies migrate towards land upwards (Myers and Milton, 1996). The rate of accommodation space is higher than rate of sedimentation in retrogradational stacking pattern (Van Wagoner et al., 1988a).

3.6 Facies Analysis

Seismic facies analysis utilizes seismic parameters to get other than structural information. A seismic facies entity is a sedimentary unit which is found to have varying seismic characteristics from its neighbouring units. During seismic facies analysis following parameters are taken into account: reflection amplitude, reflection polarity, dominant reflection frequency, interval velocity, reflection configuration, reflection continuity, geometry of seismic facies unit, abundance of reflections, and their relationship with other units (Roksandic, 1978) (Fig. 3.6).

Direct or indirect interpretation is carried out through seismic facies analysis. Direct interpretation is applied to determine geological reasons dependable of seismic signatures of a seismic facies unit. Through direct interpretation lithology, porosity, fluid content, overpressured shales, relative age, type of stratification, geometry and geological settings are established. Whereas depositional environments and processes, sediment transport direction and several stages of geological evolution (i.e. transgression, regression, subsidence, uplift and erosion) are ascertained through indirect interpretation.

During the present study reflection configurations, amplitude, reflection continuity, geometry, their relationship with other reflections, stacking pattern, type of stratification, depositional processes, relative sea level variations, accommodation space, uplift, sediment loading, glacial-induced subsidence and erosion were determined with help of seismic facies analysis (which will be discussed in chapter 4 and 5).

3.7 Trajectory Analysis

Trajectory analysis has a practical, conceptual as well as descriptive implementation which is facilitated to make better interpretations of rock strata and provides insight of rock successions where trajectories can not be observed directly. The combination of descriptive and interpretative tool enables to enhance understanding of how sedimentary successions were generated. In addition, trajectories have a direct association with seismic data as well as GPR data (Helland-Hansen and Hampson 2009).

Trajectory analysis permits genetically related advancement or retreat of a shoreline or shelf edge being an element of incessantly on-going depositional system, assists to recognize variations in depositional environments (Fig. 3.7). On the other hand, trajectory analysis does not help to predict depositional successions and does not assist for any assertions about mechanisms of sequence development (Helland-Hansen and Hampson 2009).
The shelf-edge trajectory is a large scale and long term response of variable relative sea level and sediment supply. Significant elements like bathymetry, eustatic sea-level variations, sediment supply and subsidence (including subsidence associated with sediment loading and compaction) control shelf edge trajectory.

A basic difference between shelf edge and shoreline exhibits thus shelf edge is usually fixed or basinwards accreting, while shorelines may migrate towards basin or land, eventually forming diversified and complex trajectories (Helland-Hansen and Hampson 2009).

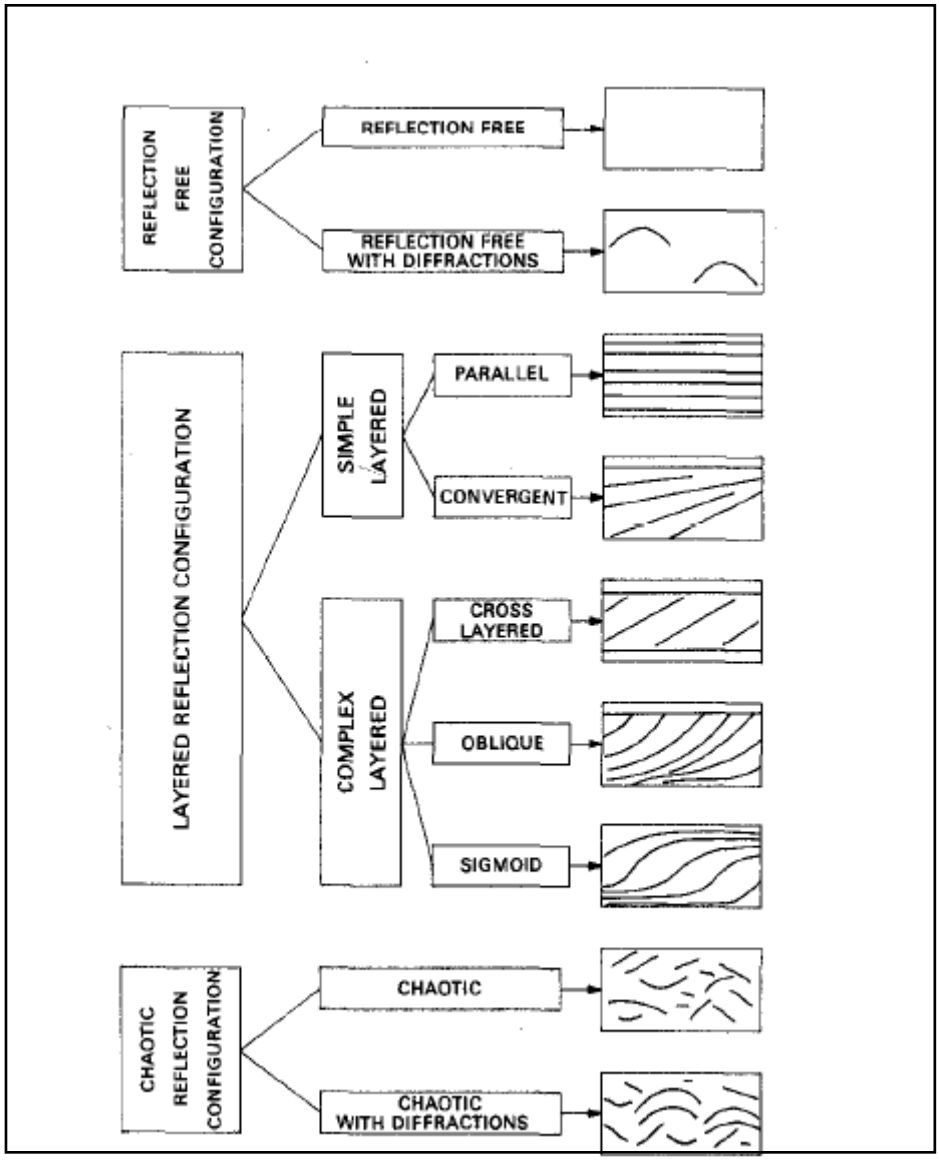

Figure 3.6 Various types of reflection configurations which are significant for seismic facies analysis (from Roksandic, 1978).

Shelf edge trajectories may be analyzed with help of seismic data. Variations in shelf-edge trajectory directions are determined with help of seismic data. Individual reflectors are at scale of parasequence and shelf edge clinoforms (Helland-Hansen and Hampson 2009). Palaeo-shelf edge trajectory was determined through trajectory analysis in this study (Figs. 5.6 & 5.7).

3.8 Chronostratigraphic Chart

Sequence stratigraphy deals with interpretation of depositional systems in time and space. However, chronostratigraphic charts reveal time relationships of systems as well as their relationship to various surfaces, e.g. surface of non-deposition, erosion and condensation.

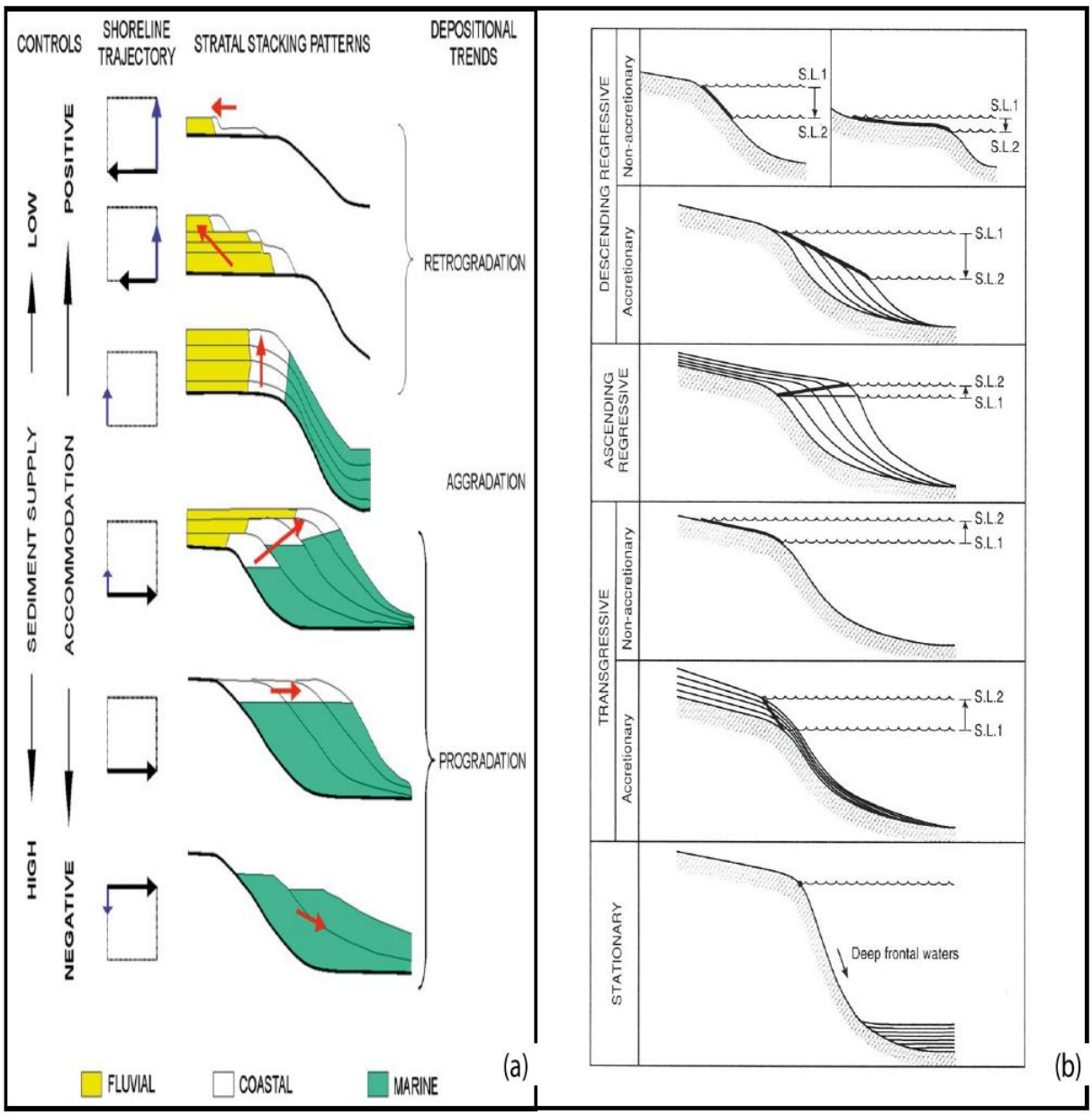

Figure 3.7 (a) illustrating stratal stacking patterns and depositional trends together with trajectory analysis (after Martins-Neto & Catuneanu 2010), (b) shoreline trajectory classes from Helland-Hansen and Hampson, 2009).

Chronostratigraphic charts emphasize significance of these surfaces by showing them in time dimension. The chronostratigraphic charts prove the interpretation in time and space.

Moreover a chronostratigraphic chart demonstrates time along vertical axis and distance along horizontal axis. Chronostratigraphic chart was constructed from seismic data in present study as depositional units were provided with better understanding of time and space.

3.9 Procedure to interpret the seismic data and analyze the seismic sequences

The present study was carried out through following procedures:

- The interpretation was started on a dip line which was having the area of interest.
- Maximum flooding surface was identified with help of downlaps against it, however erosional unconformity on regional scale was identified with the help of toplaps below it and there were onlaps above that erosional unconformity at different positions. The URU was interpreted to be an unconformity in east whereas it became a correlative conformity in west.
- Few consecutive dip lines were interpreted following first dip line as the reflectors were demonstrating comparable amplitude, geometry and orientation.
- Sequence boundaries have been identified while keeping in mind the processes related with glacial and interglacial events.
- Therefore, 32 seismic sequences have been interpreted in; this study, inferred 32 glacial events, which were separated by sequence boundaries, sequence stratigraphic framework is given in next chapter.
- Afterwards, cross-tying strike lines were interpreted and previous interpretation was inspected. Petrel has capability to show cross points between strike and dip lines (Fig. 3.8). Thus making it easier to interpret and inspect. In addition, complex features i.e. inter-fingering was interpreted with assistance of strike lines.

- Thickness of megasequences was calculated by converting milliseconds two-way travel time into meters by applying velocity taken from Reemst et al., 1996; Storvoll et al., 2005; Rise et al., 2010.
- Furthermore, time thickness maps of four megasequences were generated using Petrel to observe time thicknesses during different time periods in study area.
- Shelf edge trajectory was analyzed through offlap breaks of clinoforms which was a great input for establishing facts like relative sea-level variations, subsidence, climate and depositional processes.
- In the end, a chronostratigraphic chart was constructed in order to visualize the sequence development through time and space (see discussion chapter).

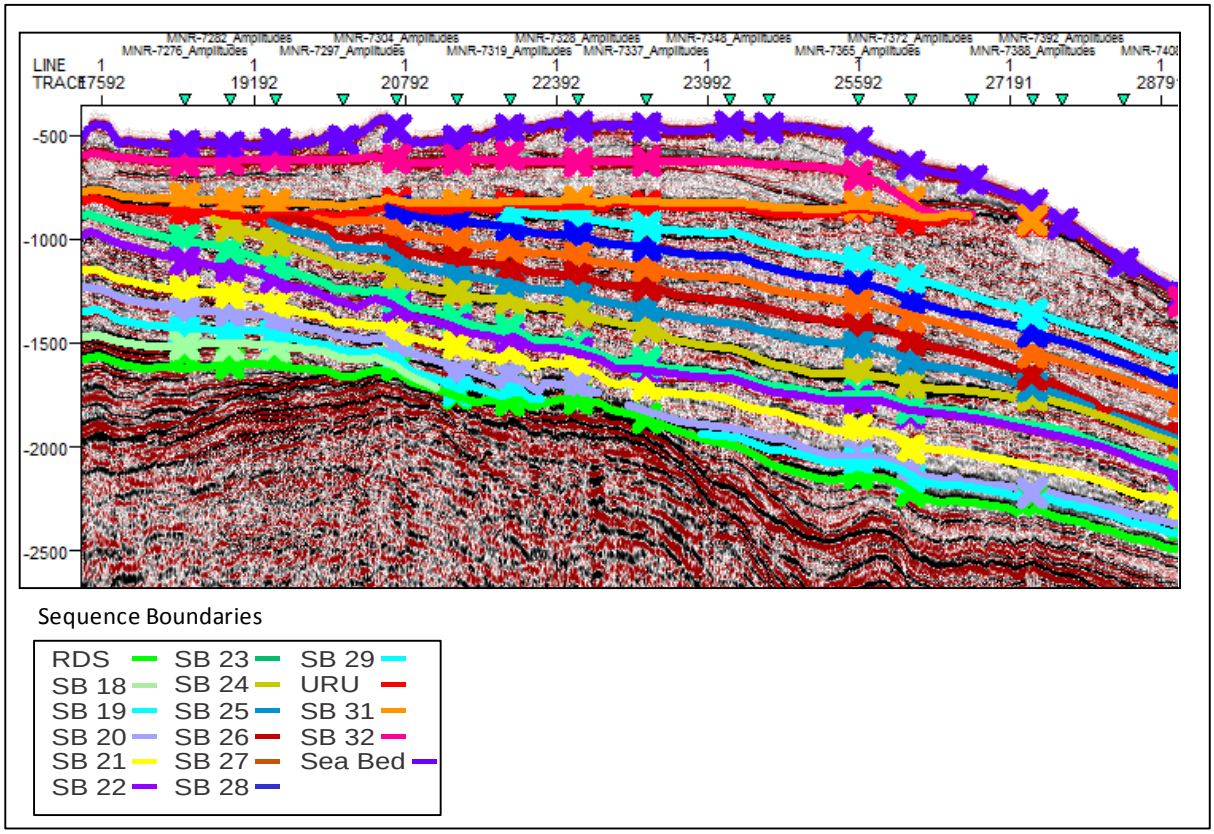

Figure 3.8 Strike line illustrating cross-ties between the dip lines and the strike line J after interpretation. See Fig. 4.2 for legends too.

Challenges

Some problems were encountered during interpretation. When reflectors were lying very close to other reflectors then tuning effects were created and destructive interference made difficult to interpret the lateral extension of original reflector (Fig. 3.5 and key seismic lines D, F, G and H in Figs. 4.5, 4.7, 4.8 and 4.9 respectively). Furthermore, steeper and tightly packed clinoforms generated destructive interference. Moreover MNR survey has time-shift thus created miss-ties between strike lines and dip lines to a certain extent while interpreting.

Drawbacks

Seismic resolution and processing quality was high in seismic sections. The image of reflections became poor due to this gas chimney effect. In addition, well cores and drilling well logs were lacking while interpreting which could possibly enhance confidence for depths and compositions of units to interpret depositional environments in this study.

4. Seismic Interpretation and Results

4.1 Description and Interpretation of seismic sequences

Seismic sequence stratigraphic analysis assisted to understand the source-to-sink relationship, tectonics and climate changes for the Late Cenozoic outbuilding of the mid-Norwegian continental margin. Seismic sequence stratigraphy proved to be the most important tool for interpretation of the Pliocene-Pleistocene clastic wedges of the present study area. Toplap truncations and onlaps define events of the fall in relative sea level, whereas downlap seismic surface demonstrate rise in relative sea level. The identification of rise and fall in relative sea level is of major significance for constructing the role of the important controlling factors on sedimentary facies and architectural style, including basin hinterland tectonics, changes in climate and eustacy.

The RDS (Regional Downlap Surface) exists in all seismic lines of the provided dataset. The clinoforms downlap against the RDS. It also shows high amplitude and high acoustic impedance contrast. Across RDS seismic velocities drop dramatically from glaciomarine sediments to Miocene strata giving high acoustic impedance contrast (Reemst et al., 1996).

The URU (Upper Regional Unconformity) of Vorren et al., 1992 and Henriksen et al., 1996 has high amplitude and the underlying depositional surfaces in the sequences make toplaps below it. The majority of the clinoforms of the Naust Formation have not their offlap breaks preserved and are truncated by the angular unconformity defined as the URU. The URU demonstrates various channels incising into underlying sequences at different levels, caused by glacial erosion which is controlled by various factors i.e., uplift, relative sea level, location of the ice streams and thickness of the ice sheets.

The Naust Formation is comprised of the succession from RDS to the seabed (Hjelstuen et al., 2005; Ottessen et al., 2009; Rise et al., 2005, 2010) (Fig. 4.1). The Naust Formation exhibits gentler clinoforms than those of the deltaic Molo Formation (Fig. 4.4). The Naust Formation has been subdivided into four magasequences in the present study. Megasequence-1 ranges from RDS to SB 11, megasequence-2 from SB 11 to SB 21, megasequence-3 from SB 21 to

URU and megasequence-4 from URU to the seabed. These megasequences are altogether further divided into 32 sequences (Fig. 4.1), all being demarcated by sequence boundaries.

Rise et al., 2010 subdivided the Naust Formation into N, A, U, S and T units which are equivalent to subdivision of the Naust Formation in this study as follows: SS 1-SS 17 are equivalent to unit N, SS 18-SS 25 to unit A, SS 26-SS 28 to unit U, SS 29 to unit S and SS 30-SS 32 to unit T.

These 32 seismic sequences reveal 32 glacial periods separated by sequence boundaries deposited during interglacial periods (Fig. 4.1). These sequences developed by 32 glacial periods have been divided into four megasequences based upon their clinothem configurations, stratal stacking pattern, angles of clinothems, seismic amplitude and lateral distribution.

Westward prograding thick clastic wedges were formed during glacial and interglacial periods along almost 160 km wide area. Rapid uplift and erosion during Northern Hemisphere glaciations (Jarsve et al., 2010) caused c. 1500 meters (1600 ms TWT) thick deposits of the Naust Formation (Late Pliocene). There was a significant role of tectonics, eustacy, sediment supply and rate of accommodation for Late Cenozoic outbuilding of the shelf in the northernmost North Sea and mid-Norwegian continental margin.

Depositional processes in the Naust Formation correspond to uplift, eustacy, relative sea-level, subsidence, sediment supply, rate of accommodation and climatic changes. Seismic facies in the Naust Formation are characterizing sliding, slumping, glaciomarine and stratified sediments.

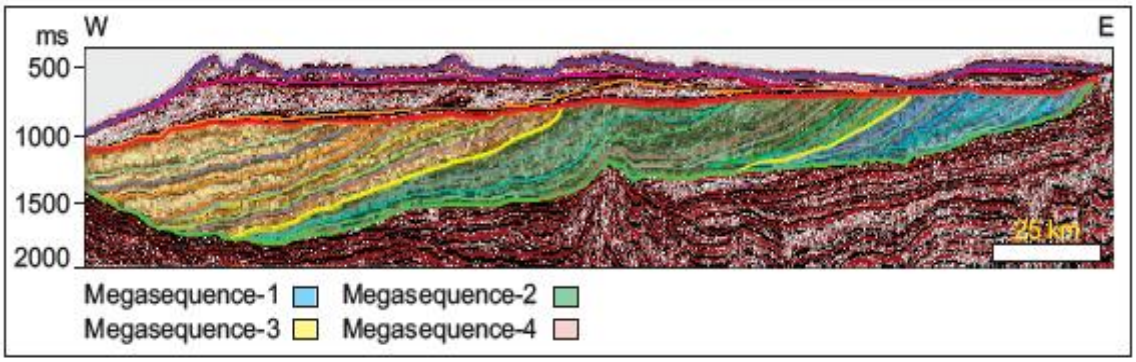

Figure 4.1 Random Seismic line showing four megasequences comprised of 32 seismic sequences.

4.1.1 Line A

The dip line is selected from the southern most part of the data set in the area. It extends up to 380 km from the Trøndelag Platform to the Lava Front (Fig. 3.1).

The seismic line A is interpreted to have 29 sequences out of 32 sequences. SS 5, 6 and 13 are found to be missing in seismic line A demonstrating tat they were not deposited or might have been eroded (Fig. 4.2).

Megasequence-1 contains very thin sequences and the steeply prograding clinothems make oblique wedge. Prograding clinothems make downlaps with RDS. The maximum composite thickness of megasequence-1 is 310 ms TWT (c. 280 m) (assuming sound velocity of 1800 m/s) on the Trøndelag Platform. Megasequence-2 has comparatively gentler clinoforms and its maximum thickness is approximately 710 ms TWT (c. 640 m) on the Nordland Ridge. Individual sequences make lenticular wedges and internal sequences have disrupted to chaotic and low amplitude reflections. Megasequence-3 has relatively more extended clinoforms which make oblique wedge. The maximum thickness of megasequence-3 is about 790 ms TWT (c. 710 m) in the Rås Basin. Megasequence-4 shows aggradation mainly and it thickens from the east to the west. The thickness of the megasequence-4 is about 330 ms TWT (c. 300 m) with the difference of 340ms TWT between URU and seabed. The sequence boundaries make downlaps against RDS and toplap against URU. Generally the sequences of megasequence-2 are thicker as compared to the other megasequences below URU (Fig. 4.2).

SB 1 coincides with RDS and forms the lower boundary of SS 1 and SB 2 makes its upper boundary. SB 2 is oblique and SS 1 is very thin. The clinothems show basinward progradation. The offlap breaks of SS 1 to SS 4 are preserved. The offlap breaks from SS 16-SS 18 are eroded. SS 16 makes downlaps above SB 16. SS 19-SS 20 show positive offlap break trajectory. SS 25-SS 28 are truncated against URU; consequently their offlap breaks are not preserved. SS 30 to 32 show mainly aggradation; nevertheless some downlap surfaces are found in SS 31. The seabed shows curvi-linear, cross-cutting lineations incising less than 10 m and look like troughs. Moreover ridges and channel-like bodies are found on seabed which will be discussed in chapter 5.

SS 4 shows a chaotic internal reflection pattern, SS 9 relatively high amplitude reflections, SS 11 and 15 disrupted reflections, SS 12 disrupted to irregular, and SS 18 shows high amplitude

reflections in the foreset and irregular to chaotic in the bottomset. In addition, SS 19 to 32 contain disrupted, irregular and chaotic internal reflections. Whereas the ridge-like feature is characterized by contorted to chaotic internal reflections (Fig. 4.2b). The seabed demonstrates cross-cutting furrow like features also illustrated in Fig. 4.2a.

4.1.2 Line B

This dip line is located north of line A and it is acquired along a distance of 405 km, extending from the Trøndelag Platform to the Lava Front (Fig. 3.1). The line B contains 30 sequences whereas SS 8 and SS 30 are missing which were not deposited or might have been eroded.

Prograding clinothems have oblique to sigmoid-oblique stratal configuration in megasequnec-1. The maximum thickness of megasequence-1 in line B is about 320 ms TWT (c. 290 m) in the Helgeland Basin. Megasequence-1 demonstrates the disrupted to chaotic, low amplitude reflections. SS 1 to 5 illustrate a progradational pattern with shingled clinoforms. Clinothems make downlaps with RDS. Megasequence-2 shows sigmoid-oblique clinothems (Fig. 4.3). Seismic sequences in megasequence-2 make sigmoidal wedge which is prograding westwards. Maxim thickness of megasequence-2 has been calculated as 760 ms TWT (c.690 m) in the Dønna Terrace. Internal reflections of sequences have low amplitude, disrupted and chaotic configuration. The downlaps are found in SS 16 above SB 16 (Fig. 4.3b). SS 12-20 demonstrate hummocky clinoform pattern following the underlying topography (Fig. 4.3a).

Megasequence-3 has a maximum thickness of almost 840 ms TWT (c. 760 m) in the Rås Basin. Megasequence-3 is characterized by sigmoid-oblique clinothems. Internal reflections have low amplitude and disrupted geometry. Some clinoforms have their offlap breaks preserved and internal reflections show low amplitude. SS 29 show markedly contorted to chaotic reflections. Maximum thickness of megasequence-4 is almost 250 ms TWT (c. 230 m) which was represented by 257ms TWT (two-way travel time). SS 31 demonstrates some prograding reflections.

Chaotic to contorted internal reflections are observed beneath ridge-like features in SS 32. The seabed has some morphological features inferred to represent erosional channels, iceberg plough marks and lateral moraine ridge (Fig. 4.3), see later in Discussion.

4.1.3 Line C

Line C is located to the north of the line B, and it extends up to 395 km from the Trøndelag Platform to the Lava Front (Fig. 3.1).

The Naust Formation is located stratigraphically above and west of the steeper clinoforms of the Molo Formation (4.4). There are 30 seismic sequences recorded along this line, whereas SS 9 and SS 30 are missing. Megasequence-1 has prograding clinothems with low amplitude, chaotic and disrupted reflections. Many clinoforms do not preserve their offlap breaks in this megasequence. The clinothems make sigmoid-oblique wedge. These seismic sequences have hummocky geometry in their foresets and bottomsets pointing towards processes of sliding, slumping and mud diapirs (Fig. 4.4d). Megasequence-1 has maximum thickness of about 230 ms TWT (c. 210 m) in the Helgeland Basin. The URU forms a broad channel-like depression above these sequences which shows aggraded infill (Fig. 4.4a). Megasequence-2 shows low amplitude, oblique, and parallel to sub-parallel clinothems. Maximum thickness of this megasequence is about 650 ms TWT (c. 590 m) on the Trøndelag Platform. SS 18 and SS 20 have their offlap breaks preserved; nevertheless, the offlap breaks of megasequence-3 have been truncated against URU (Upper Regional Unconformity).

The maximum thickness of megasequence-3 is almost 900 ms TWT (c. 810 m) in the Rås Basin. Sediments appear to have been bypassed the slope and deposited on the toe of SS 24-SS 28. SS 29 shows contorted reflections and there are homogeneous reflections on its base.

Megasequence-4 has maximum thickness of approximately 250 ms TWT (c. 230 m) and SS 30 is missing in this seismic line. There are onlap fill above channel-like feature of URU. There are some prograding reflections in SS 31 (Fig. 4.4b) and chaotic to contorted reflections in ridge-like features of SS 32 (Fig. 4.4c).

4.1.4 Line D

The line D extends from the Trøndelag Platform to the Lava Front, covering a distance of 402 km (Fig. 3.1).

This line contains all of the seismic sequences. Megasequence-1 exhibits from the RDS (Regional Downlap Surface) to SB 11. Maximum thickness of megasequence-1 is

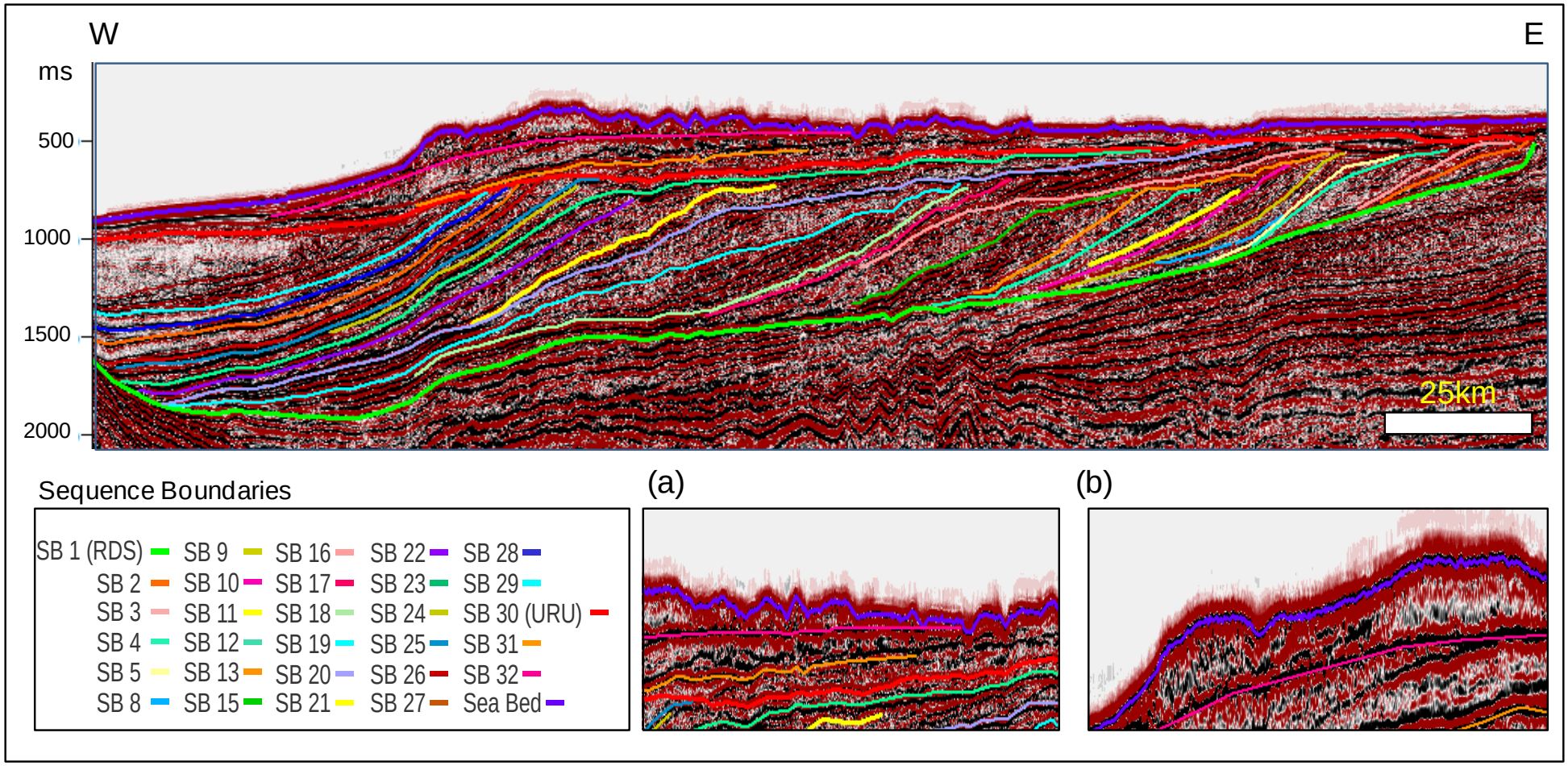

Figure 4.2 Seismic line A showing dominantly oblique to sigmoid-oblique wedges prograding westwards (a) cross-cutting furrows on the seabed (b) moraine ridge. SB 1 is coincident with RDS in east and SB 30 is coincident with URU.

approximately 420 ms TWT (c. 380 m) in the Helgeland Basin. The seismic sequences have oblique tangential clinothems and form wedges. SS 4 to 8 have internal clinoforms with mounded pattern in bottomsets (Fig. 4.5b). Clinoforms have not preserved their offlap breaks and reflections are chaotic and disrupted. The thickness of sediments increases in seismic sequences from east to west in the megasequence-2. Maximum thickness of megasequence-2 is almost 590 ms TWT (c. 530 m) and the clinoforms are sigmoid-oblique.

The reflections demonstrate aggradation and then progradation in megasequence-2. The internal reflections are low amplitude, chaotic and disrupted. SS 23-SS 25 demonstrate increased thickness in bottomsets which refer to the sediment bypass (Fig. 4.5d) and will be discussed in chapter 5. Megasequence-3 has maximum thickness of almost 860 ms TWT (c. 780 m) in the Rås Basin. There is an increased thickness in bottomsets of SS 23 and 25 (Fig. 4.5d). Chaotic to contorted reflections are present in SS 29. The Sklinnadjupet Slide is very clear in this seismic line (Fig. 4.5a). Megasequence-4 has maximum thickness of almost 600 ms TWT (c. 540 m) calculated by 600 ms TWT at the Skjoldryggen area. SS 30 reveals lenticular shape of seismic section as illustrated in Fig. 4.5c. SS 31 shows the prograding and aggrading reflections. There are channel-like features with disrupted internal reflections. SS 32 reveals mound-like structure in this seismic line (Fig. 4.5).

4.1.5 Line E

This seismic line extends from the Trøndelag Platform to the Lava Front and covers a distance of 401 km (Fig. 3.1).

This line contains 30 seismic sequences, whereas SS 10 and SS 11 are either eroded or were not deposited. Megasequence-1 has maximum thickness of about 360 ms TWT (c. 330 m) in the Helgeland Basin. The clinothems make oblique tangential geometry in this megasequence. Most of the clinoforms in the megasequence do not have their offlap breaks preserved and the sequences are truncated by URU. The URU contains a channel-like depression (which is 90 m deep and 180 m wide) in eastern part of Line E in the Helgeland Basin (Fig. 4.6). SS 4-SS 8 define mounded-like features in their toe ends. The internal reflections show mainly irregular and chaotic configuration.

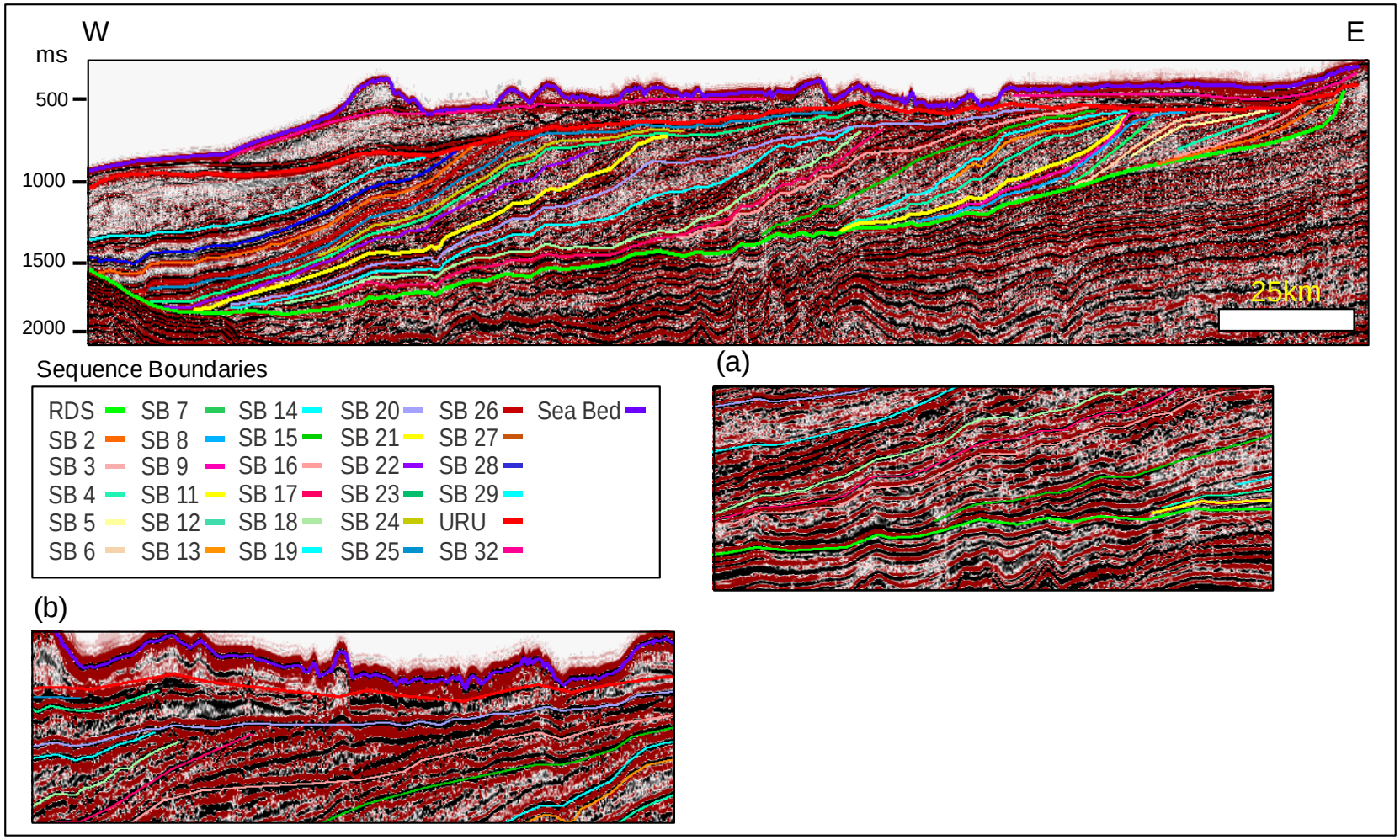

Figure 4.3 Seismic line B showing. Megasequence-1 with shingled progradational to sigmoidal clinothems (a) hummocky clinoforms in megasequence-2 and (b) prograded onlap fill making downlaps above SB 16 showing fall in relative sea level. See Fig. 4.2 for legends too.

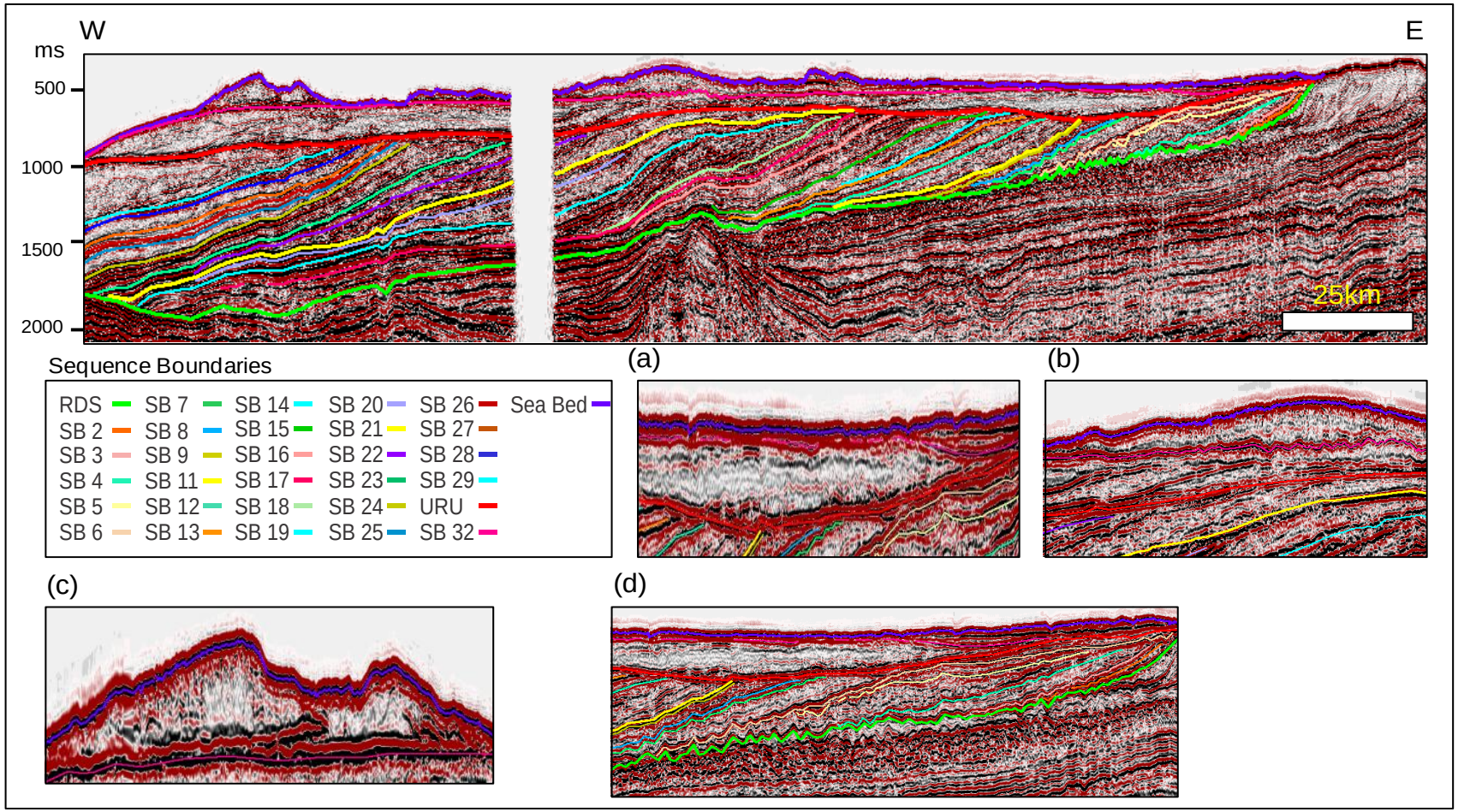

Figure 4.4 Seismic line C showing sliding and slumping in megasequence-1, (a) aggraded infill above channel in URU. (b) Prograding reflections in SS 31 (c) chaotic internal reflections in lateral moraine ridge in SS 32 and (d) hummocky clinoforms in foresets and bottomsets in megasequnece-1 indicating sliding and slumping and mud diapirs. See Fig. 4.2 for legends too.

Megasequence-2 starts from SB 13 because SS 11 is missing in this key line. The whole megasequence has clinoforms with oblique to sigmoid-oblique geometry. This megasequence forms a marked progradational wedge with an overall maximum thickness of about 660 ms TWT (c. 600 m). The internal reflections also have medium to low amplitude, irregular to disrupted pattern.

Megasequence-3 has maximum thickness of about 860 ms TWT (c.780 m) in the Vøring Basin, calculated from the difference between RDS and URU of 865 ms TWT (two-way travel time). There is an increased sediment thickness in the bottomset of SS 26 and SS 28 (Fig. 4.6c). The amplitude of the clinoforms is high whereas internal reflections have low amplitude. SS 29 shows contorted and chaotic reflections (Fig. 4.6a). Megasequence-4 has a maximum thickness of about 330 ms TWT (c. 300 m) in this seismic line. SS 30 makes a lense, and the internal reflections are disrupted. A channel incising the underlying sequences is shown in Fig. 4.6 b. SS 31 reveals some progradational reflections and mainly aggradational stacking pattern. The ridge-like and channel-like structures as well as curvi-linear furrows are found on the seabed formed during the last glacial age (Weichselian).

4.1.6 Line F

The seismic line F extends from the Trøndelag Platform to the Lava Front, a distance of 431km (Fig. 3.1).

The seismic line contains all 32 sequences. Megasequence-1 shows maximum thickness which is almost 440 ms TWT (c. 400 m) in the Helgeland Basin. The clinoforms are parallel to sub-parallel and oblique tangential. Many of the offlap breaks are not preserved in megasequence-1, whereas SS 2 and SS 10 have preserved their offlap breaks.

Maximum thickness of megasequence-2 is about 600 ms TWT (c. 540 m) in the Vøring Basin. The offlap breaks of several clinoforms are preserved. SS 11-SS 20 generated the descending (negative) offlap break trajectory, likely representing fall in relative sea level (see Discussion).

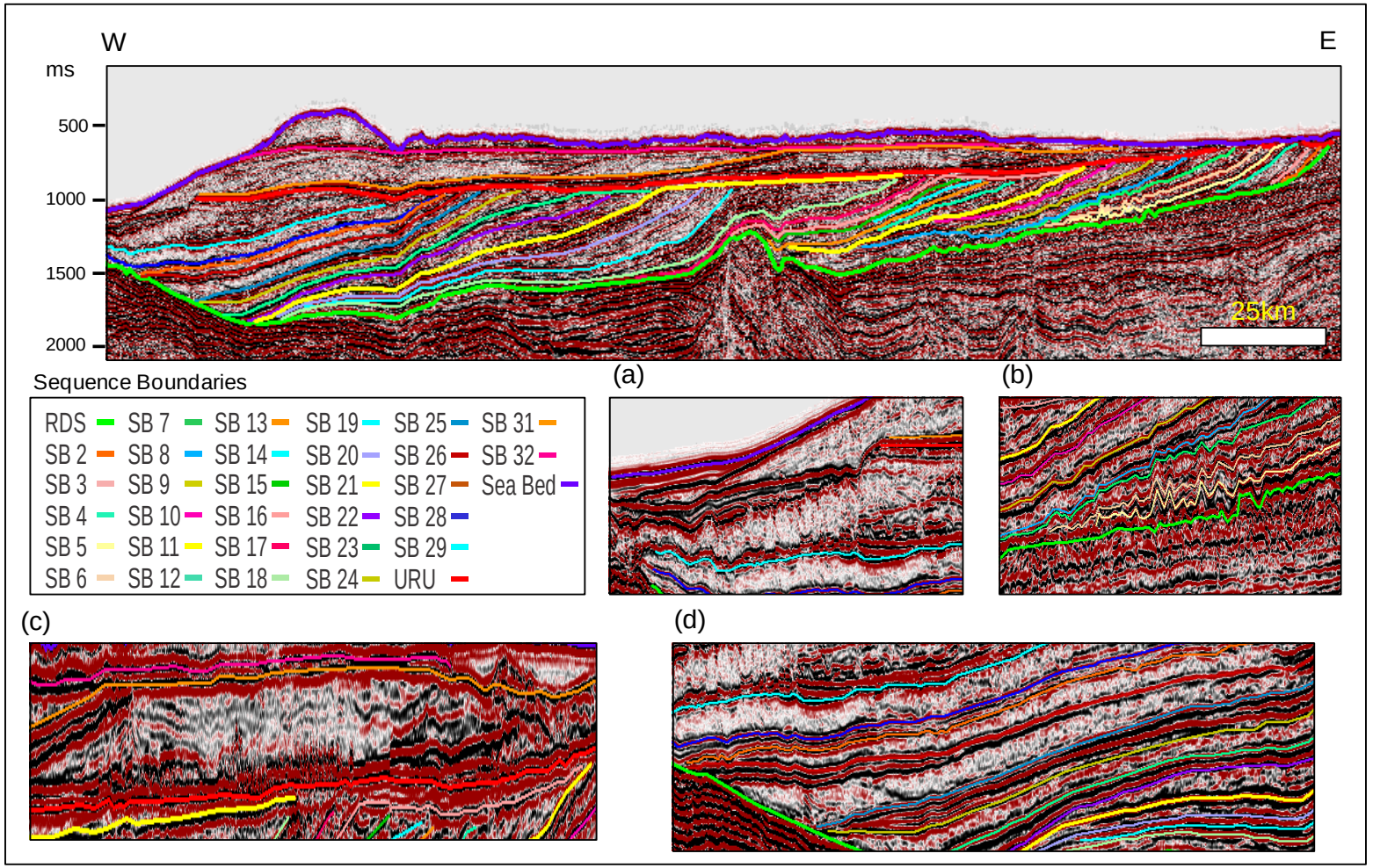

Figure 4.5 Seismic line D illustrating the section extending from east to west on mid Norwegian shelf. (a) The slide headwall of the Sklinnadjupet Slide in SS 29 (b) megasequence-1 showing sliding and mud diapirs (c) SS 30 forming lense and (d) SS 23 to 25 showing sediment-bypassing. See Fig. 4.2 for legends too.

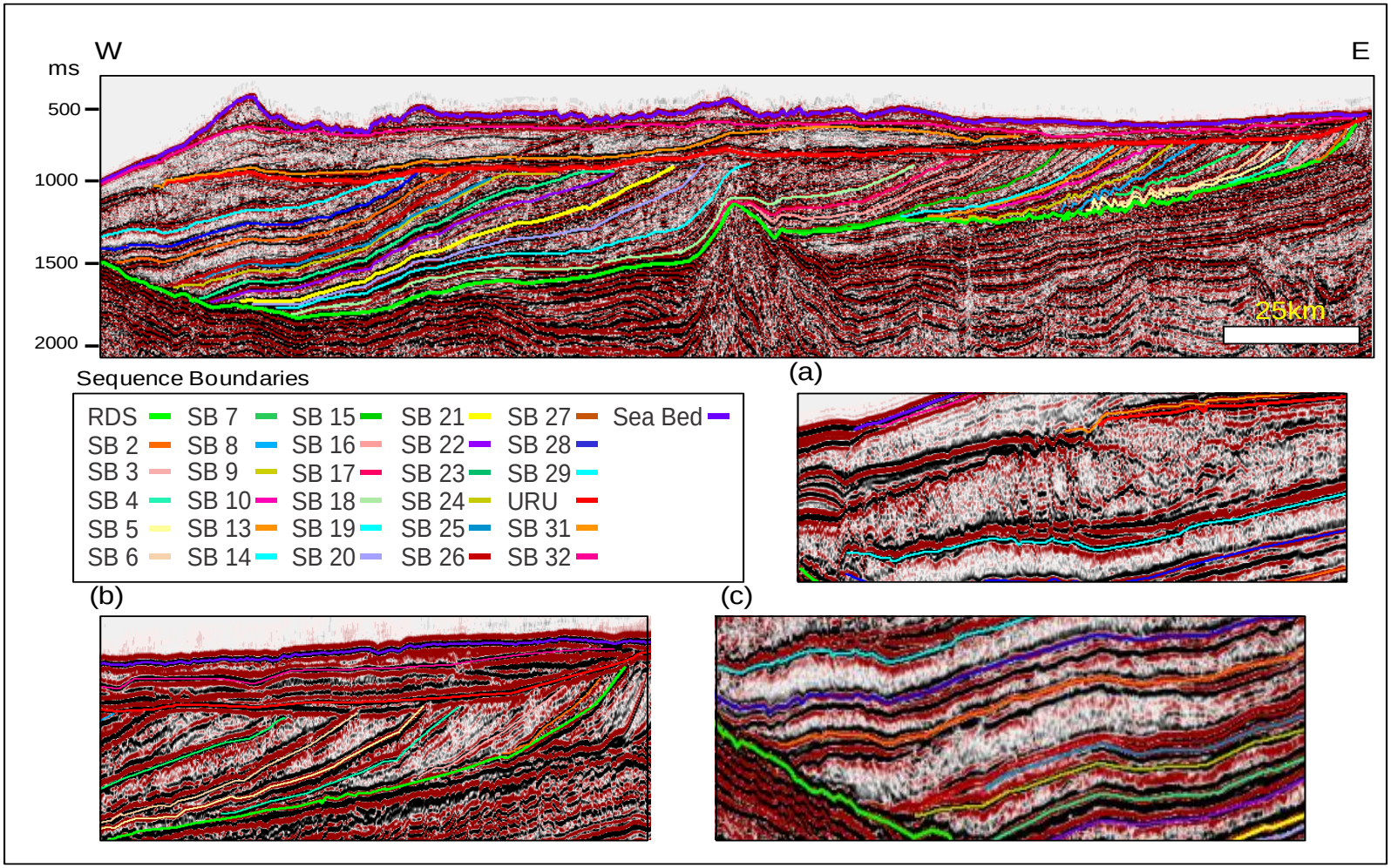

Figure 4.6 Seismic line E illustrating the mounded pattern of the clinoforms of megasequence-1 and channel in URU above megasequence-1. (a) contorted and mounded reflections of SS 29 (b) Channel in SS 30 (c) increased thickness in bottomsets of SS 26 and SS 28. See Fig. 4.2 for legends too.

Megasequence-3 has a maximum thickness of approximately 830 ms TWT (c. 750 m). There is an ascending offlap break trajectory between SS 12-SS 14. The clinoforms have high amplitude in megasequence-3, whereas internal reflections become chaotic particularly in the bottomsets. The sequences show oblique clinoforms. The Sklinnadjupet Slide is observed east of the Helland-Hansen Arch (Fig. 4.7b).

The maximum thickness of megasequence-4 is 330 ms TWT (c. 300 m). SS 30 demonstrates lenticular geometry. The internal reflections are chaotic. SS 31 shows some progradational reflections. SB 32 forms a major sequence boundary and the internal reflections are disrupted and chaotic. There are found crescentic ridges in SS 32 in the eastern part of this seismic line (Fig. 4.7a). The seabed reveals depression-like features and ridges with internal contorted reflections (Fig. 4.7). Mud diapir is observed on the seabed west of the Helland-Hansen Arch as depicted in Fig. 4.7c.

4.1.7 Line G

This is the reference line in the present study. The line extends from the Trøndelag Platform to the Lava Front, covering a distance of 447 km (Fig. 3.1).

The seismic line includes all of the identified 32 sequences. Maximum thickness of megasequence-1 is 550 ms TWT (c. 500 m) in the Trøndelag Platform. The clinoforms are parallel to sub-parallel and have sigmoid- oblique profile. The offlap breaks of SS 3, 7 and 10 are preserved in megasequence-1. The offlap break trajectory is ascending between SS 2 and 4 (Fig. 4.8). A descending, negative offlap break trajectory occurs between SS 6 and 7, and again an ascending offlap break trajectory between SS 10 to 12 (Fig. 4.8). The offlap breaks of SS 15 to 19 are not preserved. The topset beds are truncated by URU.

Megasequence-2 has maximum thickness of about 720 ms TWT (c. 650 m) in the Vøring Basin. The clinoforms of megasequence-2 have sigmoid-oblique profile. The internal reflections of megasequence-2 are low amplitude, irregular, disrupted and chaotic. There are toplap truncations against URU. The offlap breaks of SS 11 are truncated against SB 13. Thickness of sequences in megasequence-2 is relatively more as compared with sequences of other megasequences (see for discussion in chapter 5).

Megasequence-3 has a maximum thickness of 1080 ms TWT (c. 980 m) east of the Helland-Hansen Arch. There is aggrading stacking pattern between SS 21-SS 22. The clinoforms have high amplitude in megasequence-3 whereas the internal reflections have amplitude and are disrupted to chaotic. The clinothems are characterized by oblique tangential profile and form wedge prograding basinwards. SB 29 makes major sequence boundary against which SS 23-SS 28 are truncated.

Maximum thickness of megasequence-4 is about 310 ms TWT (c. 280 m). SS 30 show lensoid geometry (Fig. 4.8). SS 31 has irregular, low amplitude and chaotic reflections. The internal reflections of the SS 32 are chaotic to contorted. The seabed shows ridges and channel-like depressions which are further discussed in chapter 5.

4.1.8 Line H

The seismic line H extends from the Trøndelag Platform to the Lava Front and covers a distance of 448 km (Fig. 3.1).

This line consists of 31 seismic sequences while SS 31 is missing. Maximum thickness of megasequence-1 is 570 ms TWT (c. 520 m) in the Trøndelag Platform. The clinothems correspond to oblique to sigmoid-oblique profile. Many of the clinoforms in this sequence have preserved offlap breaks. The internal reflections are low amplitude, irregular and chaotic. Clinothems demonstrate ascending offlap break trajectory followed by the descending and the ascending again.

Megasequence-2 starts from SS 11, and the whole megasequence has clinothems with sigmoid-oblique geometry. The reflections are progradational followed by an aggradational stacking pattern of the sequences, forming the complete megasequence wedge with a maximum thickness of about 770 ms TWT (c. 700 m) in the Træna Basin. The sequence boundaries do not show the normal succession as SS 16 is underlain by SS 17 and overlain by SS 18 (Fig. 4.9). This abnormal succession was picked during tying with strike line L and a random strike line. This change in succession represents the inter-fingering of sequences deposited adjacent to each other, probably by separate ice streams coming from various directions. Another reason of this inter-fingering due to ice streams is proved that the URU was continuous above inter-fingered sequences in a trough indicating that the trough was not formed during erosion at level of URU (see Discussion chapter).

Megasequence-3 has a maximum thickness of almost 1130 ms TWT (c. 1020 m) calculated by the difference between RDS and URU of 1132 ms TWT in the Vøring Basin. The clinoforms reveal high amplitude, whereas internal reflections have low amplitude and are disrupted to chaotic. SS 29 is characterized by contorted and mounded reflections.

Megasequence-4 has a maximum thickness of about 250 ms TWT (c. 230 m) in this seismic line. SS 30 makes a lensoid geometry and shows disrupted, aggrading internal reflections. Furthermore, SS 30 contains a ridge-like feature (Fig. 4.9a) which is discussed further in chapter 5. SS 31 has contorted internal reflections and the sea bed shows mounds, ridges and cross-cutting furrows formed by the last glacial age (Weichselian) (see chapter 5).

4.1.9 Line I

This dip line lies north of line H and it is acquired along 439 km distance. This seismic line extends from the Trøndelag Platform to the Lava Front (Fig. 3.1). This line contains 28 seismic sequences however SS 9, 12, 17 and 31 are missing.

The maximum thickness of megasequence-1 in seismic line I is 570 ms TWT (c. 520 m). Internal reflections are low amplitude, irregular and disrupted to chaotic (Fig. 4.10). Megasequence-1 shows oblique tangential to sigmoid-oblique profile of clinothems with westward progradation. There is ascending offlap break trajectory between SS6 and SS 7 as illustrated in Fig. 4.10a. Megasequence-2 indicates disrupted to chaotic reflections. However, there are some high amplitude reflections in the bottomsets. This sequence shows sigmoid-oblique clinoforms. The sequence boundaries are not truncated against URU abruptly and offlap breaks have been preserved to a certain limit. Maximum thickness of this megasequence is 810 ms TWT (c. 730 m) in the Træna Basin.

Whereas maximum thickness of megasequence-3 is about 1210 ms TWT (c. 1090 m) and clinothems reveal sigmoid-oblique profile. The clinoforms show high amplitude though

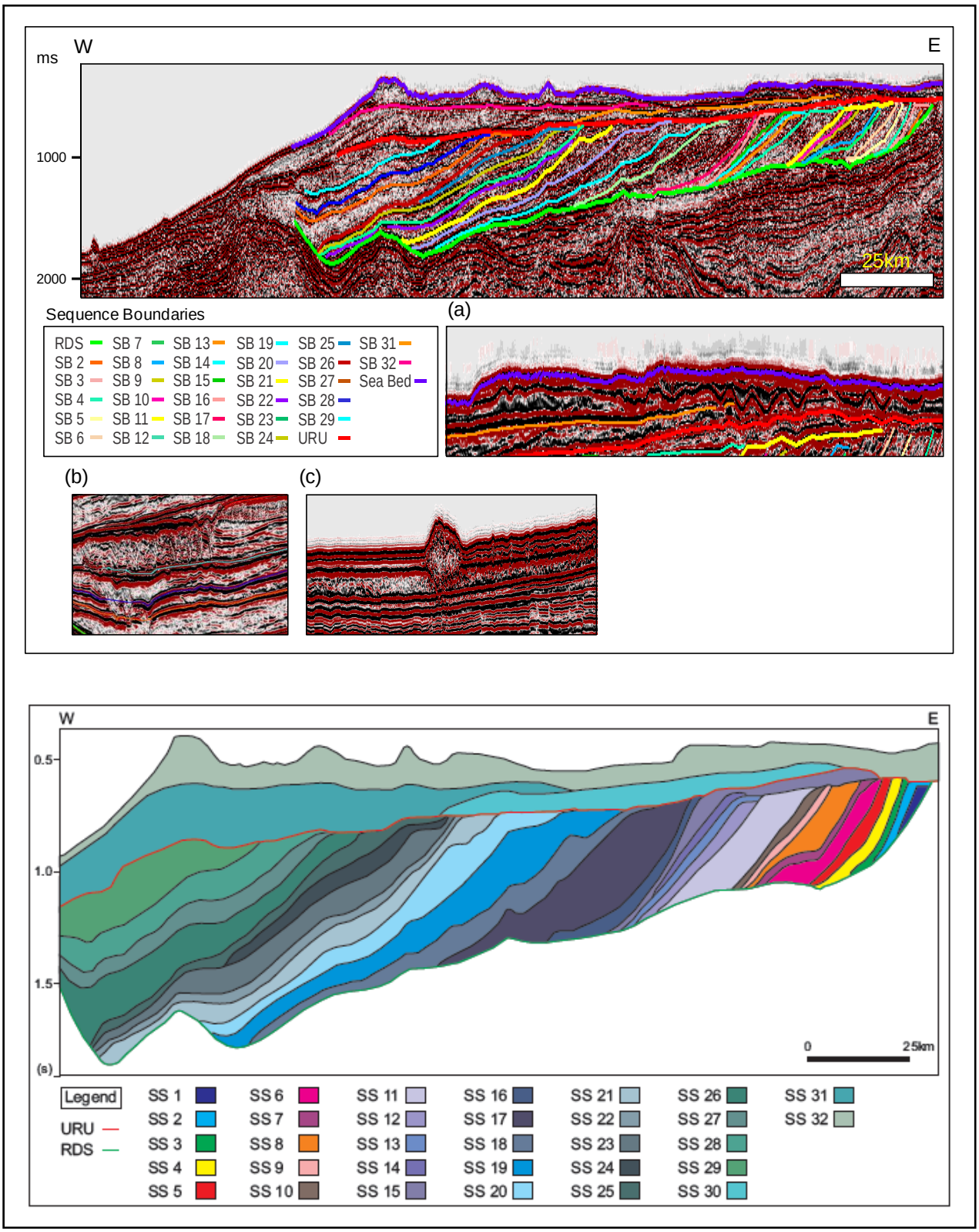

Figure 4.7 Seismic Line F and its cross-section, ascending offlap break trajectory between SS 23-SS 24 in megasequence-3. (a) crescentic ridges in SS 32 (b) Sklinnadjupet Slide east of the Helland-Hansen Arch and (c) mud diapir. See Fig. 4.2 for legends too.

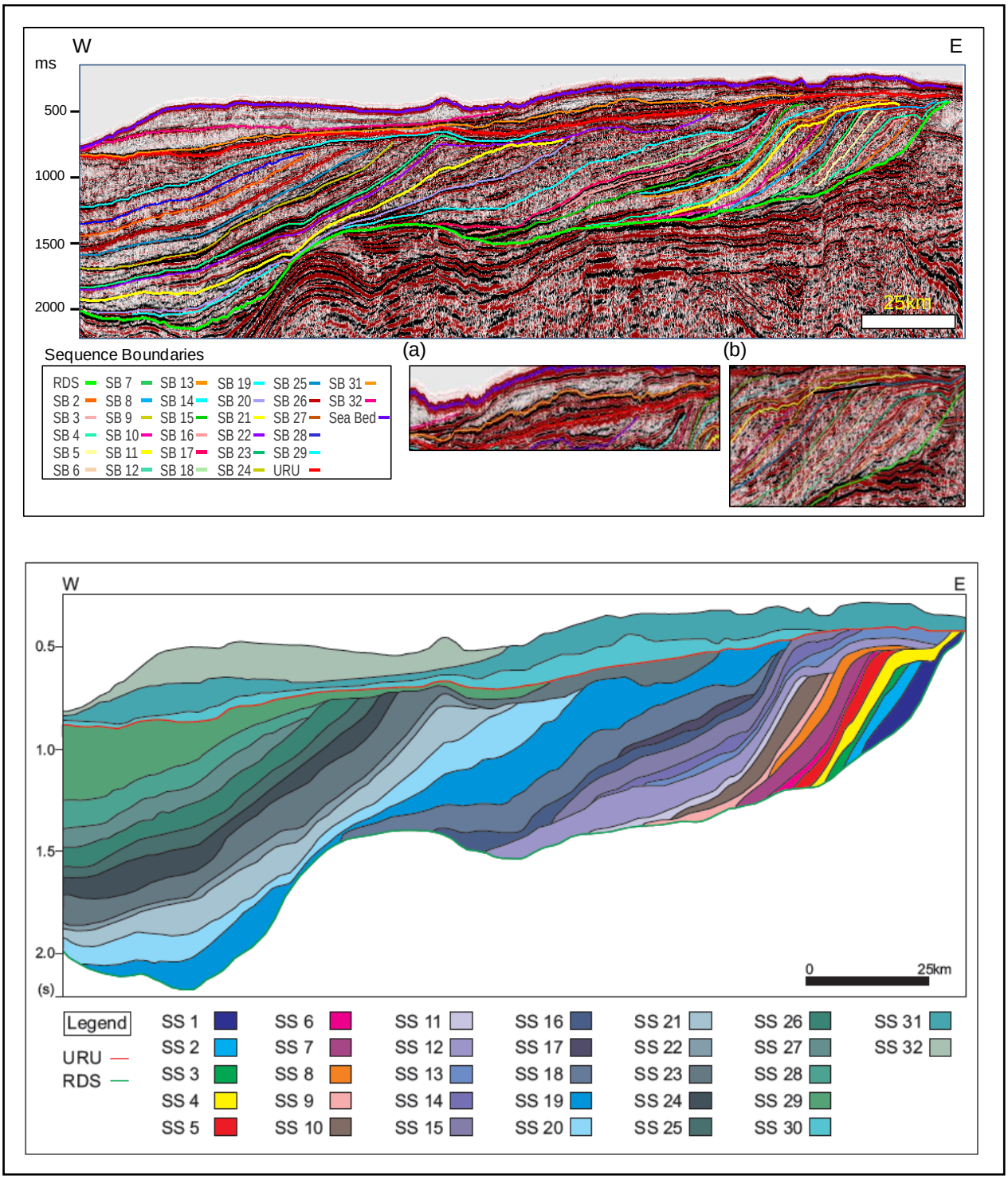

Figure 4.8 Seismic Line G along with its cross-section illustrating oblique to sigmoid-oblique clinoforms of megasequence-1 having positive and then negative offlap break trajectory. (a) lense in SS 30 (b) descending offlap break trajectory between SS 7-SS 10. See Fig. 4.2 for legends too.

beds of SS 21-SS 23 have their offlap breaks preserved. Topset bed of SS 28 is also preserved. SB 29 forms a major sequence boundary and SS 24-SS 28 make toplaps with SB 28. SS 30 shows chaotic to contorted internal reflections. The sequences above the URU demonstrate aggradation and the internal reflections are predominantly contorted and chaotic.

The shelf and clinoforms become steeper towards the north and the offlap breaks of megasequences-2 and 3 are also preserved as displayed in Fig. 4.11.

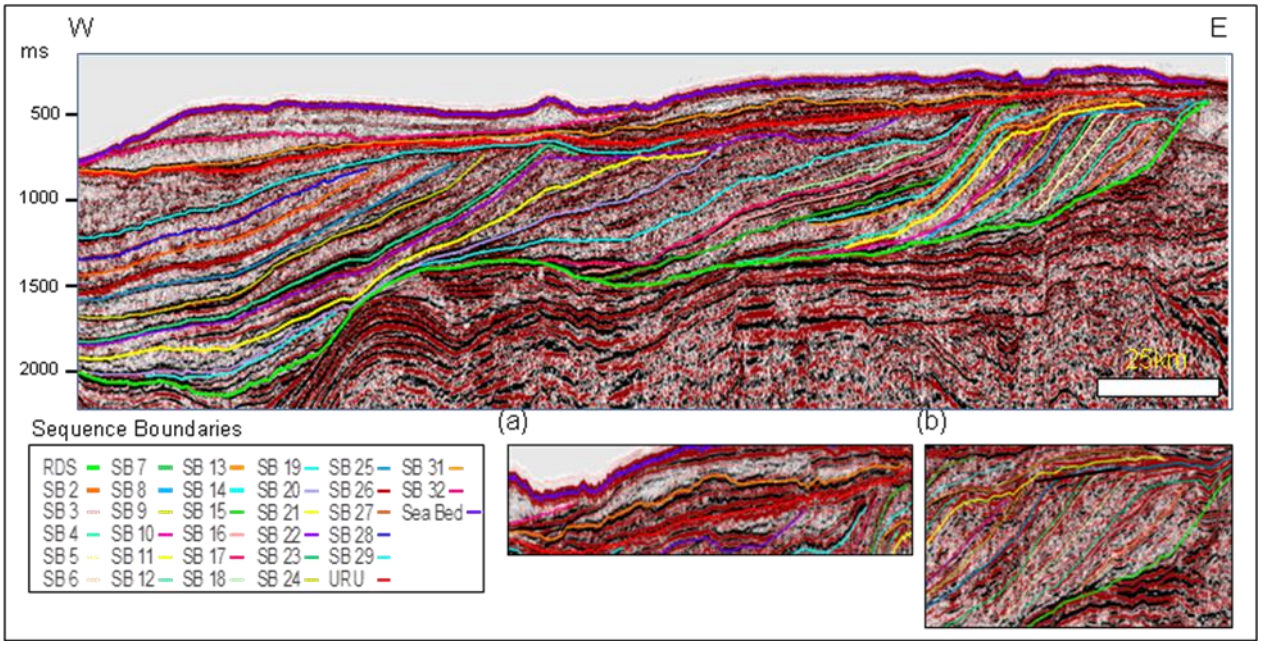

Figure 4.9 Seismic Line H showing sigmoid-oblique wedge of megasequence-1 prograding towards west, sigmoid wedge of megasequence-2 and oblique tangential wedge of megasequence-3. (a) showing ridge in SS 30. See Fig. 4.2 for legends too.

4.1.10 Line J

The strike line J is extending up to 495 km (Fig. 3.1), starting from the Vøring marginal high to the Froan Basin. The sequences become younger towards the north.

Megasequence-2 starts from SB 18 in south as displayed in Fig. 4.12. Maximum thickness of this megasequence is 730 ms TWT (c. 660 m). The reflections are disrupted to chaotic and they prograde northwards (Fig. 4.12). The clinothems prograde from east to the west in dip lines and from south to north in the strike lines suggesting that the sedimentary succession

prograded from SE to NW. The reflections make toplaps against URU and downlap against the RDS.

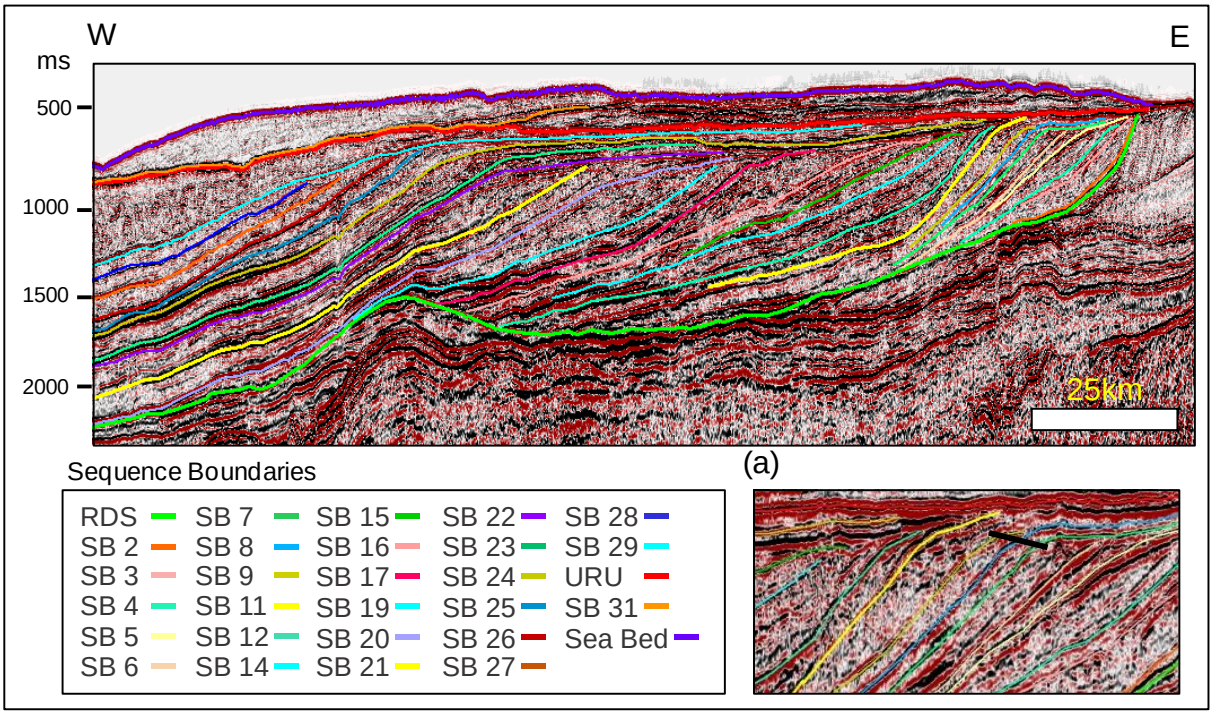

Figure 4.10 Seismic Line I illustrating oblique tangential to sigmoid-oblique clinoforms in megasequence-1, sigmoidal clinoforms in megasequence-2 and sigmoid-oblique clinoforms in megasequence-3. (a)The ascending offlap break trajectory between SS 6 and SS 7 is illustrated. See Fig. 4.2 for legends too.

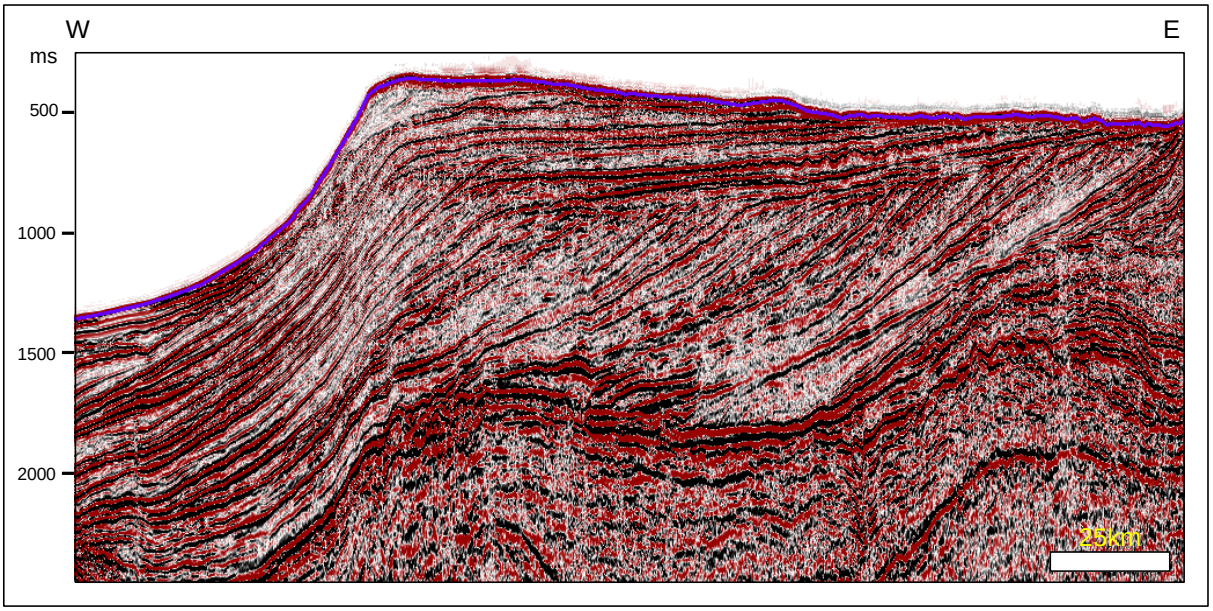

Figure 4.11 Random Seismic Line is one of the northern most of the lines in data showing the steeper shoreline along with steeper and preserved clinoforms.

Megasequence-3 has a maximum thickness of almost 1060 ms TWT (c. 960 m). The clinoforms have high amplitude. Nevertheless, the internal reflections are disrupted to chaotic. SS 29 has contorted internal reflections. Maximum thickness of megasequence-4 is about 350 ms TWT (c. 320 m). SS 30 makes a lenticular symmetry (Fig. 4.12a). Some prograding reflections are observed in SS 31 and SS 32 in the northern part of this seismic line as shown in Fig. 4.12. The low amplitude internal reflections are chaotic and disrupted in SS 31and SS 32. SS 31 demonstrates valley-like features which will be discussed in chapter 5. The seabed contains the ridges, channel-like depressions and cross-cutting furrows.

4.1.11 Line K

The strike line K is 463 km long; it runs north-south and extends from the Vøring Basin to the Froan Basin. This seismic line is located east of the previous line (Fig. 3.1). The sequences become younger towards north.

In the south megasequence-2 starts from SB 15 and the maximum thickness of this megasequence is almost 630 ms TWT (c. 570 m) (Fig. 4.13). The internal reflections are disrupted to irregular and chaotic and reveal northward progradation. The clinothems make wedge and downlaps against the RDS in the Nordland Ridge.

Megasequence-3 has a maximum thickness of approximately 910 ms TWT (c. 820 m). The clinoforms have high amplitude. Nevertheless, the internal reflections are chaotic. There is a channel-like feature along SS 20 which is incising underlying sequences. Maximum thickness of megasequence-4 is about 300 ms TWT (c. 270 m) and SS 30 makes lenticular geometry. SS 31 and 32 contain some prograding reflections. The internal reflections are chaotic in SS 31and SS 32. The reflections below the ridges are contorted. The seabed contains ridges, channel-like features and cross-cutting furrows (Fig. 4.13).

4.1.12 Line L

The strike line L covers a distance of 252 km, it runs north-south, extending from the Vøring Basin to the Trøndelag Platform. This seismic line is located east of the previous line (Fig. 3.1).

Megasequence-1 starts from SB 1 in the south. Maximum thickness of megasequence-1 is almost 350 ms TWT (c. 320 m) in the Helgeland Basin. The clinoforms have high

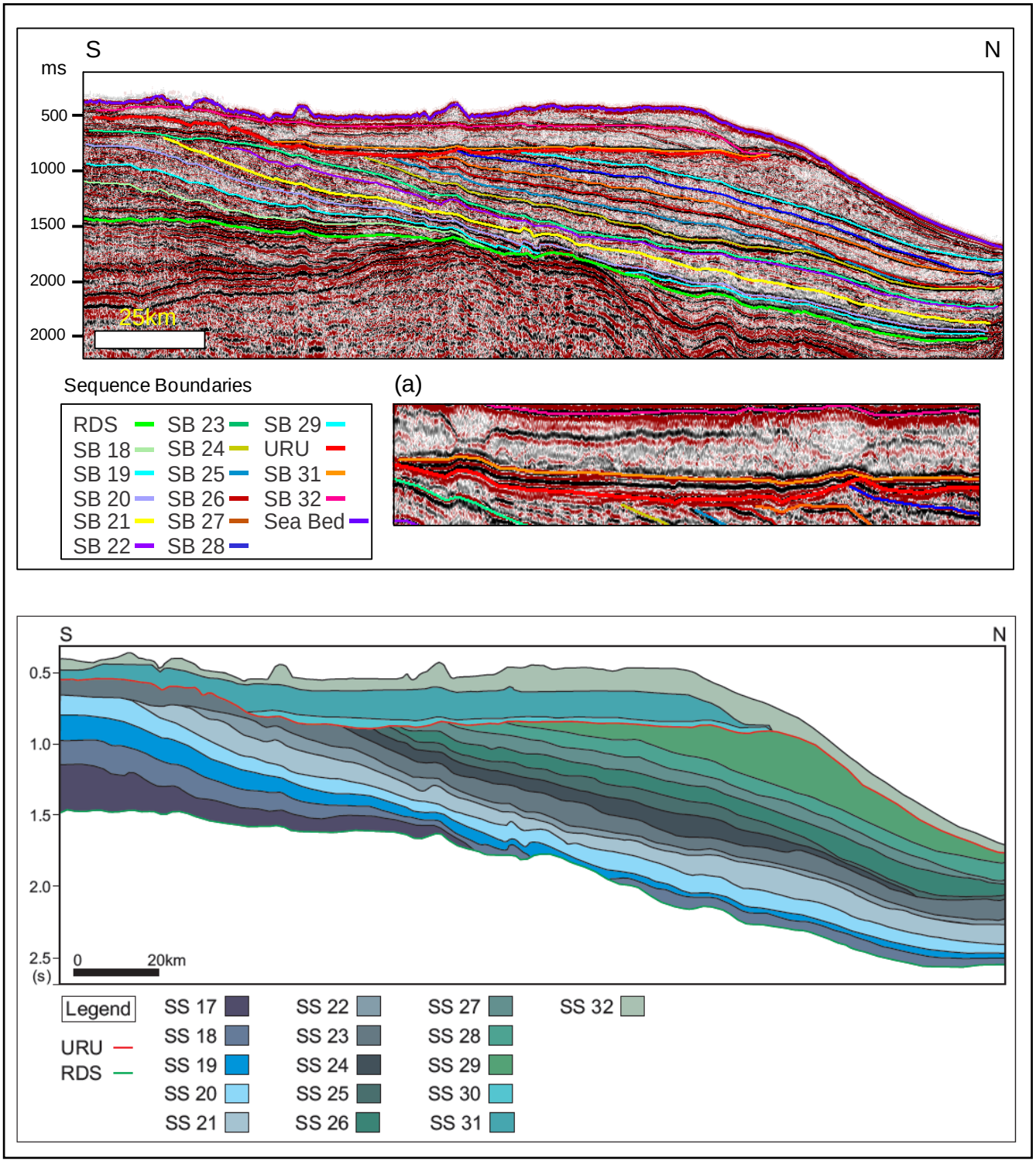

Figure 4.12 Seismic Line J together with its cross-section illustrating progradation. (a) SS 30 illustrating lense. See Fig. 4.2 for legends too.

amplitude; however the internal reflections are irregular, disrupted to chaotic. Clinothems make a wedge and reveal a northward progradational stacking pattern. The reflections downlap against the RDS and make toplap with the URU.Megasequence-2 has a maximum thickness of about 740 ms TWT (c. 670 m). The internal reflections are disrupted to chaotic. There are wedges in megasequence-2 which are building out northwards and southwards (Fig. 4.14). The reflections are inter-fingering in a trough in the Træna Basin as shown in Fig. 4.14. The URU defines a big channel-like structure which has incised underlying sequences (Fig. 4.14). Maximum thickness of megasequence-3 is almost 130 ms TWT (c. 120 m). While thickness of megasequence-4 is about 270 ms TWT (c. 250 m). The reflections are aggrading in SS 30 and the reflections make the onlapping fill in the channel-like structure. The sea bed contains the ridges and channel-like feature. Several crescentic ridges are found in SS 32 (Fig. 4.14) (for detail see chapter 5).

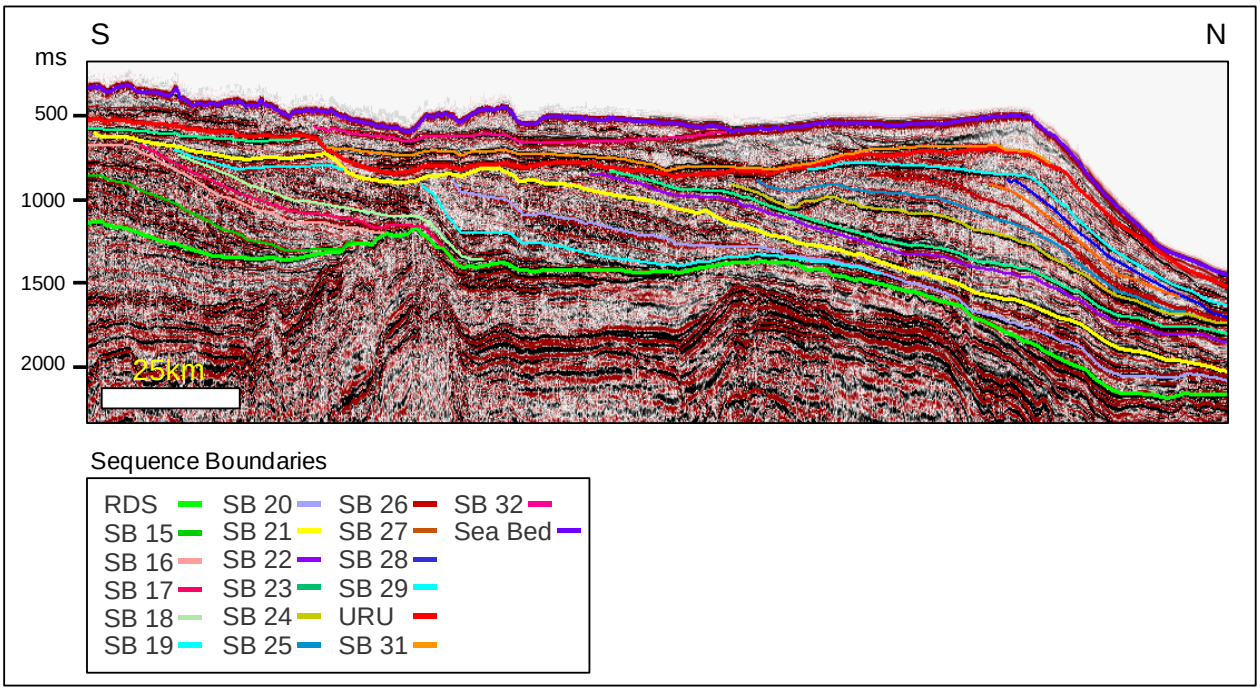

Figure 4.13 Seismic Line K illustrating progradation development towards north. The clinoforms show collectively oblique to sigmoidal wedges. See Fig. 4.2 for legends too.

4.2 Seismic Sequence Analysis

The prograding wedges of four megasequences are interpreted to have been formed from deposition of glacigenic detritus of Pliocene-Pleistocene ice sheets that moved from mainland Norway in the east into a rather deep marine basin in the west (Dahlgren et al.,

2005; Ottesen et al., 2005). In the mountainous hinterland area to the east, glacial ice eroded and huge amounts of debris were transported in ice streams down to the coastal lowland. At the edge towards the deep water basin, the ice sheets broke up and produced ice berg along a calving front (Dowdeswell et al., 2010; Graham et al., 2011). Through repeated glacial-interglacial cycles the shelf was widened by the accretion and procreation of new sediment wedges. Clastic wedges formed during individual glacial periods when ice sheets entered the shelf and sediments were deposited at the ice front and beneath floating ice sheets.

The clastic wedges thus formed glacial sequences enveloped by sequence boundaries formed as unconformities by glacial erosion in areas where the ice sheet was grounded and by surfaces representing low rate of sedimentation in interglacial periods in the marine realm at and ahead the ice front (Dahlgren et al., 2005; Rise et al., 2005, 2010). Internal clinoforms of individual sequences represent depositional events, interrupted by events or periods of reduced rate of sedimentation. The clastic wedges and sequences are formed with largely sigmoidal to oblique sigmoidal geometry as a result of reducing rate of sedimentation basinwards from the ice front. The bottomsets of the clinothems downlap onto the RDS. Offlap breaks get preserved when the ice sheet is floating at the front. Clinothem topsets have been preserved when the next ice was floating across the shelf with sediments aggraded beneath the ice sheet. Topsets and offlap breaks were truncated when the next ice sheet was grounded and eroded, as typically beneath the URU.

Factors controlling deposition or erosion from the glacier ice sheets depended on a series of factors, such as (1) ice sheet thickness and ice stream flow rate, (2) amount of glacial debris transported by the glacial ice, (3) rate and amount of fall and rise in glacial eustacy, and (4) changes in water depth due to tectonic/isostatic subsidence and sediment compaction.

The seismic features formed by the dynamic sedimentation during glacial periods and the following interglacial periods assisted to interpret the depositional environments, existence and extension of the ice sheets and ice streams and the sediment provenance. This will be further described and discussed below.

4.2.1 Seismic Sequence 1 (SS 1)

Characteristics

This thin seismic sequence contains parallel to sub-parallel reflections. SB 1 forms its lower boundary (coincident with RDS) and the upper boundary is SB 2. SB 2 makes concordant relationship with this sequence. The clinoform geometry is oblique in south and becomes oblique tangential in north as illustrated in seismic lines A-I (Figs. 4.2-4.10). The topset beds and offlap breaks are not preserved and are truncated by URU. The low amplitude internal reflections are irregular and chaotic. SS 1 thickens from south to north as displayed in seismic line A-I (Figs. 4.2-4.10).

Interpretation

SS 1 along with rest of megasequence-1 demonstrates the continuous depositional environment. In most of the interpreted lines this sequence represents the parallel to sub-parallel reflection configuration indicating the uniform rates of deposition on a shelf with uniform subsidence or a stable basin plain settings. The divergent geometry of the reflections is in accordance with the lateral outbuilding.

The foreset and the bottomset represent the hummocky reflection geometry indicating that debris flow deposits were accumulated e.g. found in the lines C-E (Figs. 4.4-4.6). The offlap breaks are not preserved indicating a grounding ice sheet, either by erosion from the contemporaneous ice sheet or from the next or/and later ice sheets.

4.2.2 Seismic Sequence 2 (SS 2)

Characteristics

SS 2 is bounded by SB 2 on base and SB 3 on its top. SB 2 and SB 3 have concordant relationship with each other. SS 2 thickens and becomes oblique to oblique tangential from

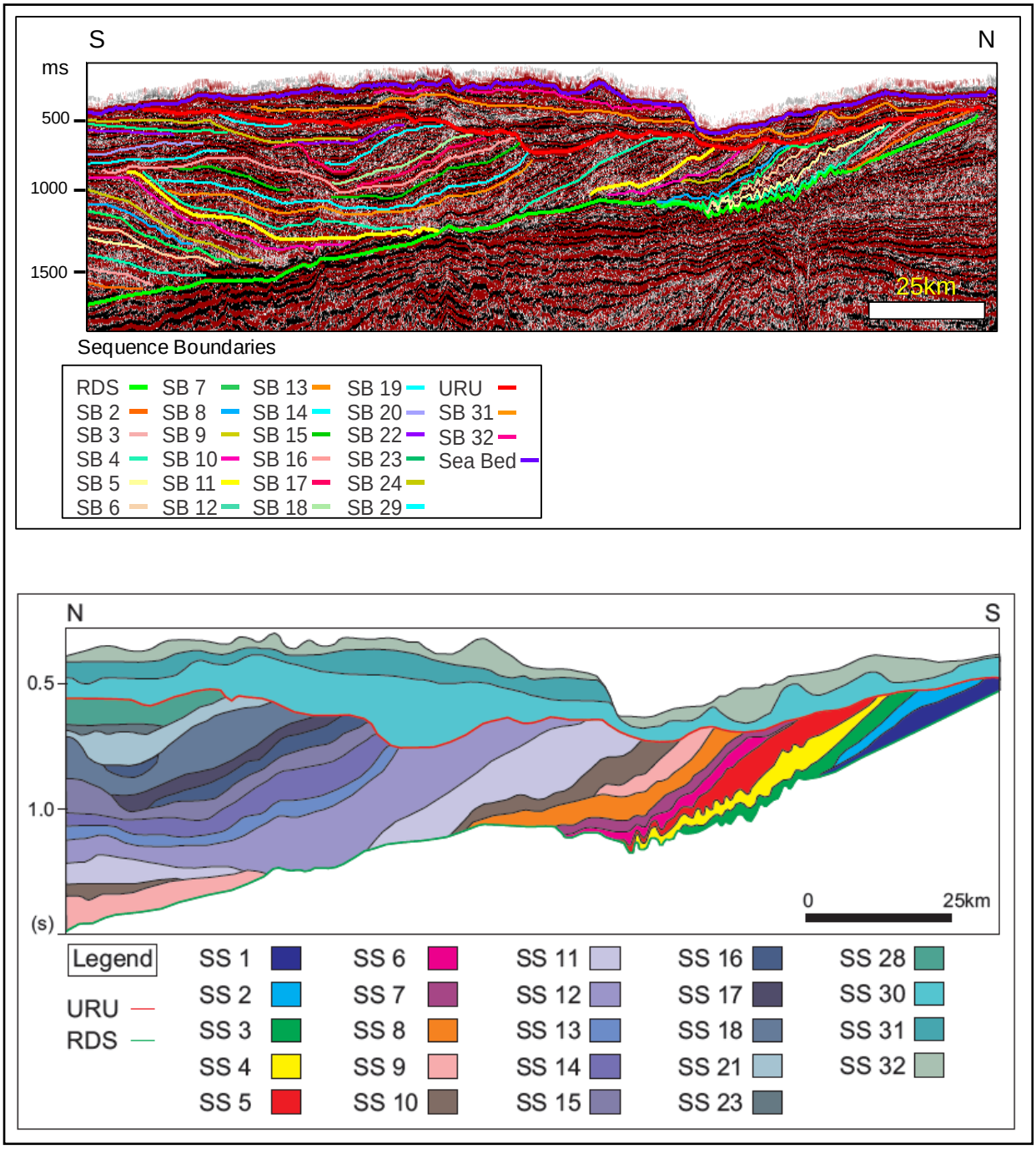

Figure 4.14 Seismic Line L illustrating inter-fingering of SS 16, 17 and 18 and wedges building out towards north and south. See Fig. 4.2 for legends too.

south to north as illustrated in seismic profiles A-I (Figs. 4.2-4.10). This seismic sequence is characterized by low amplitude, parallel to sub-parallel, chaotic and disrupted internal reflections. Oblique geometry in southern seismic lines is confirmed with evidence that topset beds are truncated against the URU nevertheless topset beds are preserved in many

seismic lines lying in north. SS 2 progrades westwards in seismic dip lines and northwards in strike lines making wedge. Reflections downlap against RDS making gentle angles.

Interpretation

The homogeneous sediments illustrate glacial sediments representing till, debris flow and slide deposits (Dahlgren et al., 2005). Parallel to sub-parallel geometry reveals the uniform depositional rates. The reflections outbuild in the northwest direction as displayed in seismic lines A-I (Figs. 4.2-4.10).

4.2.3 Seismic Sequence 3 (SS 3)

Characteristics

SB 3 makes its lower boundary and SB 4 bounds it from top. SB 3 and SB 4 have concordant relation. SS 3 makes a wedge prograding westwards in dip lines and northwards in strike lines. Clinothems become oblique to oblique tangential form south to north as depicted in seismic line A-I (Figs. 4.2-4.10). SS 3 shows thinning towards north. Topset beds are not preserved in SS 3 in most of seismic lines and are truncated by the URU. Reflections downlap with RDS making gentle angles. Internal reflections are low amplitude, parallel to sub-parallel, disrupted and chaotic.

Interpretation

As far as disrupted and chaotic reflections are concerned they are related to glacial and interglacial environment and are known to be generated through multiple lobes (Dahlgren et al., 2005) of debris flow on the outer shelf. They correspond to the transparent seismic facies on the seismic as depicted in key line E (Figs. 4.18).

4.2.4 Seismic Sequence 4 (SS 4)

Characteristics

SS 4 is bounded by SB 4 on its base and SB 5 on its top. SB 4 and SB 5 are concordant to each other. The offlap breaks are not preserved on most of the lines. The reflections make downlaps with RDS and toplaps with URU. The seismic unit contains parallel to sub-

parallel, low amplitude, disrupted and chaotic reflections. Clinoforms in this seismic sequence are oblique and demonstrate hummocky pattern in its foreset ad bottomset e.g. seen in lines C, D and E (Figs. 4.4-4.6).

Interpretation

The mounded reflections present in foreset and bottomset of SS 4 indicate debris flow deposits (Berg et al., 2005) and acoustically transparent facies (as illustrated in part of seismic section E in Fig. 4.18). The rate of the sedimentation was high during the deposition of the earlier deposited sequences as revealed by local sliding found on lines C, D and E (Figs. 4.4-4.6).

Mud diapirs (Hjelstuen et al., 2004b) have also caused the mounded pattern in this sequence (Fig. 4.18). Glide planes are supposed to have been provided by stratified deposits of hemipelagic or contouritic sediments (Dahlgren et al., 2005). Hemipelagic or pelagic sediments are interpreted to have provided planes for sliding and slumping of glacial debris from the ice sheet front into deeper water. The mounded, hummocky clinoforms represent acoustically transparent facies likely and it is noteworthy to mention that they are formed by glacigenic debris flows.

4.2.5 Seismic Sequence 5 (SS 5)

Characteristics

SS 5 is bounded by SB 5 on its base and SB 6 on its top. The clinoforms are oblique and topset beds are not preserved in southern lines however topset beds are not truncated by URU abruptly in northern seismic lines, for instance line I (Fig. 4.10). Internal reflections are disrupted and chaotic, furthermore make downlaps with RDS. Reflections show sediment progradation towards northwest, as interpreted with help of the strike and dip lines. The internal reflections are mounded and show hummocky pattern on foresets and bottomsets (Figs. 4.4-4.6 and 4.18). In addition, intensity of hummocky pattern increased from south to north as displayed in lines C and D to E.

Interpretation

The mounded reflections illustrate glacigenic debris flows and acoustically structureless facies represent slide debrites (Fig. 4.21). The high rate of debris flow sedimentation is thought to have been triggered by rapid accumulation of fine-grained material with high pore water content at the ice front. This generated slide and debris flows in addition with the hemipelagic or contouritic sediments. Debris flow is assisted with presence of shale deposited during interglacial periods and mud diapirs (Hjelstuen et al., 2004b) also exist in this sequence (Figs. 4.4-4.6 and 4.18). However, this sequence also contains acoustically structureless facies (Dahlgren et al., 2005) which is inferred from disrupted, irregular and chaotic reflections. The structureless seismic facies represent slide debrites.

4.2.6 Seismic Sequence 6 (SS 6)

Characteristics

SB 6 makes its lower boundary and SB 7 forms its upper boundary. Clinoforms are oblique and topset beds are not preserved and are truncated by URU. The reflections are low amplitude, parallel to sub-parallel, disrupted and chaotic. Some seismic sections C, D and E (Figs. 4.4-4.6) illustrate mounded geometry in the foresets and bottomsets.

Interpretation

High rate of sedimentation and high pore water content have likely caused the acoustically poor reflections (Dahlgren et al., 2005) with the transparent character of seismic facies. In addition, the mounded reflections represent lobes of glacigenic debris flows (as illustrated in Fig. 4.18). During glacial period rate of sedimentation was higher than rate of accommodation space creation which caused prograded slopes as well as considerable amount of pore water was retained in sediments. High amount of water in pores destabilized slope sediments; moreover muds deposited during interglacial period were also involved in the debris flows and mud diapirs.

4.2.7 Seismic Sequence 7 (SS 7)

Characteristics

SS 7 is bounded by SB 7 on its base and SB 8 on its top. SB 8 has high amplitude as compared with other sequence boundaries close by. The topset beds are not preserved and truncated by the URU. Internal reflections are disrupted, chaotic and have low amplitude. The hummocky pattern is found in the internal reflections in some seismic lines C, D and E (Figs. 4.4-4.6). SS 7 along with other sequence of megasequence-1 makes a wedge prograding northwest according to strike and dip lines.

Interpretation

Low amplitude, irregular and chaotic reflections demonstrate the deformed sediments and theses are deduced to be caused by debris flows and slide debrites (Figs. 4.18 and 4.21). As well as high pore water may also be reason of the poor image of theses reflections. The high rate of sediment supply to the shelf break during the shelf edge glaciations may have caused the slope failures and debris flows.

4.2.8 Seismic Sequence 8 (SS 8)

Characteristics

SB 9 makes its upper boundary whereas SB 8 makes its lower boundary. SS 8 becomes oblique tangential to oblique from south to north as displayed in seismic sections A-I (Figs. 4.2-4.10). Clinoforms become gentler as compared with older sequences of megasequence-1. The topsets are truncated by URU and bottomsets make downlaps with RDS. However, topsets have high amplitude and make toplaps against RDS. The internal reflections have low amplitude and are chaotic, irregular and disrupted. On lines C, D and E (Figs. 4.4-4.6) internal reflections show mounded and hummocky pattern in the foresets and bottomsets.

Interpretation

High amplitude in clinoforms may be due to high acoustic impedance contrast and also by glacier-induced compaction. However, the internal reflections being chaotic and irregular demonstrate the deformed sediments due to sliding and slumping as well as mud diapirs are

present in this sequence. Hummocky clinoforms represent the glacigenic debris flows. However, the internal reflections show transparent facies and reveal glacigenic debris flows.

4.2.9 Seismic Sequence 9 (SS 9)

Characteristics

SS 9 is bounded by SB 9 on its lower side and SB 10 makes its upper boundary. The clinoforms have oblique tangential geometry in south to oblique in north. Topset is truncated by URU and in seismic profiles F, G and H (Figs. 4.7-4.9) clinoforms make toplaps with SB 11. Internal reflections are low amplitude, irregular and chaotic. Reflections make downlaps with RDS. Intensity of mounded geometry is reduced from SS 8-SS 9.

Interpretation

Increased rate of subsidence accompanied with high rate of sedimentation are thought to have generated longer clinothems.

4.2.10 Seismic Sequence 10 (SS 10)

Characteristics

SB 11 forms a major sequence boundary and makes upper boundary of SS 10. This sequence is the last sequence of megasequence-1. Clinoforms have oblique tangential to sigmoid-oblique configuration in south and north respectively as shown in seismic lines A-I (Figs. 4.2-4.10). SB 11 has high amplitude particularly in its bottomset. Internal reflections have low amplitude and are disrupted and chaotic. Topsets are truncated by URU in most of the seismic profiles. Whereas offlap break of its upper boundary (SB 11) is preserved in seismic profiles F, G and H (Figs. 4.7-4.9) where clinoforms of the lower sequences make toplaps against it. SB 11 has high amplitude in the bottomset.

Interpretation

The high amplitude of SB 11 indicates glacial-induced compaction shown in seismic profile D (Fig. 4.5). The topset of SS 10 is preserved in many of the interpreted lines showing subsidence occurring on the margin. Otherwise in the prograded successions the topset beds

might be eroded with relative sea level fall. Because progradation take place due to low ratio between rate of accommodation and rate of sedimentation. Moreover, high amplitude may be result of sediment loading, compaction during interglacial period due to low rate of sedimentation providing more time for compaction. It is also noteworthy at this moment to mention that high acoustic impedance s\contrast is generated in accordance with variation in lithology due to change from glacial to interglacial period. Since diamictons and till are deposited during glacial period while shale is deposited during interglacial period as displayed in lines A-I (Figs. 4.2-4.10). Furthermore, shale is more prone to be compacted as compared with till and diamictons.

4.2.11 Seismic Sequence 11 (SS 11)

Characteristics

This sequence is oldest in megasequence-2 and the reflections become gentler as compared to the previously generated sequences of megasequence-1 (for instance line B, Fig. 4.3). SB 11 makes its lower boundary and SB 12 makes its upper boundary. The internal reflections have high amplitude in topsets; however, amplitude is lower in the foresets and bottomsets. The mounded structures are found in the internal reflections in this sequence. Clinoforms have oblique geometry. Internal reflections are low amplitude and chaotic.

Interpretation

The accommodation space is increased through subsidence and increase in rate of sedimentation along with relative sea level rise resulted into the aggradation. The mounded reflections represent the glacigenic debris flows (lines C, D and E) shown in Figs. 4.4-4.6, and there could possibly be effect of the currents in bottomsets.

4.2.12 Seismic Sequence 12 (SS 12)

Characteristics

SS 12 is bounded by SB 12on its base and SB 13 on its top. Clinoforms are oblique to sigmoid-oblique as illustrated in seismic lines A-H (Figs. 4.2-4.9). Topset beds are preserved in few lines and in other seismic lines topsets are not preserved. There is thinning of SS 12

form south to north. SB 13 has high amplitude but the amplitude of the internal reflections is low. The internal reflections are disrupted and chaotic and have mounded geometry in the bottomsets. SS 12 progrades northwest as demonstrated by strike and dip lines.

Interpretation

The outbuilding of the wedges with the aggradation is inferred to be the result of increase in sediment supply, relative sea level rise and as well as by increase in rate of subsidence (for example line H, Fig. 4.9). The mounded geometry of reflections in bottomset beds reveals that there may probably be enhanced contouritic effect due to glaciomarine or marine environment.

4.2.13 Seismic Sequence 13 (SS 13)

Characteristics

SS 13 is bounded by SB 13 on its base and SB 14 on its top. Clinoforms in this sequence have oblique to oblique tangential geometry from south to north (seismic profiles B-I in Figs. 4.3-4.10). Clinoforms demonstrate high amplitude in the topset and bottomset (line H, Fig. 4.9). Internal reflections have low amplitude in foreset. Reflections in bottomset have hummocky pattern. Amplitude of SB 14 becomes too low in bottomsets in many seismic lines which makes it difficult to follow its extension. Offlap breaks of the clinoforms are not preserved in this sequence.

Interpretation

Megasequence-2 demonstrates aggradation and then progradation towards west. SS 13 shows progradation followed by aggradation resulted by the increase in rate of sedimentation and relative sea level fall (line H). Prograding units show that the rate of sedimentation was higher than rate of accommodation.

4.2.14 Seismic Sequence 14 (SS 14)

Characteristics

SS 14 is bounded by SB 14 on its base and SB 15 on its top. Clinoforms are oblique and internal reflections are disrupted and laminated (seismic profile A, Fig. 4.2). Reflections show high amplitude in foreset however low amplitude in the topset and bottomset. The reflections make toplaps against the URU and downlaps with the RDS (lines A-I).

Interpretation

Low amplitude of reflections may be due to less lithology contrast between two reflections; in addition, disturbed sediments may show low amplitude and disrupted reflections. SS 14 builds the progradation towards west in dip lines and makes wedge collectively with other sequences of megasequence-2 (lines A-I, Figs. 4.2-4.10) indicating high ratio between rate of sedimentation and rate of accommodation.

Furthermore, laminated reflectors reveal acoustically laminated facies which indicate hemipelagic and/or contouritic sediments (Dahlgren et al., 2005) (Fig. 4.22).

4.2.15 Seismic Sequence 15 (SS 15)

Characteristics

SS 15 is bounded by SB 15 on its base while SB 16 makes its upper boundary. Its upper boundary which is SB 16 is sigmoid-oblique to oblique from south to north. SB 16 acts like major sequence boundary with high amplitude. In south (seismic lines A and B, Figs. 4.2-4.3) topset beds are preserved whereas topset beds are not preserved in SS 15 in northern seismic profiles (C, E-H). Internal reflections in seismic sections (A and F) are sigmoid-oblique and depict mounded geometry in the bottomsets.

Interpretation

The topset beds are not preserved which makes it difficult to deduce relative sea level. On line B (Fig. 4.3) there is progradational stacking pattern after aggradation indicating relative sea level fall. Moreover the rate of sedimentation and rate of accommodation remained high

during formation of this megasequence as indicated by increased thickness in sequences of megasequence-2 including SS 15. In seismic lines B and C (Figs. 4.3-4.4), SS 16 contains some reflections which downlap against SB 16, showing the relative sea level fall in SS 16. Moreover, laminated reflections in SS 15 of seismic profile B (Fig. 4.3) demonstrate fine grained sediments indicating marine or glaciomarine depositional environment.

4.2.16 Seismic Sequence 16 (SS 16)

Characteristics

The lower boundary of SS 16 is formed by SB 16 however upper boundary is formed by SB 17. Clinoforms make oblique to oblique tangential profile form south to north. SS 16 extends up to long distances, showing the continuation of the sedimentation (for example in line B, Fig. 4.3). In seismic line B this sequence extends from east of the Dønna Terrace to east of the Helland-Hansen Arch (Fig. 4.3). Internal reflections are low amplitude, irregular and chaotic. Reflections make toplaps with the URU and downlaps with RDS. Internal reflections of SS 16 downlap against SB 16 and these reflectors are observed in seismic line A and B. Strike line L (shown in Fig. 4.14) show inter-fingering between SS 16, SS 17 and SS 18 in a trough in the Træna Basin. SS 16 in seismic line F (Fig. 4.7) reveals laminated reflectors.

Interpretation

The inter-fingering of SS 16, SS 17 and SS 18 is observed in the Træna Basin in few strike lines including key line L (Fig. 4.14). These reflections are marked on dip lines with help of strike line L and a random line which is displayed in chapter 5 (Fig. 5.16). The inter-fingering of the sequences demonstrate the deposition by ice streams coming form the north and the south as shown in Figs. 4.14 and Fig. 5.26. URU remained continuous above trough showing inter-fingering of SS 16, SS 17 and SS 18. It mentions that this trough was formed through ice streams and was not incised by processes occurring during development of URU. Presence of ice streams in the Træna Basin also refer that there was relative sea level rise. Ice streams developed due to shift from glacial period to interglacial period. This will be further discussed in chapter 5.

Furthermore, laminated reflections in SS 16 of seismic profile F (Fig. 4.7) correspond to the acoustically laminated facies (Fig. 4.22) which characterize contouritic or hemipelagic sediments.

4.2.17 Seismic Sequence 17 (SS 17)

Characteristics

SS 17 is bounded between SB 17 as lower boundary and SB 18 makes its upper boundary. SS 17 has oblique tangential clinoforms and they followed underlying topography. SB 18 has high amplitude however internal reflections show medium to low amplitude (line C, Fig. 4.4). Amplitude of reflections is lowered in northern lines which makes difficult to interpret its extension. Further in line I (Fig. 4.10) SS 17 is missing. Maximum extension of SS 17 is 111 km lying form the Trøndelag Platform to east of the Helland-Hansen Arch found in line D (Fig. 4.5). The reflections are disrupted to chaotic. This sequence dips in the northwest direction as shown by dip and strike lines. For the reason that dip lines demonstrate sequences dipping towards west (lines A-H, Figs. 4.2-4.9) while in strike lines the sequences prograde towards north (lines J and K, Figs. 4.12 and 4.13 respectively). Topset beds are not preserved of SS 17 and are truncated against the URU.

Interpretation

The sequence boundaries do not show the normal succession in few seismic lines as SB 18 is underlying SB 17 and SB 19 overlies it (Strike line L in Fig. 4.14). This change in succession represents the inter-fingering of the sequences deposited by ice streams coming from different directions above the ice sheets. These ice streams were flowing and they deposited sediments in a trough and these sediments show inter-fingering. Ice streams indicate relative sea level rise. SB 18 was eroded in further northern seismic lines (for instance line I, Fig. 4.10). Furthermore, the truncation of topset beds against URU are attributed to relative sea level fall, and/or increase in thickness of ice sheets eroding sediments as well as erosion by ice streams.

4.2.18 Seismic Sequence 18 (SS 18)

Characteristics

SS 18 has its lower boundary as SB 18 and upper boundary as SB 19. SS 18 has clinoforms which have oblique geometry and in northern lines geometry is oblique tangential while following underlying topography (for instance in seismic line E, Fig. 4.6). The clinoforms seem to show a hummocky geometry in bottomset and seems to be caused by topography. SS 18 exhibits one of the most extended sequences in megasequence-2 (line H, Fig. 4.9) extending from the Træna Basin to north of the Helland-Hansen Arch.

The topset beds are truncated bellow the URU. SB 19 depicts the high amplitude; however, the internal reflections of SS 18 have low amplitude. Internal reflections reveal laminated pattern in line A (Fig. 4.22). SS 18 overlies SS 16 inline H and strike line L and a random line given in Fig. 5.26.

Interpretation

Chaotic to disrupted reflections show deformation due to glaciomarine and marine environment affecting through currents. Inter-fingering of the sequences was interpreted through strike lines (L and a random strike line) (Figs. 4.14 and 5.26). The inter-fingering of the sequences shows the presence of ice streams. These ice streams eroded sediments and deposited them with reduced energy. SS 18 thins out in its bottomset making a lenticular wedge. Bottomset of SS 18 makes downlaps with RDS.

4.2.19 Seismic Sequence 19 (SS 19)

Characteristics

SS 19 is bounded by SB 19 on its base and SB 20 makes its upper boundary. Clinoforms show sigmoidal to oblique profile from south to north. The amplitude of SB 20 is high; however, the internal reflections of SS 19 have low amplitude and are disrupted to chaotic. SS 19 extends from Trøndelag Platform to east of the Helland-Hansen Arch (152 km) in line A. SS 20 makes downlap surfaces above SB 20 particularly in topset. It is significant to

mention that there are onlap surfaces above SB 20 (For instance line F in Fig. 4.7). Moreover, there are also onlap surfaces within SS 19 (line F in Fig. 4.7).

Interpretation

The preservation of the offlap break of SB 20 in lines (A, B, F and I, illustrated in Figs. 4.2, 4.3, 4.7 and 4.10) may have been caused by rising relative sea level, controlled by subsidence of the basin margin and/or by eustatic changes. In addition, in lines A and B (Figs. 4.2 and 4.3) there are downlaps above SB 20 indicating that SB 20 was acting as flooding surface and then there was relative sea level fall in SS 20.

Areas where topset beds of SS 19 are not preserved may indicate presence of ice streams (for instance seismic lines C, D, E, G and H, Figs. 4.4-4.6, 4.8 and 4.9). It may probably be caused by erosion during next glacial cycle which deposited SS 20 afterwards. Moreover submarine onlaps above SB 20 and within SS 19 demonstrate submarine onlaps.

4.2.20 Seismic Sequence 20 (SS 20)

Characteristics

SB 21 makes the upper boundary of megasequence-2 and SS 20 is the youngest sequence deposited in megasequence-2. SB 20 makes the lower boundary of SS 20 whereas SB 21 forms its upper boundary. Clinoforms have sigmoid-oblique to oblique profile and show high amplitude. Topset beds are preserved in seismic lines) C and D, Figs. 4.4 and 4.5) whereas seismic lines (B, E, H and I) demonstrate that topset beds are truncated against the URU. The internal reflections have low to medium amplitude.

Interpretation

The amplitude is increasing from east to the west (as demonstrated in lines A-I, Figs. 4.2-4.10) and it might be caused by the glacier-induced compaction. It suggests that the glacier-induced compaction is enhanced in the west of the Rås Basin and above the Helland-Hansen Arch (Line D, Fig. 4.5). The thickness of SS 20 increases in the bottomset showing the sediment-bypass along the slope as illustrated in (Fig. 4.8) of line G.

4.2.21 Seismic Sequence 21 to Seismic Sequence 28 (SS 21 to SS 28)

Characteristics

Clinoforms demonstrate predominantly high amplitude and have sigmoid-oblique to oblique tangential profile. Clinoforms followed the underlying topography (for instance line G, Fig. 4.8). Internal reflections are low amplitude, chaotic, disrupted in SS 21-SS 28 (lines B-G, Figs. 4.3-4.8) and become contorted predominantly in bottomsets in SS 21-SS 28 (lines A-I, illustrated in Figs. 4.2-4.10). The internal reflections also become stratified as compared to the previously deposited sequences (SS 23) of line H, Fig. 4.9. The sequences start from the Dønna Terrace and they extend through the Rås Basin and downlap against RDS east of the Helland-Hansen Arch in southern lines (line A and B).

Interpretation

SB 22-SB 29 have high amplitude which may indicate glacial-induced compaction (Fig. 4.15), whereas the internal reflections have poor amplitude in the bottomsets (Fig. 4.16) (see chapter 5 for discussion). The stratified sediments are found which demonstrate the hemipelagic or contouritic sediments and they play role as gliding planes for the slides in the glaciomarine deposits. The sediment bypass is occurred in some of the interpreted lines

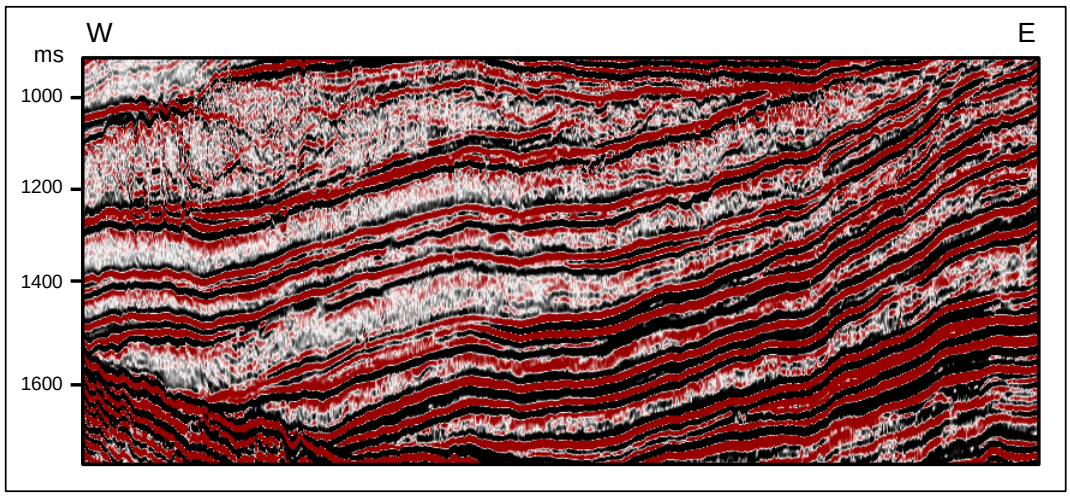

Figure 4.15 Seismic line (section of key line E) showing the sequence boundaries of the megasequence-3 with high amplitude. See figure 4.6 for seismic stratigraphic framework.

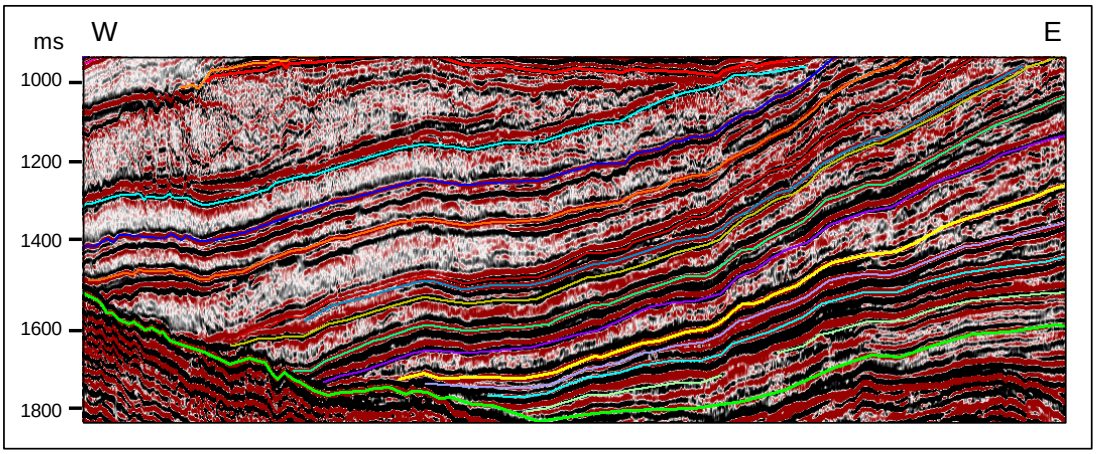

Figure 4.16 Interpreted seismic line (section of key line E) showing low amplitude reflections in bottomsets of megasequence-3. See figure 4.6 for seismic stratigraphic framework and see Fig. 4.2 for legends.

illustrating the movement of the sediments along the slope. The huge extension of these sequences likely represents the high rate of subsidence with enough rate of sedimentation and high rate of accommodation.

4.2.22 Seismic Sequence 29 (SS 29)

Characteristics

URU makes the upper boundary of this sequence and SB 29 forms its lower boundary. Seismic lines show stratified reflections on the base of SS 29. Several valley-like bodies are present on lower part of SS 29. The disrupted to chaotic reflectors are found in lower part (e.g. Fig. 4.5). The URU abruptly bends down in east of the Helland-Hansen Arch in seismic lines making the slide head wall (D, E and F, Figs. 4.5-4.7).

Interpretation

SS 29 consists of the contorted and mounded reflections showing the debris flow deposits (Fig. 4.12). And there are also acoustically structureless seismic facies representing the slide debrites. The mounded structures are due to debris flow (King et al., 1996; Nygård et al., 2005; Dahlgren et al., 2005). The URU bend is interpreted to reveal the Sklinnadjupet Slide which shows change of more or less horizontal reflections to steeply dipping reflections. The slide headwall and the base of the slide are also observed (Figs. 4.5-4.7). The base of the Sklinnadjupet Slide shows the stratified sediments suggesting the marine to distal glacial

marine environment. These stratified reflections are supposed to be fine grained sediments which provided the glide plane for the Sklinnadjupet Slide (e.g. found in Line F, Fig. 4.7) (see chapter 5 for discussion).

The contorted reflections in sequence are due to effect of the contouritic currents particularly in bottomsets. The slide scars above the Sklinnadjupet Slide were depicted in the seismic lines suggesting the removal of the sediments through the slide deposits.

4.2.23 Seismic Sequence 30 (SS 30)

Characteristics

Megasequence-4 starts from the URU as its lower boundary and the seabed as its upper boundary. The URU contains some erosional structural depressions that may represent scours or channels formed by glacial erosion. These erosional depressions have subsequently been filled by prograding or onlapping sediments. SS 30 also contains some channels and the internal reflections show aggradation to progradation.

Interpretation

Megasequence-4 shows the high rate of erosion through the fast moving ice streams which are interpreted as acoustically transparent reflections. This sequence preserved some lenses which are referred to be formed by the floating ice sheets (Fig. 4.6) discussed in the chapter 5. The aggrading glacial till is preserved in SS 30 (Line L, in Fig. 4.14).

4.2.24 Seismic Sequence 31 (SS 31)

Characteristics

SB 32 forms the upper boundary of this sequence and SB 31 makes the lower boundary. Many of the internal reflections are overlapping and few make the downlaps against SB 31. Downlaps depict high amplitude and high acoustic impedance contrast. The reflections are chaotic while the amplitudes are low. Valley-like bodies are found in this sequence and internal reflections demonstrate chaotic configuration.

Interpretation

SS 31 shows presence of the floating ice sheet and aggrading glacial till with some prograding reflections (Line F, Fig. 4.7). Acoustically poor and homogeneous sediments reveal the glacial sediments representing tills, debris flows and slide deposits. The erosive action of the thick ice sheets and ice streams was quite enough during the formation of this sequence thus, forming chaotic to transparent reflections. The contorted to transparent facies of SS 31 represents the galciomarine sediments of slide scars. The downlaps shows high acoustic impedance contrast while internal reflections are disrupted to transparent indicating difference of composition of deposited sediments. These differences are probably due to different environmental processes. The valley-like bodies represented molten water valleys. The disrupted to transparent internal reflections of this sequence support several phases of erosion (during Saalian).

4.2.25 Seismic Sequence 32 (SS 32)

Characteristics

The reflections are contorted and the amplitude of the reflections is low. Some of the better amplitude reflections show the aggradation and the reflections below the mounds on the seabed have contorted configuration. On seismic line F (Fig. 4.7) small anastomosing to sub-parallel crescentic ridges are found in SS 32. On the seabed ridges; curvi-linear, cross-cutting linear features and channel-like most striking features are found. There are large arcuate ridges met on seabed, whereas the largest one is located in the Skjoldryggen area. The valley-like features are found in SS 32 in line I as shown in Fig. 4.10.

Interpretation

The contorted to transparent seismic facies show glacimarine in-fill of the slide scars (King et al., 1996; Nygård et al., 2005; Dahlgren et al., 2005). The crescentic ridges on lines F and L are inferred to be formed by ground moraine (Fig. 4.7 and 4.14). The ground moraine generated these ridges due to ice-push, overriding palaeo-ice stream (Graham et al., 2009; Graham et al., 2011).

The curvi-linear, cross-cutting line-like features are interpreted to be formed by break-up of the ice sheet. These are inferred to be iceberg plough marks. During the Weichselain, fast-moving ice streams eroded older sediments and transported them towards palaeo-shelf edge and these deposits are found as lateral moraine on seismic section. Lateral moraine ridge becomes most prominent due to increased amount of sediments in Skjoldryggen area (area located on the present shelf edge) (e.g. Fig. 4.5, line D).

Moraines are considered to be reflecting the deglacial phase more willingly than related to the Late Weichselain maximum (Graham et al., 2011).

The channel-like features are formed by incision through melt waters for instance illustrated in Fig. 4.17. The sediments are deformed due to repeated erosion and processes like debris flows. Due to high rate of sedimentation sediments could not get stabilized and compacted during glacial periods and rise in relative sea level causes those sediments to be more destabilized. Therefore, sediments are found to be involved in mass wasting processes during deposition of the Naust Formation. The ridges on the Helland-Hansen Arch are found i.e. in line E (Fig. 4.6) which are formed by debris flow deposition.

Contorted reflections in SS 32 represent modification of sediments by effect of the contouritic currents (King et al., 1996; Nygård et al., 2005; Dahlgren et al., 2005) hence indicating glaciomarine or pure marine processes.

The erosion of the offlap breaks is increased from the south to the north (Line A to Line E) which might be reason of the existence of the ice stream or increased thickness of the ice sheets grounding the previous sediments. And then the offlap breaks remain preserved towards the further north (Fig. 4.11) suggesting lesser intensity of the ice streams.

4.3 Seismic Facies Analysis

Facies are characterized by different properties such as appearance, composition and biologic content between various rock or lithostratigraphic units or their components. Likewise, different elements of sequences exhibit varying seismic appearance. Therefore a seismic facies corresponds to a particular lithostratigraphic or seismostratigraphic unit or

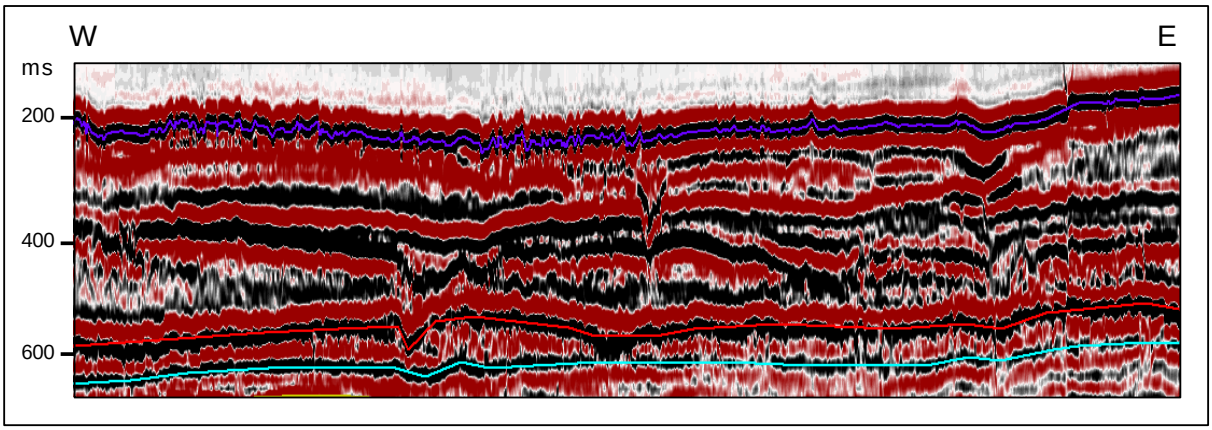

Figure 4.17 Seismic profile I illustrating melt water channel stacking in SS 32. See figure 4.10 for seismic stratigraphic framework.

element of such unit having particular seismic characteristics discernible from other units. This seismostratigraphic unit may be related with subunit of a sedimentary sequence between two distinguishing markers mapable over a significant area (Roksandic, 1978).

Four types of seismic facies have been deduced on basis of the reflection configurations in the seismic sections in this study area which are following.

4.3.1 Mounded acoustically transparent facies

Hummocky and chaotic reflections are found in megasequence-1 (SS 4 to SS 8) of seismic profiles C, D and E (for instance demonstrated in Fig. 4.18). SS 29 of megasequence-3 exhibits chaotic and hummocky reflection pattern in lines (A-I). Furthermore, SS 31 of megeasequence-4 displays chaotic reflections in seismic sections A, D and E (Figs. 4.2, 4.5 and 4.6).

These hummocky and chaotic reflections characterize mounded acoustically transparent seismic facies corresponding to glacigenic debris flows (Dahlgren et al., 2005). It is significant to mention that intensity of hummocky configuration of SS 4-SS 8 reflections in seismic lines C, D and E; (Figs. 4.4-4.6) intensify in the northern most seismic line (E). This indicates that debris flows were intensified due to the relative sea level rise.

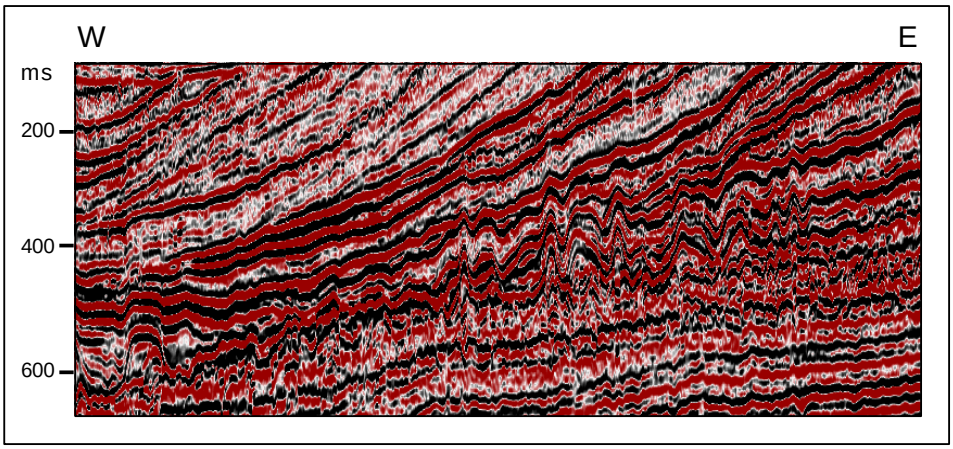

Figure 4.18 Seismic section E depicting mounded acoustically transparent facies in SS 4-SS 8. See figure 4.6 for seismic stratigraphic framework.

4.3.2 Contorted to transparent facies

Foresets and particularly bottomsets of megasequences below URU reveal contorted, irregular and disrupted reflections (lines B-G) particularly in bottomsets. Whereas SS 29 of megsequence-3 reveals contorted and chaotic reflections (lines A-I). In addition, megasequences above URU exhibit contorted and irregular reflections in seismic lines A-I (for example shown in Fig. 4.19). Furthermore, lateral moraine (Roksandic et al., 1978) has dominantly contorted reflections in SS 32 as illustrated in seismic profiles A-F (Figs. 4.2-4.7) and (Fig.4.20) which has focused lateral moraine ridge and megasequence-3. Predominantly contorted reflections are characterized by contorted to transparent facies. Contorted character of reflections became pronounced particularly in bottomsets as depicted.

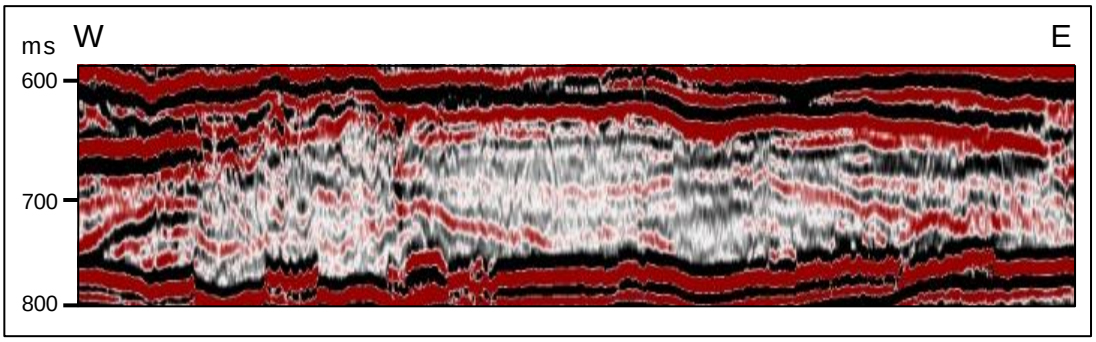

Figure 4.19 Seismic section E illustrating contorted to transparent facies in SS 30. See figure 4.6 for seismic stratigraphic framework.

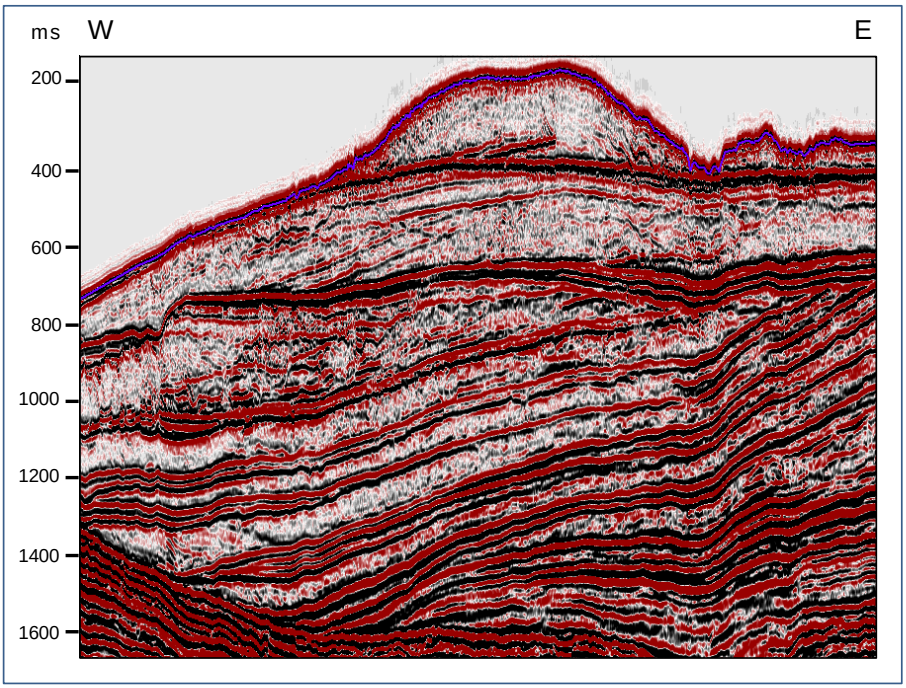

Figure 4.20 Seismic profile D showing contorted to transparent facies in SS 25-SS 29 and lateral moraine. See figure 4.5 for seismic stratigraphic framework.

in key lines A-I (Figs. 4.2-4.10). Contorted to transparent facies are associated with glacimarine sediments (Dahlgren et al., 2005)

4.3.3 Acoustically structureless facies

SS 25-SS 29 in megasequence-3 reveal pronounced irregular, chaotic to structureless reflections in seismic profiles (C-F). Seismic lines in further north (G and I) show considerable intensity of structureless reflections in SS 20-SS 29 west of the Helland-Hansen Arch. Structureless reflections occur in SS 31 and SS 32 and intensity of stuctureless reflections increase in western parts of seismic lines of (B, C, D, E and F) also illustrated in Fig. 4.21.

These structureless facies correspond to slide debrites (Dahlgren et al., 2005).

4.3.4 Acoustically laminated facies

First of all, sequence boundaries are associated with interglacial periods and largely shales are deposited during interglacial period. Due to variation in lithology from glacial deposits

(diamictons and till) shales demonstrated high acoustic impedance contrast along sequence boundaries. Sequence boundaries show prominently laminated facies.

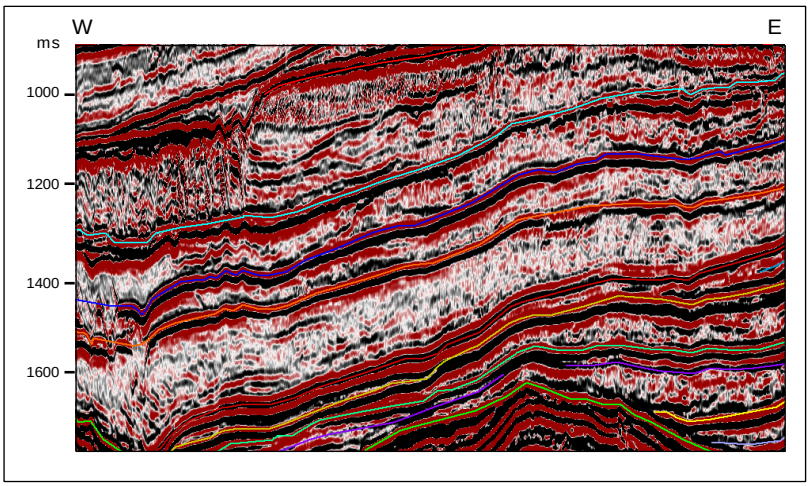

Figure 4.21 Seismic section F displaying acoustically strauctur4eless facies in SS 25-SS 29. See figure 4.7 for seismic stratigraphic framework.

Laminated facies mainly correspond to hemipelagic/contouritic sediments (Dahlgren et al., 2005). Secondly laminated reflections are observed on base of the Sklinnadjupet Slide in SS 29 in megasequence-3 in line A illustrated in Fig. 4.22. Furthermore, homogeneous (laminated) reflections are found in SS 9, SS 14 and SS 18 of line A, SS 15 and SS 18 of line

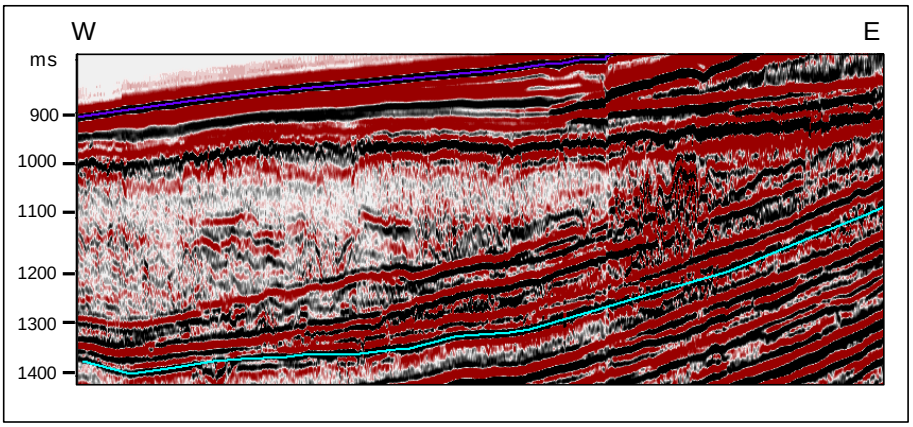

Figure 4.22 Seismic profile A illustrating acoustically laminated facies in SS 29. See figure 4.2 for seismic stratigraphic framework.

B, SS 18 of line C, SS 16 of line F and SS 21-SS 29 of line H. SS 30 also represents the homogeneous reflections in seismic line G.

5. Discussion

Late Cenozoic basin development in the northernmost North Sea and mid-Norwegian continental margin is revealed by approximately 1600 ms TWT (c.1500 m) thick deposits of Late Pliocene Naust Formation along c. 160 km wide area. Thick prograding successions of the Naust Formation refer to the rapid uplift and erosion during Northern Hemisphere glaciations (Jarsve et al., 2010). 32 glacial periods are interpreted during this study based on 32 seismic sequences within the Naust formation. These glacial periods are very significant during which erosion of eastern source areas took place. Eastern flanks of the northernmost North Sea and mid-Norwegian continental margin uplifted and during almost 32 glacial periods, ice sheets and ice streams eroded sediments form eastern areas during the Late Pliocene.

The Late Cenozoic continental shelf offshore Mid-Norway represents a prograding shelf succession which for the latest Pliocene and Pleistocene is delineated into 32 sequences in this project. The Pliocene to Pleistocene sequences demonstrate the events of erosion and renewed deposition. There is a significant interplay between the tectonics, eustacy and sediment supply in the basin development. The seafloor spreading and mantle plume activity in the North Atlantic domain are suggested as triggering mechanisms for Cenozoic uplift of the mainland Norway, creation of accommodation space and basin subsidence (Smelror et al., 2007; Faleide et al., 2010).

Tectonics played the most important role for high rate of sediment supply, sea-level fluctuations, rate of accommodation, climatic variations, glacial and inter-glacial periods (Martinsen et al., 1999; Jarsve et al., 2010). In NW European margin basinward progradation took place during Early Cenozoic tilting (c. 60-50 Ma). Wedge progradation diminished and contourite deposition occurred in deep-water basins during Mid-Cenozoic sagging (c. 35-25 Ma). Uplifting along inner margin and offshore highs caused basinward progradation during Late Cenozoic tilting (< 4±0.5 Ma). Mantle-lithosphere interactions are inferred for km-scale vertical movements related with uplifting (Praeg et al., 2005).

Eastern source and uplifting during the Late Pliocene have been confirmed with westward tilting of basin below the URU (Upper Regional Unconformity) and its angular relationship

with underlying megasequences-1, 2 and 3 illustrated in seismic lines A-I (Figs. 4.2-4.10). Sandy and silty muds were eroded from NE Atlantic and shelf areas during glacial periods and clastic sediments together with diamictons and till sediments deposited building clastic wedges making downlaps with the RDS (Regional Downlap Surface) displayed in lines A-I (Figs. 4.2-4.10).

Thickness of the Naust sediments increased from SE to NW which is displayed in time-thickness map of the Naust Formation (Fig. 5.21). Moreover, ice streams were developed in bathymetric troughs and they deposited sediments in NW of area (Figs. 5.21 and 5.23).

Megasequence-1 reveals relatively steeper clinothems with mainly oblique configuration making prograding stacking pattern. Megseqeuence-1 is separated from megasequence-2 through high amplitude SB 11 across which stacking pattern varies from strongly prograding to aggrading pattern (e.g. in line G, Fig. 4.8). Stacking pattern becomes aggrading to prograding in megasequence-2. However megasequence-1 makes oblique wedge whereas megasequence-2 forms sigmoidal wedge for instance in line A (Fig. 4.2). SS 4-SS 8 in megasequence-1 show debris flow deposits with sliding and slumping and mud diapirs. Mounded acoustically transparent facies of SS 4-SS 8 show higher rate of sedimentation. Higher rate of sediment supply caused high pore water to be retained in sediments generating sliding, slumping and mud diapirs. Steeper clinothems of megasequence-1 were deposited closer to source areas and on steeper slopes which is illustrated in line A (Fig. 4.2). Lateral extension of SS 11-SS 20 of megasequence-2 is greater than megasequence-1.

Megsseqauenec-2 exhibits larger part of the Naust Formation below URU. Seismic sequences of megasequence-2 in seismic sections reveal laminated facies indicating hemipelagic contouritic sediments (Dahlgren et al., 2005). Topography changed considerably during megasequence-2. Megasequence-2 is separated from megasequence-3 through high amplitude SB 21. SS 21-SS 29 have clinothems oblique tangential to oblique. Clinoforms related to megasequence-3 have relatively higher amplitude showing glacial-induced compaction. Mid-Norwegian margin reveals highest subsidence on slope and outer shelf (Dahlgren et al., 2005). Sigmoid-oblique clinothems of megasequence-3 also represent subsidence, for instance in seismic profiles A and B (Figs. 4.2 and 4.3) and illustrated in Fig. 5.2. SS 30 in seismic line G (Fig. 4.8) indicate aggradations more or less equal rates of accommodation and sedimentation

(A/S). Moreover slide debrites are characterized by structureless facies (Dahlgren et al., 2005), SS 31 and SS 32 in seismic lines B-F (Figs. 4.3-4.7).

Megasequences below URU show submarine onlaps above sequence boundaries and with in sequences (for example onlaps above SB 3, within SS 3 in key line A, above SB 4, SB 5, SB 8, SB 10, SB 21, SB 26, within SS 11, within SS 17, SS 19 etc in key line F (Fig. 4.7). Icebergs released sediments and they accumulated along slopes and toes of slopes which are demonstrated by onlaps above sequence boundaries and with in glacial sequences.

Reflections reveal aggradation and tilting of the continental margin had stopped and rise in relative sea-level is indicated by increase in accommodation space during development of megsequence-4. Tunnel valleys in SS 29 in lines A-I (Figs. 4.2-4.10) reveals Elsterian glacial period (Graham et al., 2011). The cross-cutting furrow-like features on seabed are attributed to iceberg plough marks which represented break-up of ice sheets in this region during Late Pleistocene (e.g. seismic lines A and B) (Figs. 4.2 and 4.3). Increased thickness of SS 32 at the Skjoldryggen area reveals lateral moraine deposits (illustrated in line D, Fig. 4.5). Whereas ground moraine (Roksandic et al., 1978) shown by crescentic ridges in SS 32 represents ice-push and super imposition of palaeo-ice streams (Graham et al., 2009; 2011). These features on seismic sections represent that same processes might have been going on during older glacial and inter-glacial periods.

5.1 Ages of the sequences

Ages of sequences in this study were correlated with five units related to Naust Formation assigned by Rise et al. (2010) (Fig. 5.1). The oldest unit of the Naust Formation represents age of 2.8-1.5 Ma (Eidvin et al., 2007; Rise et al., 2010) and SS 1 to SS 17 were correlated to this unit. The base of the Naust Formation was dated to be 2.8 Ma depending upon biostratigraphic correlation of lower glacial deposits of Naust with deep sea core samples (Eidvin et al., 2000). Moreover, during 2.8 Ma considerable increase in ice-rafted debris was noticed in the Norwegian Sea (Ottesen et al., 2009) as well as this age was perceived for the beginning of the Quaternary (Gibbard et al., 2009).

Many seismic sequences in this study indicated an average glacial cycle duration of about 0.1 Ma. These sequences downlaped 20-30 km east of the Helland-Hansen Arch (Rise et al., 2010). Seismic sequences of megasequence-1 described in chapter 4 have mounded reflections along with dominant transparent internal reflections which revealed glacigenic debris flows (Dahlgren et al., 2005) (Fig. 4.6).

The cores taken from above URU (Upper Regional Unconformity) were interpreted to be

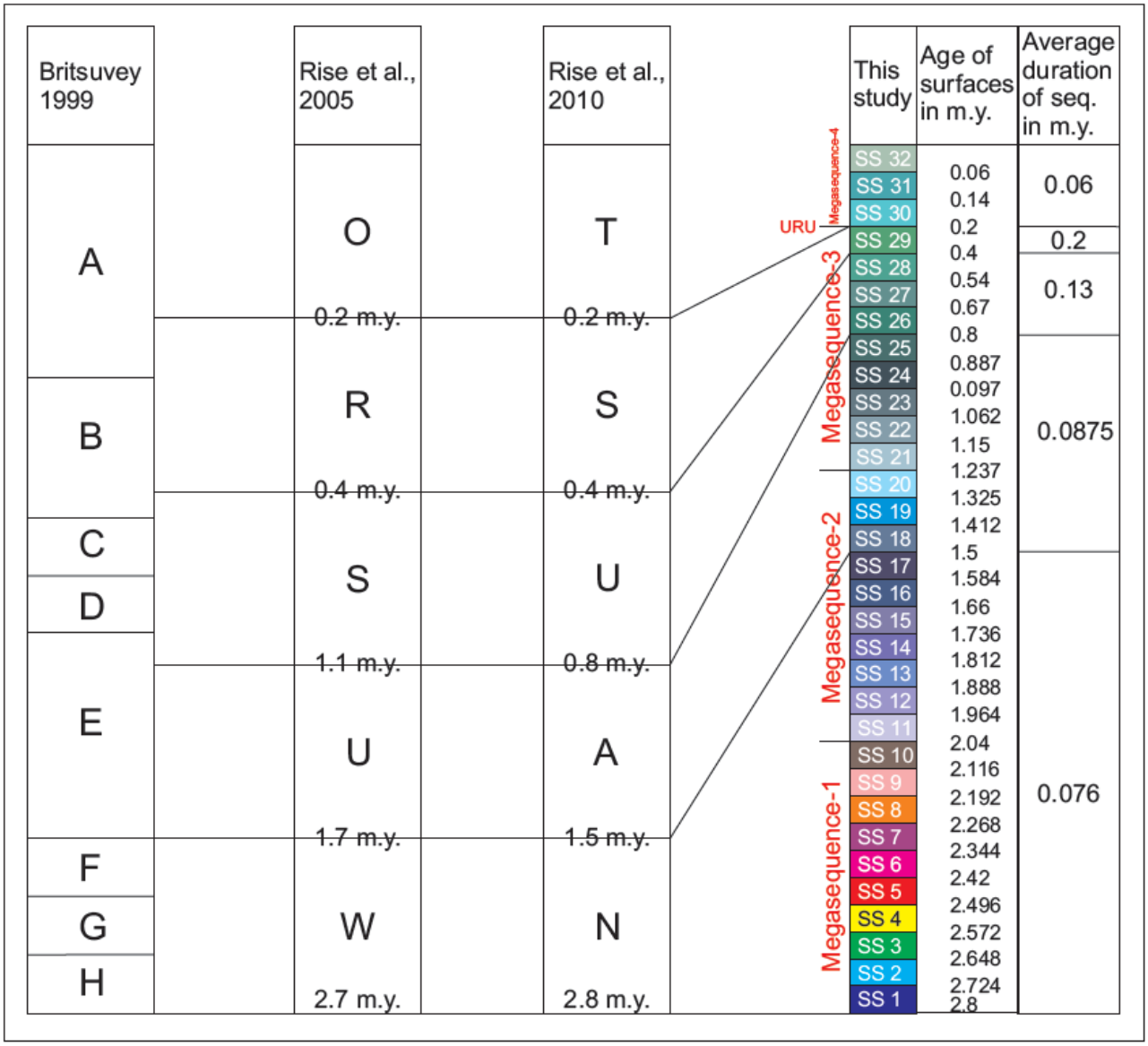

Figure 5.1 The proposed ages of SS 1 to SS 32 integrated to the Naust units of Britsurvey (1999) and Rise et al., 2005 and 2010 (modified from Rise et al., 2005; Hafeez, 2011).

younger than 0.5 Ma (Stoker et al., 1994; Sættem et al., 1992; Rise et al., 2002; Dahlgren et al., 2005). Age of URU is considered to be 0.2 Ma as illustrated in Fig. 5.1 which supports age given by Stoker et al., 1994. During the Saalian, Weichselian and following interglacial periods of about 200,000 years, SS 30 to SS 32 were deposited on shelf and uppermost slope (Hjelstuen et al., 2004b; Rise et al., 2005, 2010) (Figs. 4.2-4.10).

5.2 Creation of the accommodation space

Tectonics played a significant role for Late Cenozoic outbuilding of mid-Norway. During the Pleistocene the landward part of the Norwegian margin has undergone uplift and erosion. However, the subsidence has occurred in the outer shelf (Dahlgren et al., 2002a; Dahlgren et al., 2005). The pattern of the deposition and subsidence along the Mid-Norwegian margin reveals that sediment loading played a significant role for the subsidence (Dahlgren et al., 2005). The important contribution of the loading-induced subsidence has been evaluated through modeling studies (Ceramicola et al., 2005; Dahlgren et al., 2005). A huge amount of sediments were eroded in mainland Norway by glacial mechanisms, transported by grounded ice and deposited from ice streams. Sediment overburden and loading of grounded ice sheets likely generated compaction of the previously deposited sediments. The sedimentary successions with high acoustic impedance in megasequence-3 (SS-20 to SS-28) deposited in the west indicate glacial-induced compaction.

The isostatic movements associated with advances of glaciers on the shelves of NW Europe were diminutive and temporary in character (Nygård et al., 2004; Dahlgren et al., 2005). They are recognized to be negligible to have any direct impact on the depositional pattern (Dahlgren et al., 2005). The rates of the subsidence have been considered to vary between 0.1 and 0.2 m/ka (Solheim et al., 1996; King, 1996; Lebesbye and Vorren, 1996; Dahlgren et al., 2002b; Hjelstuen et al., 2004b; Dahlgren et al., 2005). The parts of the Mid-Norwegian margin are considered to have the highest subsidence rates furthermore; the highest subsidence takes place on the outer shelf and slope (Dahlgren et al., 2005).

The stratal stacking pattern is result of the combination of changing degree of sediment supply, depositional processes and accommodation space. The accommodation space is attributed to the tectonic movements and/or loading induced subsidence as well as eustatic sea

level fluctuations (Dahlgren et al., 2005). Accommodation space and rate of sediment supply was increased during deposition of (SS 11 to SS 20) which is depicted by increased thickness of this megasequence (Fig. 4.14). Aggrading units of glacial till, representing multiple glacial advances, over the URU and cover a large area (Dahlgren et al., 2005) (Fig. 4.6).

Aggradation of the prograding wedges preserved the palaeo-shelf break terminations through the burial of the underlying strata which is referred to be syn-depositional subsidence (Solheim et al., 1996; King, 1996; Lebesbye and Vorren, 1996; Dahlgren et al., 2002 a, b; Hjelstuen et al., 2004b; Dahlgren et al., 2005) (Figs. 5.2, 5.3 & 5.20).

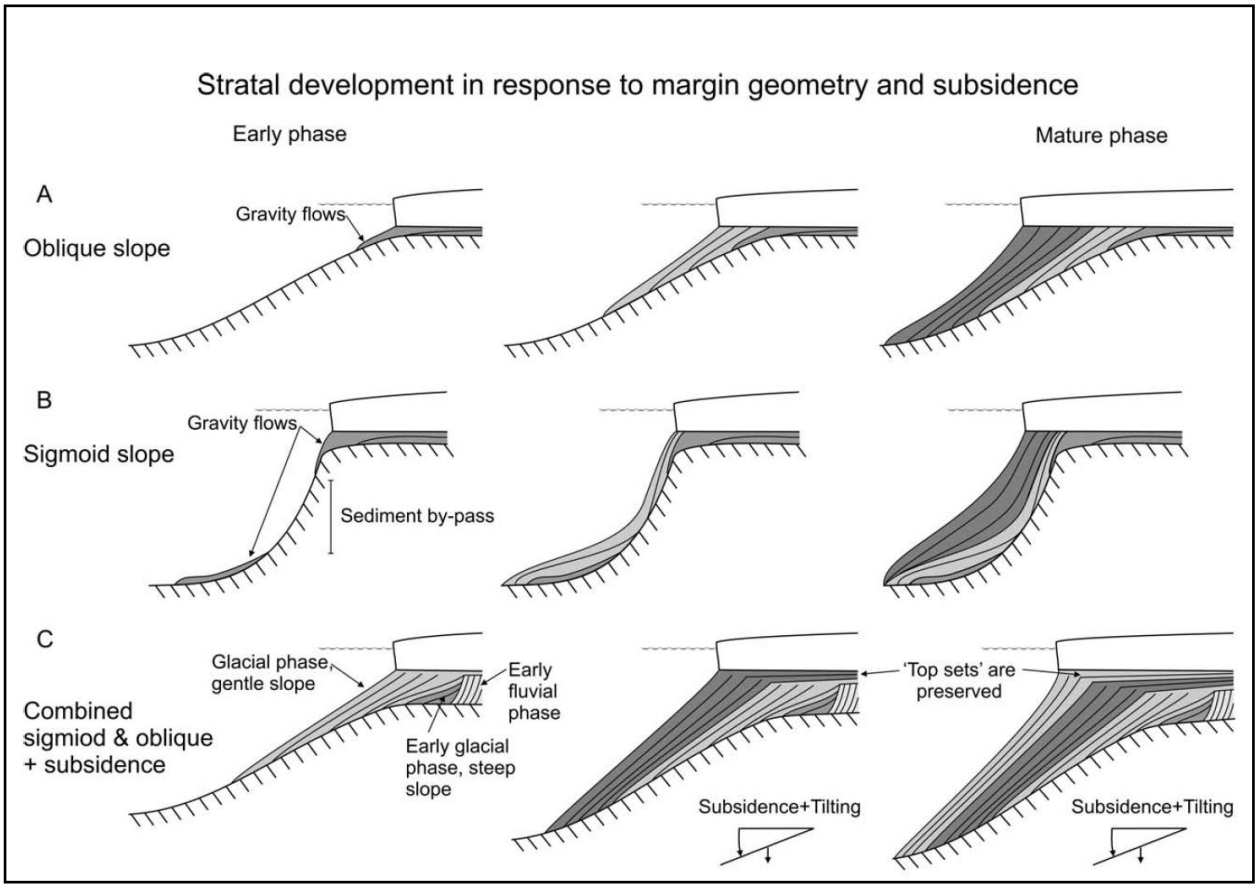

Figure 5.2 The conceptual model illustrating the influence of margin geometry and subsidence on the resulting progradation and stratal stacking pattern of the prograding wedges (Dahlgren et al., 2005).

It is noticeable that the thickness of megasequences 1, 2 and 3 increased northwards indicating comparatively lesser erosion in north (Fig. 5.3). On the other hand, dip lines

demonstrate that thickness of megasequence-4 increases from south to north and then decreases again further north (Fig. 5.3) (refer chapter 4. for thickness of megasequences).

It is evident from the studied dip-lines that thickness of megasequence-2 decreases from the east to west; however, the thickness increases further to the west. The thickness of megasequences-3 and 4 increases towards the west, representing movement of ice streams westwards which eroded sediments and deposited them further west. Moreover, accommodation space was created more towards west.

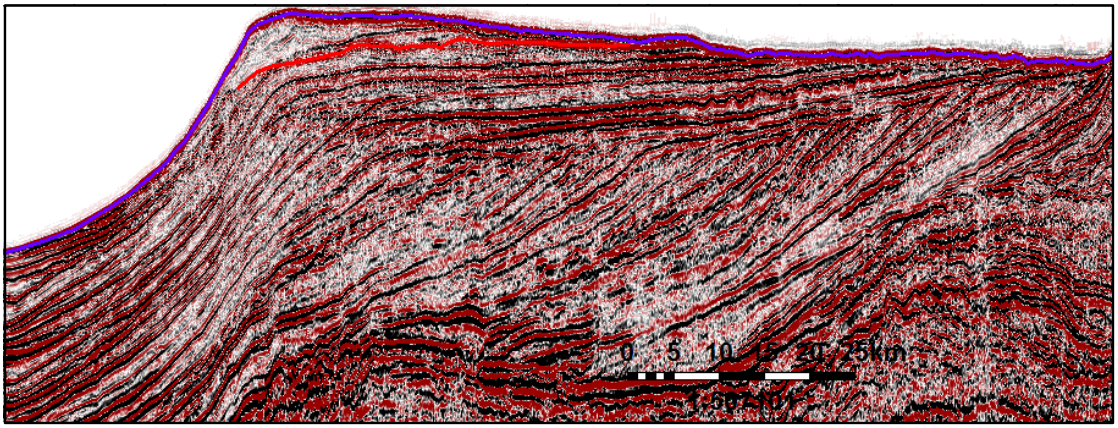

Figure 5.3 Random Seismic line (one of northernmost lines in seismic data) illustrating topsets preserved due to aggradation below URU indicating palaeo shelf edge.

5.2 Shelf edge Trajectory Analysis

The basinward progradation and wedges generate clinothems in accordance with sufficient sediment supply and water depth on either delta/shoreface scale of tens of meters or a shelf margin scale of hundreds of meters (Pirmez et al., 1998; Steel and Olsen 2002; Bullimore et al., 2005).

The shoreline trajectory analysis is a method to determine the sequential position of the shoreline of shoreface scale, recorded in clinothems in depositional, dip-oriented profiles; the geometry of the shoreline trajectory is a function of basin dynamics, as the rate in creation of

accommodation space (A) versus rate of sedimentation (S), the A/S ratio. Sediment supply, relative sea-level changes and basin physiography are controlling factors for the shoreline trajectory (Helland-Hansen & Gjelberg 1994; Helland-Hansen & Martinsen 1996). The principles developed for shoreline analysis can as well be applied on sedimentary shelf edge and platform edge trajectories (Bullimore et al., 2005; Helland-Hansen & Hampson, 2009; Glørstad-Clark et al. 2010, 2011; Helland-Hansen et al., 2012). Shelf transit times (Burgess & Hovius 1998; Muto and Steel 2002) influence sediment supply to the shelf and consequently affect shoreline and shelf edge trajectory (Porobski & Steel 2003). In the further discussion, the concepts of shelf edge trajectory, as reflected by the offlap break trajectory, will be used.

5.2.1 Positive shelf edge trajectory

Strongly progradational clinothems having each successive break of clinoform slope above and more basinward than the earlier one reveals the low angle positive shelf edge trajectory (Fig. 5.4).

The positive shelf edge trajectory represents progradation during rising relative sea-level and topsets may probably be preserved. The topset area has low ratio of accommodation space to sediment supply (A/S), yet larger than 1. The accommodation space is higher behind the shelf edge in high angle positive shelf edge trajectory as compared with low angle positive shelf edge trajectory. For example, SB 22, SB 23 and SB 24 of megasequence-3 (Fig. 4.10), SB 23, SS 23 and SS 24 of megasequence-3 of line B (Fig. 4.3), SS 3, SS 4 and SS 5 of megasequence-1 (Fig. 5.5) represent positive (ascending) offlap break trajectory which is determined from preserved offlap break of these clinothems.

5.2.2 Negative shelf edge trajectory

The negative shelf edge trajectory reveals progradation during falling and subsequent early rise of relative sea-level (Fig. 5.4). It will be demonstrating a forced regressive-falling stage systems tract (Hunt & Tucker 1992; Nummedal et al., 1992; Helland-Hansen & Gjelberg 1994; Plint & Nummedal 2000; Bullimore et al., 2005) or a lowstand wedge systems tract (Van Wagoner et al., 1988a; Posamentier & Vail 1988; Posamentier et al., 1988; Bullimore et al., 2005).

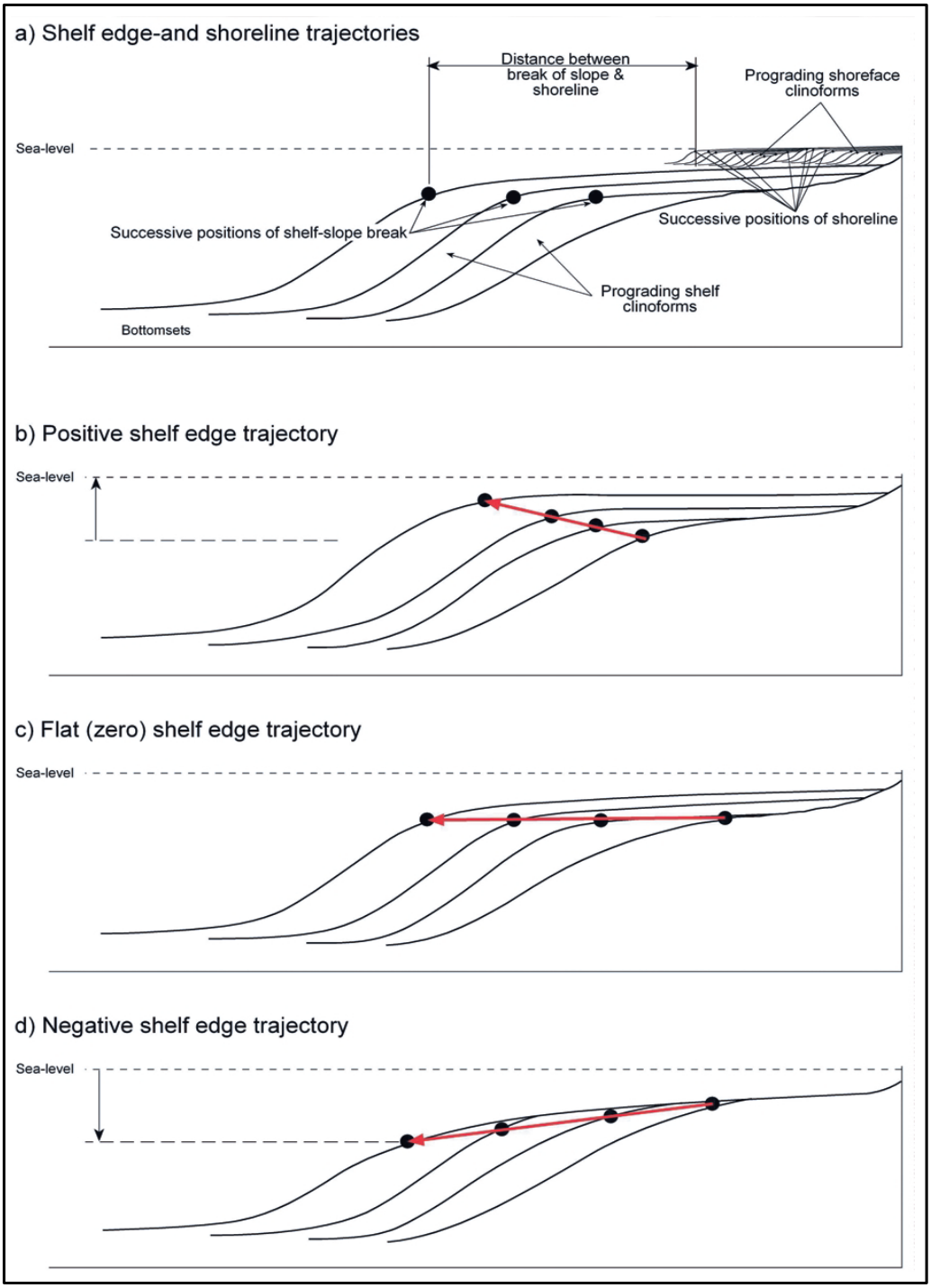

Figure 5.4 Diagram illustrating different scaled prograding shoreface and prograding shelf clinothems. Shoreline trajectory identified through successive positions of the shoreline demonstrating both forced regressive and normal regressive trends. The positive shelf edge trajectory, flat (zero) shelf edge trajectory and negative shelf edge trajectory trends are depicted (modified from Steel & Olsen 2002; from Bullimore et al., 2005).

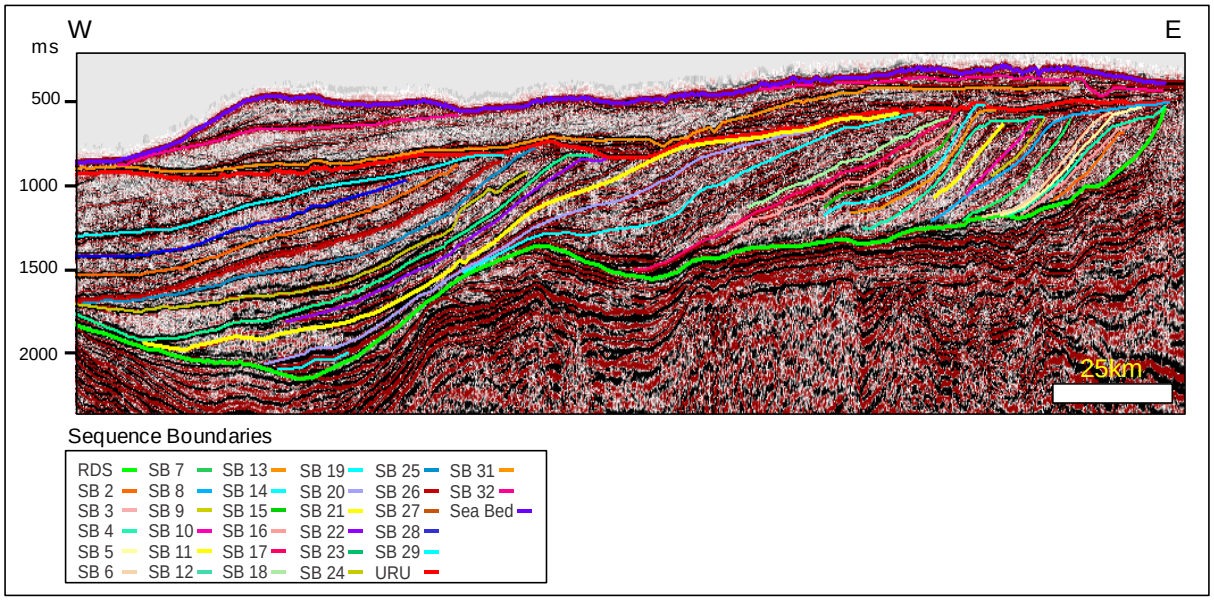

Figure 5.5 Seismic section illustrating positive (ascending) offlap break trajectory through preserved offlap breaks of clinoforms of SS 3, SS 4 & SS 5 of megasequence-1. Positive offlap break trajectory representing rate of accommodation space to sediment supply rate larger than 1 referring to rising relative sea level. See Fig. 4.2 for legends too.

Moreover, in low angle negative shelf edge trajectories, the topsets are usually eroded particularly in proximal areas, whereas they may be preserved in the most basinward areas. However, the determination of an offlap break trajectory is dependent upon preservation of offlap breaks. Negative offlap break trajectories were recognized during interpretation of the seismic sections in this study. SB 8, SB 9, SB 11 and SB 12 of line I (Fig. 4.11) represented negative (descending) offlap break trajectories, showing fall in relative sea level. SS 9 is missing, again suggesting fall in relative sea level.

SB 12, SB 13, SB 15 and SB 16 of megasequence-2 in line A demonstrate negative offlap break trajectories (Fig. 4.2). The downlapping surfaces above SB 16 in SS 16 suggested fall in relative sea level (Fig. 4.2). Sedimentary lenses preserved below several sequence boundaries, i.e. SB 20, SB 21, SB 23 and URU were inferred to have been deposited from floating ice sheets (Fig. 4.2).

The slump deposits may be present in the bottomset of some clinothems, thus referring to unstable slope related to negative shelf edge trajectory (Bullimore et al., 2005). The mounded pattern in foresets and bottomsets of clinothems of megasequence-1 in (Fig. 4.4) were inferred to be caused by slumping and slope instability associated with negative shelf edge trajectory.

However high angle negative shelf edge trajectory occurs during a falling stage systems tract. The high angle negative shelf edge trajectory results into bypass of topsets/shelf area and erosion of topset and slope of earlier deposited clinothems. Erosion represents relative sea level fall and sediments are supplied from hinterland as well as from eroded topset and foreset areas (Bullimore et al., 2005).

Considerable number of clinoforms have not preserved their offlap breaks in the line illustrated in Fig. 5.8 demonstrating relative sea level fall and likely also erosion by ice streams and thick ice sheets during the last two glacial periods. In another example, sediments were bypassed along slope and were deposited in bottomsets of megasequence-3 of SS 24 to SS 28 of line C (Fig. 4.4) and SS 26 of line E (Fig. 4.6).

5.2.3 Flat (zero) shelf edge trajectory

Low and equal rates of sediment supply and accommodation space result into flat or zero offlap break (and shelf edge trajectory) (Fig. 5.4). Flat offlap break trajectories are generally found in gently prograding to aggrading systems tracts.

5.3 Palaeo-shelf edge

During SS 1 to SS 25 westward progradation occurred extensively below present shelf edge. Progradation during deposition of SS 26 to SS 28 buried the whole Helland-Hansen Arch (Rise et al., 2006, 2010) as well as Modgunn Arch (Rise et al., 2010). The palaeo-shelf edge migrated towards its most westerly position above the shallowest crest of the Helland-Hansen Arch (Rise et al., 2010) during deposition of SS 29.

The palaeo-shelf margin trend is linear to concave (Fig. 5.6). In seismic line A which is located in south of the study area, the distance which palaeo-shelf covered is calculated to be c. 141 km (Fig. 5.6). However, in northern most seismic line given in Fig. 5.7 palaeo-shelf edge was migrated up to 87 km located in east of Någrind Syncline.

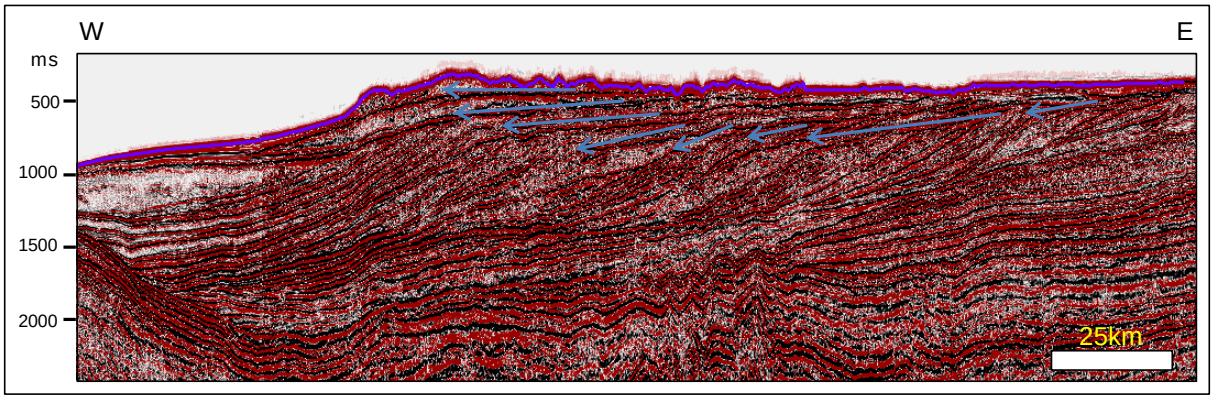

Figure 5.6 Seismic line A (also referred in chapter 4 in Fig. 4.2) illustrating linear to concave palaeo-shelf margin trend. Palaeo-shelf migrated up to 141 km located in east of the Rås Basin.

5.4 Provenance

The Cenozoic depositional pattern was strongly influenced by two Cenozoic highs, the Modgunn Arch and Helland-Hansen Arch (Rise et al., 2006, 2010). During deposition of the Naust Formation (since c. 2.8 Ma) sediments were derived through glacial erosion from the western part of the Scandinavian mountain range and inner shelf areas (Rokoengen, et al., 1995; Henriksen and Vorren, 1996; Stuevold and Eldholm, 1996; Eidvin et al., 2000; Dahlgren et al., 2002b; Hjelstuen et al., 2004a; Rise et al., 2005, 2006; Dowdeswell et al., 2010; Rise et al., 2010).

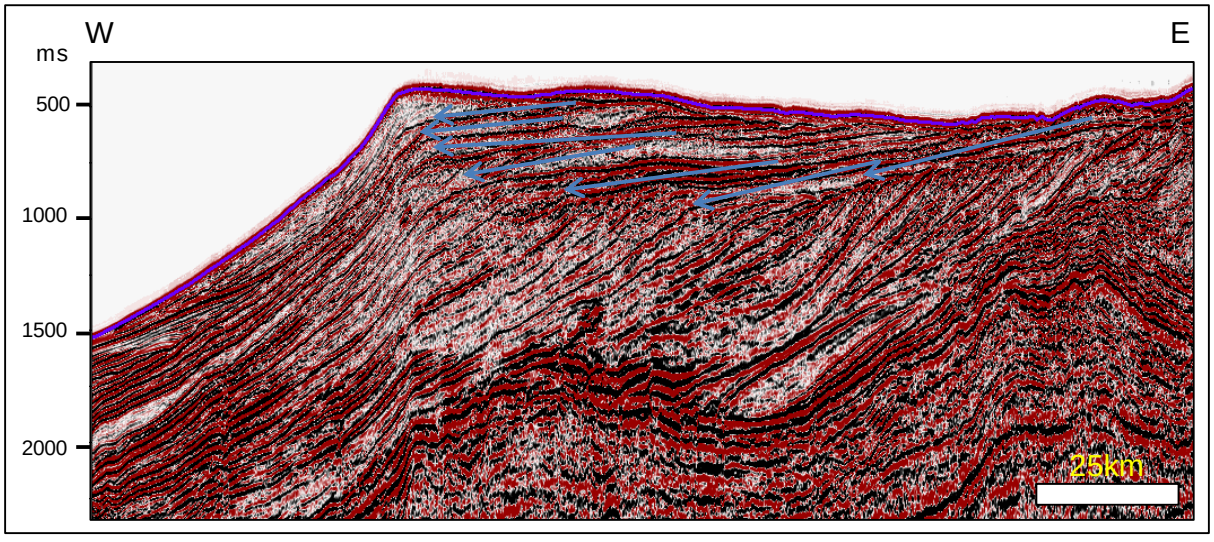

Figure 5.7 Northern most random seismic line demonstrating linear to concave palaeo-shelf margin trend. Palaeo-shelf migrated up to 87 km located in east of the Någrind Syncline.

Furthermore, provenance studies based on geochemical analysis of the youngest glacigenic debris flows in the prograding wedges off Mid-Norway also supported that they were glacially eroded and transported from proximal land and shelf areas with Caledonian bedrocks (Farmer et al., 2003).

Moreover, the progradational pattern in the early phase demonstrates the relatively steeper clinothems (SS 1-SS 10 as illustrated in key lines A-I, Figs. 4.2-4.10) with a north-eastern source and younger phase with gently sloping clinothems showing the eastern source (Dahlgren et al., 2005).

The most important finding for determining the provenance was utilization of high valued sedimentary core from the Norwegian continental shelf. The ice-rafted debris in the lower parts of the Naust Formation was comprised of clasts originating from crystalline rocks from neighboring Norwegian mainland (Ottesen et al., 2009).

5.5 Sedimentation

The shelf break migrated up to 150 km due to the deposition of the prominent prograding wedges along the continental margin of NW Europe during the Late Pliocene to Pleistocene. Furthermore, thick sediment successions were deposited through marginal to high latitude ice sheets. The geographical distribution besides stratigraphical and chronological data, suggests that deposition and construction of wedges was associated with factors like tectonic uplift, Late Pliocene to Pleistocene climate deterioration and initiation of the major northern hemisphere glaciations (Dahlgren et al., 2005).

The wedges depict gently inclined seaward prograding clinothems with chaotic to transparent acoustic facies (for instance found in line D in SS 25-SS 28, Fig. 4.5). The geometry of these clinothems varies from oblique to sigmoidal and wedges show varying degrees of the aggradation. However, the pattern may be disrupted by glacial troughs or differential compaction over structural highs (Dahlgren et al., 2005).

During SS 1-SS 25 (2.8-0.8Ma) of Naust Formation the westerly progradation took place below the present shelf. SS 26 to SS 28 (0.8-0.4 Ma) is thickest on slope in the northern part.

These sequences are considered to be glacial debris redistributed down slope from the grounding line of ice sheets.

The samples of the Naust Formation reveal that they are composed of glacigenic diamicton with interbeddings of the marine and glaciomarine sediments which are affected by bottom-currents. Debris flows have the interbeddings of slide debrites, hemipelagic marine and the glaciomarine sediments. Furthermore, the matrix of the glacigenic diamicton contains 10-40 % sand and the remaining amount consists of almost equal clay and silt (Dahlgren et al., 2005). The laminated seismic facies of the marine and glaciomarine hemipelagic and contouritic sediments inter-finger with glacigenic debris flow and amalgamated debris flow units (Dahlgren and Vorren, 2003; Dahlgren et al., 2005). The contouritic sediments might show a weaker internal stratification as compared to the hemipelagic sediments. The sediments hold large amount of water due to high rate of sedimentation which affects the seismic imaging (Laberg et al., 2001; Dahlgren et al., 2005). High rate of sedimentation had also probably effect on the seismic image of SS 4 to SS 8 in megasequence-1(Fig. 4.6).

The coarser sediments in the diamicton may have all grain sizes from gravel to boulder; however, it might contain glaciotectonic rafts (Sættem et al., 1992; Dahlgren et al., 2005). The composition of the glacigenic debris flows and shelf tills deposits are very similar, suggesting that the sediments retain their composition during the down-slope movements (Laberg and Vorren, 1995; King et al., 1996; Dahlgren et al., 2005).

The depositional pattern of the glacigenic debris flow will be influenced by the geometry of the margin (Dahlgren et al., 2002a; O`Grady and Syvitski, 2002; Dahlgren et al., 2005).
In addition, the rheology of flows and their mode of transport will have impact on the profile i.e., steep or shallow of the wedge (Elverhøi et al., 1997; Dahlgren et al., 2005). The depositional pattern of debris flow may evolve the originally steep margin to a more gently sloping margin revealed as a transformation from a concave or sigmoidal profile to a more uniform oblique profile (Dahlgren et al., 2005). The debris flows may bypass the steepest part of the slope in gullies to be deposited at the toe of the slope. If such depositional pattern continues then slope may achieve a gradient with more uniform dip and deposition takes place along whole of the slope profile. This current sliding complicates the slope profile

nevertheless; slope failure will result into a more sigmoid profile and steep gradient (Dahlgren et al., 2005).

SS 23 and SS 25 of line D (Fig. 4.5), SS 24 to SS 28 of line C (Fig. 4.4), SS 26 of line E (Fig. 4.6) and SS 23 and SS 26 in line given below (Fig. 5.8) showed increased thickness of sediments in bottomsets revealing phenomenon of sediment bypass associated with contouritic currents. These contouritic and hemipelagic sediments provided glide planes for sediment bypass and sliding. The Sklinnadjupet Slide had hemipelagic sediments at its base in megasequence-3 (for instance illustrated in line A, Fig. 4.2). Megasequence-3 has strong influence of contouritic currents. These hemipelagic sediments were characterized by stratified reflections in seismic sections in this study. Furthermore, these fine sediments showed readily glacial-induced compaction (Fig. 4.15).

The high sediment supply is related to the easily erodable sedimentary rocks along the large distances on the wide shelves (O`Grady and Syvitski, 2002). The mid-Norwegian margin reveals typically the geometry and stratal pattern depicted in C and D in (Fig. 5.2) (Dahlgren et al., 2005). The mode of transport, rheology, sediment flux and slope gradient are the controlling parameters for the stratal development on the prograding wedges (Dahlgren et al., 2005).

The sediments have been intermittently redistributed by the large slides on the wedges and further into deep sea basins (Bugge, 1980; King et al., 1996; Evans et al., 1996; Holmes et al., 1998; Laberg and Vorren, 2000; Dahlgren et al., 2005) however, the glide planes of the slides are provided by the hemipelagic/contouritic sediments (Laberg and Vorren, 2000; Bryn et al., 2003; Dahlgren et al., 2005).

The seismic facies associations and cores are used for making the conceptual depositional models (Bulat, 2003; Dahlgren et al., 2005) (Fig. 5.9). The glacigenic sediments of the prograding wedges comprise the transparent, homogeneous, chaotic and structureless seismic facies. The glacigenic deposits representing the debris flows are elongated down-slope and lensoid in cross-section. Their origin is associated to the sufficient sediment supply to the shelf break and upper slope regions during the shelf edge glaciations, down-slope transport of cohesive mud or debris flows and subsequent slope failures (Vorren et al., 1989; Dahlgren et al., 2005).

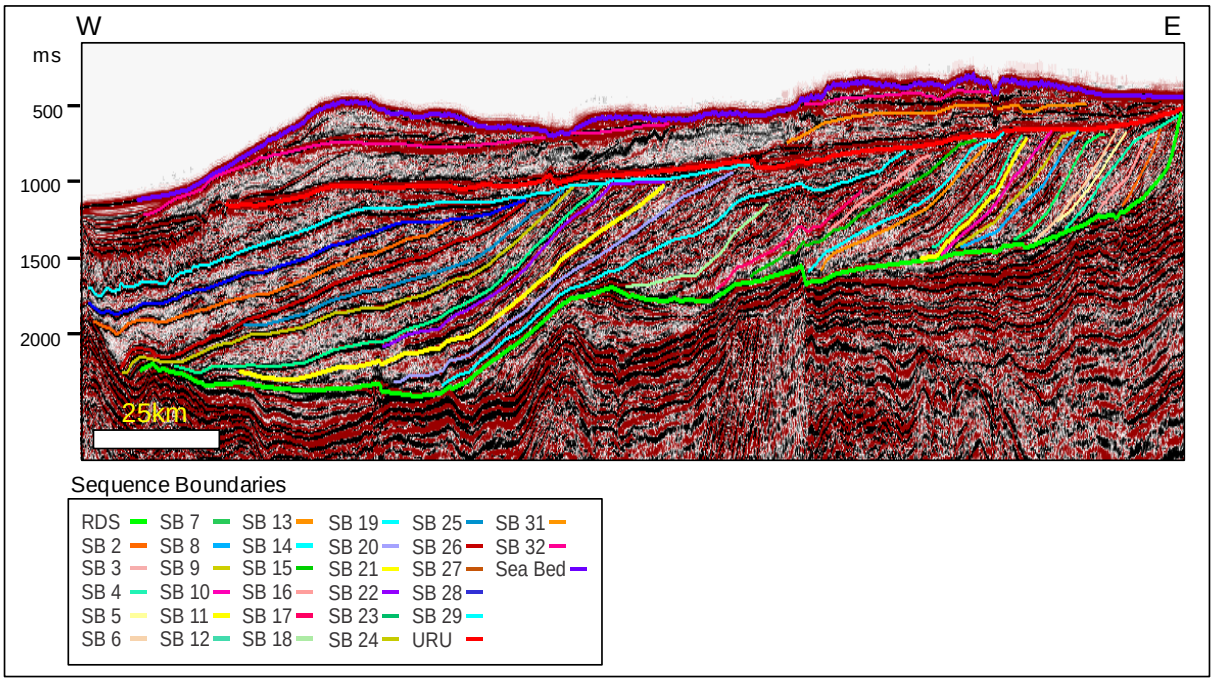

Figure 5.8 Seismic Random line illustrating increased thickness in bottomsets due to sediment bypass. See Fig. 4.2 for legends too.

Individual sequences in megasequence-1 were found to be lenticular in shape and sediment supply was quite enough which assisted mass wasting processes (lines C, D & E). These sediments were interpreted to have mounded reflections particularly in foresets and bottomsets. Lense in SS 30 is preserved indicating floating ice sheet in lines A (Fig. 4.2) and D-I (Figs. 4.5-4.10).

The units comprising many stacked flow lobes draping on the slope demonstrate acoustically transparent reflections on seismic. Their undulating surface holds the only hint of the amalgamated character (King et al., 1996; Dahlgren et al., 2002a; Dahlgren et al., 2005). Internal reflections of SS 4 to SS 8 in lines C, D and E (Figs. 4.4-4.6) showed chaotic to transparent geometry indicating sliding and slumping.

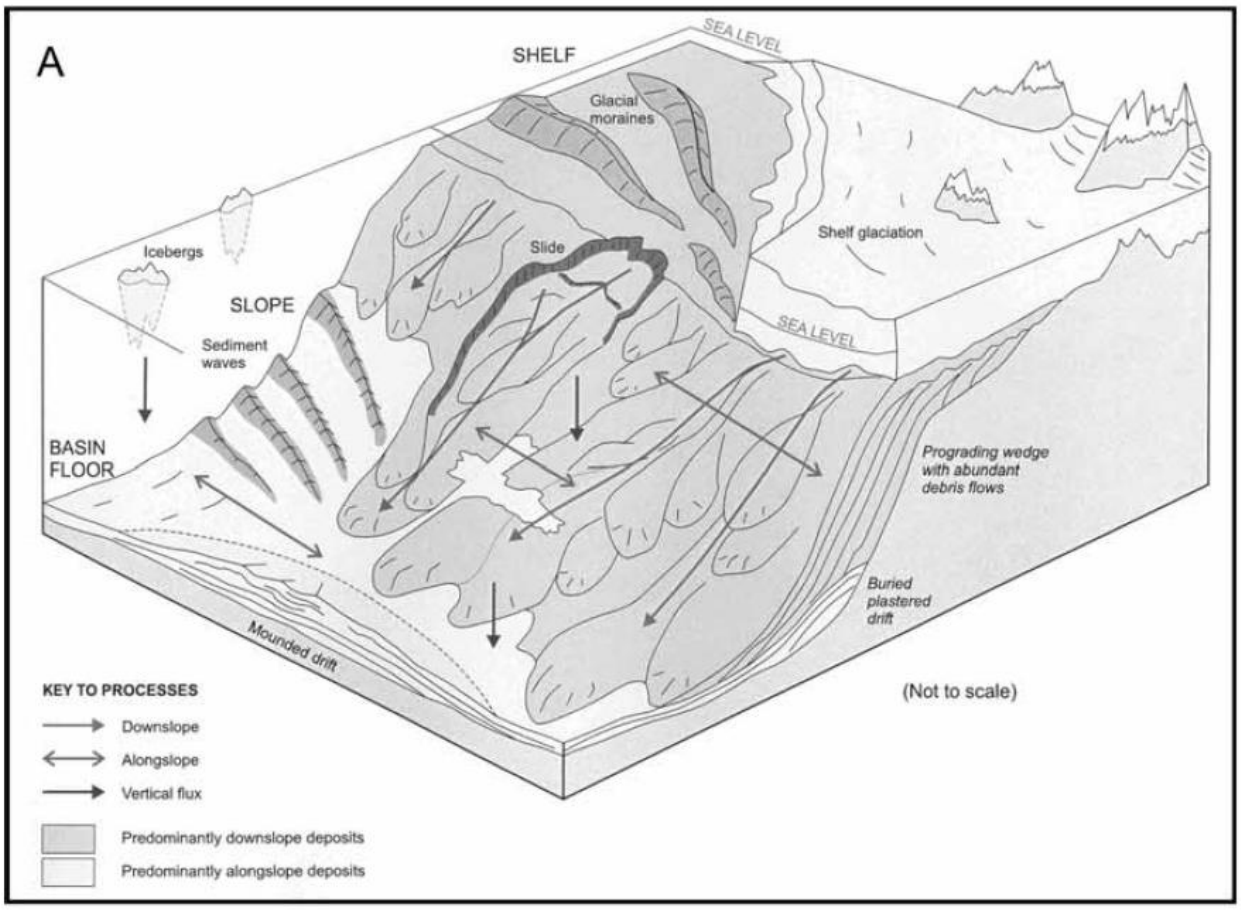

Figure 5.9 A conceptual model displaying the interaction of sedimentary processes and resulting stratal architecture of the deposits, adapted from (STRATAGEM Partners., 2002; Dahlgren et al., 2005).

5.5.1 Depositional Model

A depositional model has been proposed by Berg et al., 2005 based on the Ormen Lange area (Fig. 5.10). The depositional model has been divided into two main stages which are dependent on the climate cyclicity. Stage-1 was peak glaciation while stage-2 was comprised of periods with ice front in a retreated position, including interstadials and interglacials. However, stage-2 was considerably longer than stage-1. The model is here supposed to be generally valid for all glacial periods leaving deposits on the Mid-Norwegian continental shelf.

Hooke and Elverhøi (1996) predicted, based on study of the margin west of Svalbard that the ice front probably have been at the shelf break about 10% of the Weichselian glacial period.

The stages described earlier were differentiated on basis of strikingly different depositional processes. During stage-1, till deposition and glacial debris flow deposition were major processes on slope and outer shelf. Though, glacial marine and normal marine processes occurred on outer continental margin during stage-2 (Fig. 5.10). The glacial processes and the marine currents were influenced by climate and position of ice front, although a suite of processes largely remained same (Berg et al., 2005).

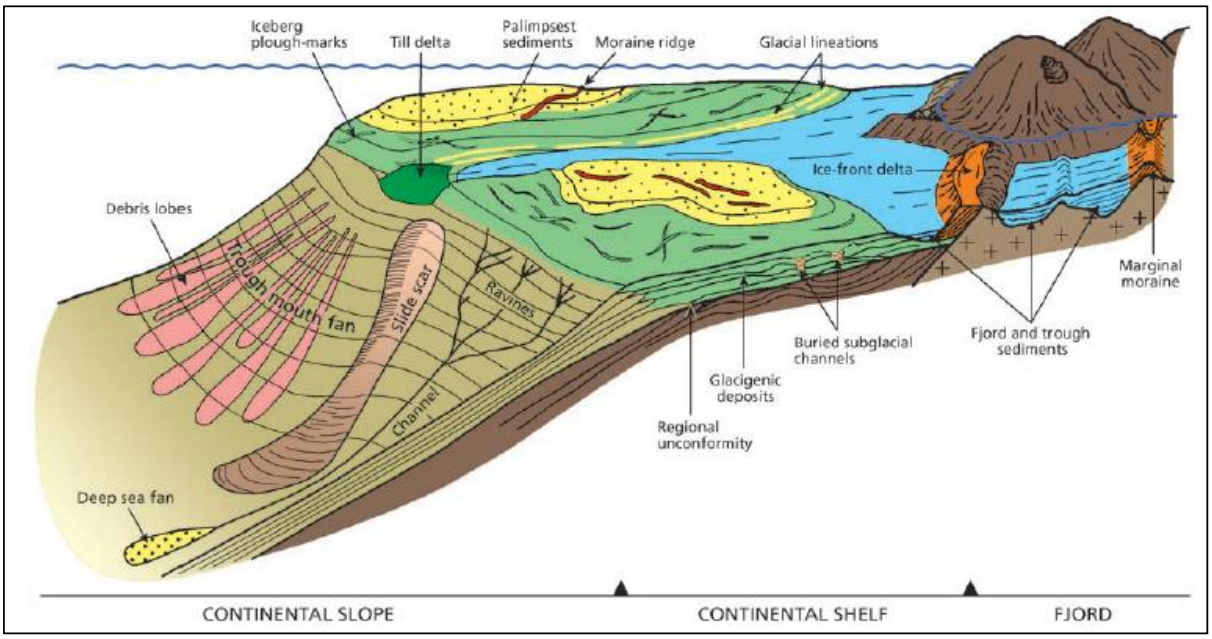

Figure 5.10 Model illustrating the main glacigenic morphological features together with lithofacies of the Norwegian continental margin, exemplified by the margin off northern Norway; modified after Vorren and Mangerud (2006); from Wohlfarth et al., 2008.

The Naust Formation is composed of diamicton with marine and glaciomarine sediments and is also influenced by bottom-currents. Cores of sediments and seismic studies have supported that the last glacial ice sheet floated over a muddy layer interpreted as till (Graham et al., 2007). During glacial periods the rate of sedimentation was very high as ice streams carried a huge amount of sediments playing a significant role for erosion and transportation of sediments.

When fast-flowing grounded ice sheets were broken-up during late Pleistocene, the icebergs were formed and curvi-linear, cross-cutting lineations formed on the seabed which represented plough marks (Figs. 4.2-4.6, 4.9, 4.10 & 5.10). Therefore, iceberg plough marks

observed on seismic lines support the process of breaking-up of ice sheets and icebergs released sediments to be deposited in glaciomarine and marine environment.

Moreover the depositional facies have varied with both climate and distance from ice margin. Various depositional processes may have taken place at various locations on the margin at each time period. Furthermore, marine or distal glacial marine sedimentation affected by currents at variable degrees has existed on the lower slope settings, whereas till was deposited on the outer continental shelf (Berg et al., 2005) (Fig. 5.10).

Sequence boundaries were interpreted during this study separating earlier glacial cycle from later one, revealing compaction of earlier glaciomarine or glacigenic sediments (Figs. 4.2-4.14). During interglacial periods (marine and glaciomarine environments) fine grained sediments were deposited and compaction took place effectively due to low rate of sedimentation.

It is worth stating that the glacial depositional systems are complex; therefore, a simplified depositional model will be described below.

5.5.1a Stage-1: Peak glaciation

Following a substantial period of climatic deterioration, the commencement of continental shelf glaciation involved a major glacial advance, developing a glacial erosion surface across the continental shelf. The sediment source such as the ice front, advanced to the shelf edge, depositional rates on the outer shelf and upper slope raised and the glacial marine sedimentation increased in the deep ocean simultaneously. Fast flowing ice streams followed topographic lows across the shelf stimulating a significant increase in sediment supply to the outer shelf and upper slope together with the IRD (ice rafted detritus) component in the deep sea. However main IRD peaks might have occurred during early deglacial periods (Berg et al., 2005). Sub-glacial layer of deformation till transporting sediments to the shelf break (Nesje et al., 1987; Alley et al., 1989; Nesje and Dahl, 1992; Hooke and Elverhøi, 1996; Berg et al., 2005) led to abrupt build-up of unstable sediment configurations in front of the ice streams, followed by predominating small-scale failures and glacigenic debris flows on the continental slope (Fig. 5.10). This set of processes was critical, causing the shelf edge progradation occurring during the peak glacial period. Recent models demonstrate how glacial debris flows

in front of a fast flowing ice stream produced shelf edge progradation and aggradation (Berg et al., 2005; and references therein). Sediments were also supplied to the margin with melt water together with floating ice. However, in general, these processes were less effective than ice stream transport of deformation till. Thick debris flow deposits belonging to stage-1 may cover huge areas of fine grained deposits from earlier stage-2 deposition (Berg et al., 2005).

It is an important aspect to point out that mass-wasting processes prevailed strongly during deposition of the Naust Formation. Since, mounded reflections in SS 4 to SS 8 in lines C, D, E and L indicated sliding and slumping. Hence, sliding and slumping might be caused by high pore water pressure due to high rate of sedimentation and unstable slope sediments. Furthermore, monoclinal seaward tilting of whole basin during Eocene to Oligocene and earthquakes along the Møre-Trøndelag Fault Zone (Bruhn and Pegrum, 2010) were also significant factors for sliding. The mud diapirs have disturbed the seafloor as illustrated in line E (Fig. 5.11). The Sklinnadjupet Slide had slide plane consisting of stratified reflections and slide eroded sediments over the Helland-Hansen Arch resulting into the scars (also illustrated

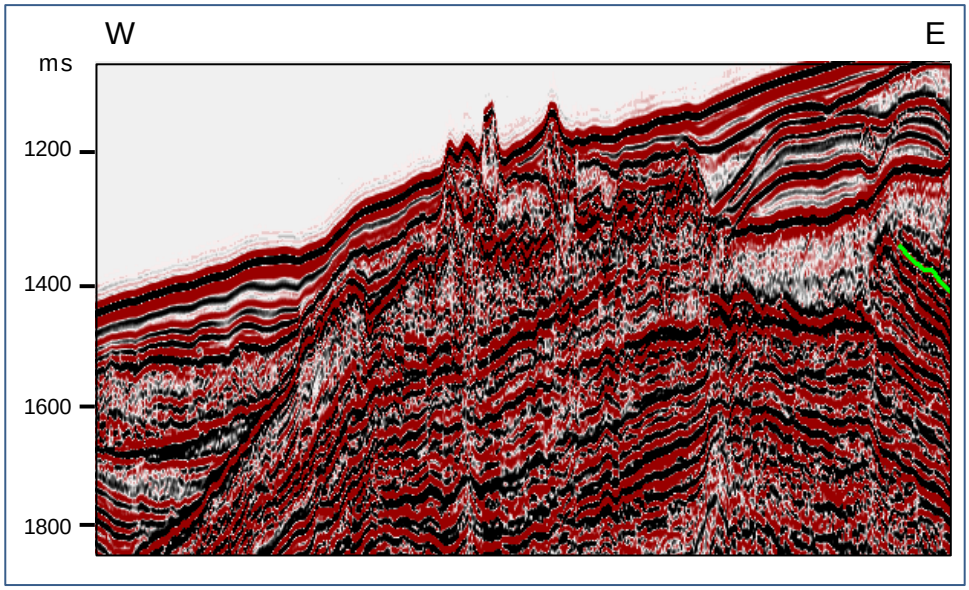

Figure 5.11 The mud diapirs have disturbed the seafloor above the Helland-Hansen Arch.

in Fig. 5.11). Furthermore, currents filled these scars with sediments which they carried with them after erosion and transportation.

Taking this fact into account that the Ormen Lange Gas Field is situated in scar of the Storegga Slide, this must therefore be recognized that the depositional processes related with

the Sklinnadjupet Slide are significant in this study. The pressurized water and perhaps gas may continue to be coming through the liquefaction pathways over the Helland-Hansen Arch (Fig. 5.12).

After climatic betterment and rise in relative sea level, the marine based ice sheet retreated efficiently. During the last glacial phase before lift-off and abrupt retreat, lodgement till was presumably deposited on the outermost continental shelf. During retreat, glacial marine deposition enhanced in front of the retreating ice front (Berg et al., 2005).

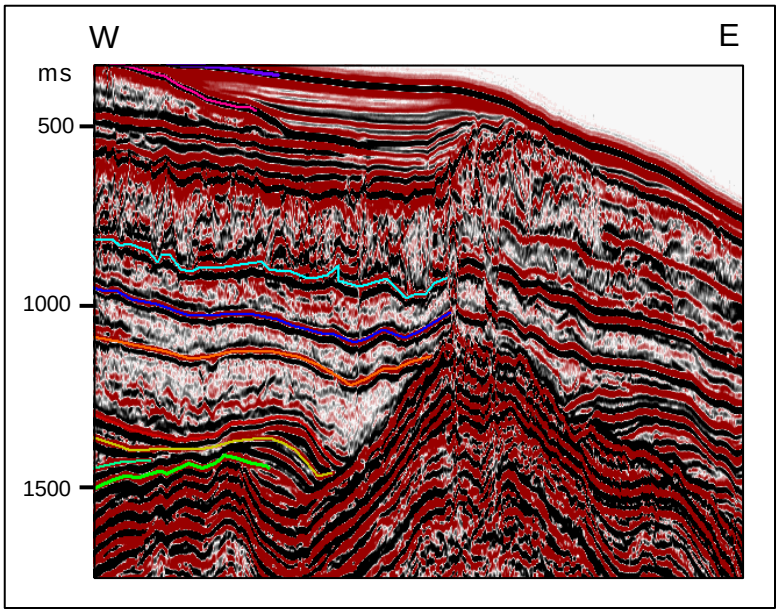

Figure 5.12 Seismic line illustrating deformed sediments and pathways above the Helland-Hansen Arch may be used for releasing the pressurized water or gas.

5.5.1b Stage-2: Periods of reduced ice cover

Stage-2 comprised 80-90% of each glacial-interglacial cycle with quite variable climatic conditions, and true interglacial periods. During stage-2 distal glacial marine and normal marine hemipelagic processes were dominant over entire margin (Fig. 5.10). The glacial marine deposits have a low preservation potential on the continental shelf (Berg et al., 2005). For the reason that erosion through ice streams and ice sheets, moreover sliding and slumping may deform sediments.

As glacial retreat began across the shelf, the development of icebergs and eventually supply of IRD enhanced (Berg et al., 2005). During the present interglacial period (Holocene) after the

Weichselian ice age, icebergs formed plough marks on the seabed in outer shelf (e.g. in lines A-D, Figs. 4.2-4.5).

Normal marine sedimentation recommenced on the slope and in the deep ocean and was partially affected by contour-following currents during the consequent period of retreated ice front (interglacial, interstadial or a limited stadial) (Berg et al., 2005) (Fig. 5.10). Sediments in lateral moraine ridge show contorted reflections corresponding to contorted to transparent facies which show contouritic current influence (lines B-F) (Figs. 4.3-4.7).

The currents might occasionally have been powerful to transport and erode fine sediments, which were re-deposited in the scars formed by previous slides (Fig. 5.10) (Solheim et al., 2005; Berg et al., 2005).

Huge submarine slides i.e., the Holocene Storegga Slide and other older slides are considered to have occurred during initial parts of stage-2 deposition (Solheim et al., 2005; Berg et al., 2005). The Sklinnadjupet Slide (found in SS 29) (e.g. Figs. 4.5-4.7 and 5.14) also probably occurred during interglacial period during relative sea level rise.

The fine grained marine, partly contouritic layers are supposed to provide the detachment levels. Contouritic sediments caused sediment bypass in SS 23 and SS 26 in megasequence-3 (Fig. 5.8). Likewise, stratified reflections in seismic sections were interpreted to be contouritic and hemipelagic sediments (fine grained), which provided glide planes for the Sklinnadjupet Slide and sliding of SS 4 to SS 8 in megasequence-1 in lines C, D and E.

The glacial-interglacial cyclicity, consequent differences in depositional processes, and physical characteristics of sediments related to stage-1 and 2 apparently controlled the sliding process (Bryn et al., 2005; Berg et al., 2005). Climatic deterioration during late stage-2, caused ice accumulation in inland areas and a new glacial period commenced resulting into a new period of stage-1 deposition (Berg et al., 2005).

5.5.2 Megasequence-1

The time-thickness map of megasequence-1 (Fig. 5.13) depicts that on dip lines (Fig. 5.14) thickness is up to approximately 300 ms TWT (c. 270 m) in the Helgeland Basin and thins out west of the Trøndelag Platform. SB 11 downlaps against RDS on east of the Dønna Terrace in

(Fig. 5.14). The strike line L (Fig. 4.14) displays that megasequence-1 is thinning out on the Trøndelag Platform and found again further north, in the Træna Basin (Fig. 4.14). The dip line I (Fig. 4.10) in north on the time thickness map, shows that megasequence-1 consists of almost 250 ms TWT (c. 220 m) in the Træna Basin at position of strike line L and SB 11 laps out before the position of strike line displayed the map (Fig. 5.13).

The first glacial advances to the Norwegian coast developed at 2.8-2.7 Ma (SS 1) as identified by the sudden increase in ice-rafted debris (IRD) in deep sea deposits on the Vøring Plateau and Iceland (Fronval and Jansen, 1996; Eidvin et al., 2000; Smelror et al., 2007). The glaciers

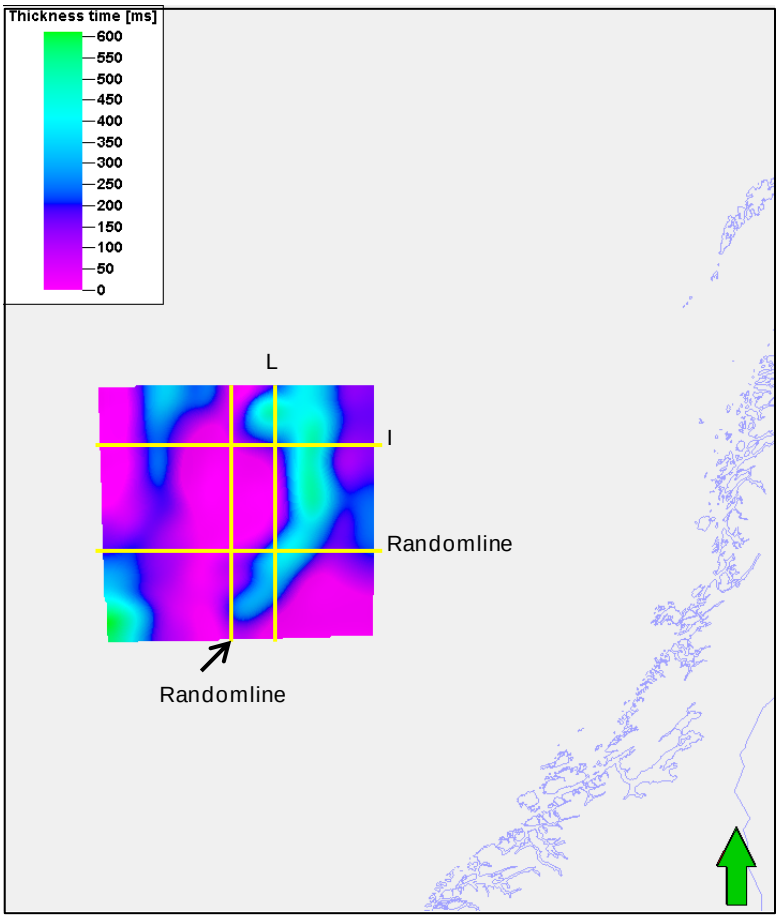

Figure 5.13 Time thickness map between SB 11 & RDS (megasequence-1). Location of key seismic lines and random lines also shown.

did not develop up to shelf and were limited to the mainland until 1.5 Ma (Bugge et al., 2004; Smelror et al., 2007).

5.5.3 Megasequence-2

Line B (Fig. 4.3) is tied with random strike line lying east of line K on the Nordland Ridge. Megasequence-2 is prograding westwards on the Dønna Terrace and thickness is increasing westwards as also shown by the time-thickness map (Fig. 5.15). The thickness is increasing from south to north and reaches up to 900 ms TWT (c. 810 m) in Træna Basin on a random dip line as displayed in the map (Figs. 5.15 and 5.17). It reduces to 700 ms TWT (c. 630 m) on the Nordland Ridge at level where K (Fig. 4.13) is tied with a random dip line (Fig. 5.5) in south of key line G (Fig. 4.8).

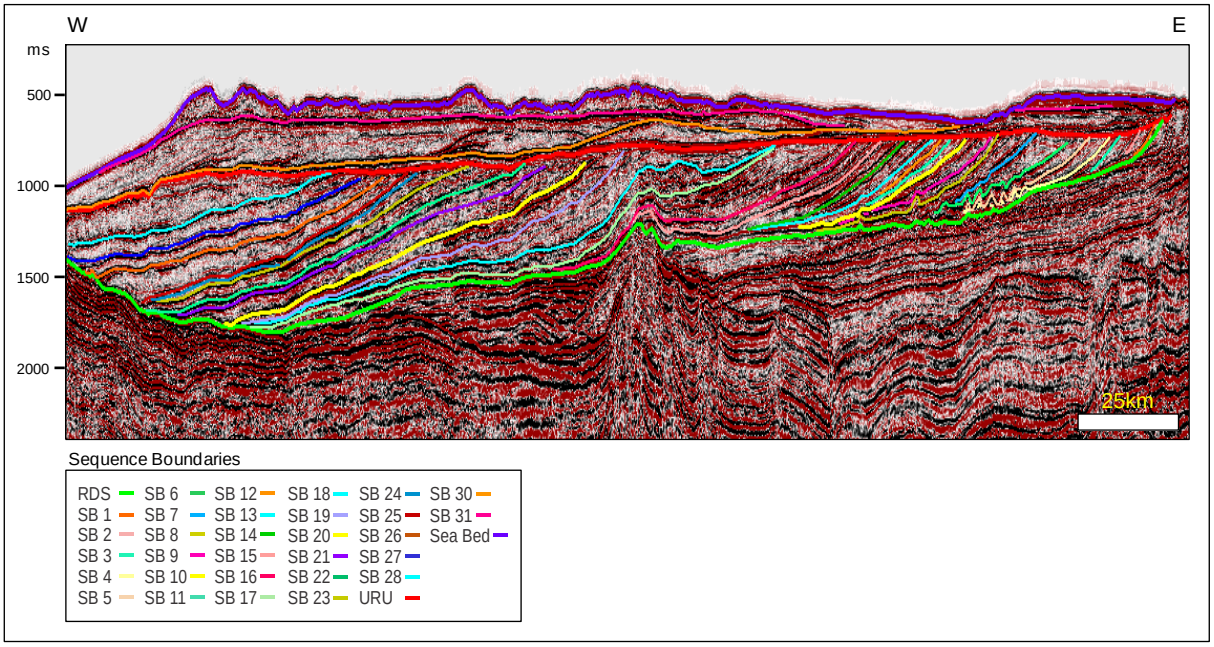

Figure 5.14 Random dip line (north of key line E) illustrating pinch out of SB 11 in east of the Dønna Terrace. See Fig. 4.2 for legends too.

5.5.4 Megasequence-3

The thickness of megasequence-3 is increasing from south to north (Fig. 5.16) while thickness on line B at tie with line J is 400 ms TWT (c. 360 m) in the Rås Basin. The thickness increases in west as shown in line C (Fig. 4.4). The thickness reaches up to 1200 ms TWT (c. 1080 m) in the Vigrid Syncline at level of J (Fig. 4.12) in line illustrated in (Fig. 5.18).

The glaciers are considered to have entered the shelf locally at various periods from 1.5 to 0.5 Ma (SS 18 to SS 27). The amount of IRD enhances greatly during at 1.1 Ma (SS 21) in the

Norwegian Sea (Jansen et al., 2000; Smelror et al., 2007) which is considered to be related with first ice stream expansion to shelf edge through Norwegian Channel (Sejrup et al., 1995; Smelror et al., 2007).

The extension of ice sheets might be estimated with assistance of tunnel valley networking (Graham et al., 2010; 2011). The subglacial tunnel valleys were found in SS 29 of lines e.g. A-I (Fig. 4.2-4.10) and will be discussed later.

5.5.5 Megasequence-4

Time-thickness map between Seabed and URU (megasequence-4) (Fig. 5.17) has almost 100 ms TWT (c. 90 m) in the Vigrid Syncline at the crossing with tied strike line J (Fig. 4.12) as shown in time-thickness map and line shown in Fig. 5.18. Megasequence-4 has thickness of almost 350 ms TWT (c. 310 m) at tied point of strike line in Rås Basin while decreasing west it pinches out in east of Helland-Hansen Arch (Line D, Fig. 4.5).

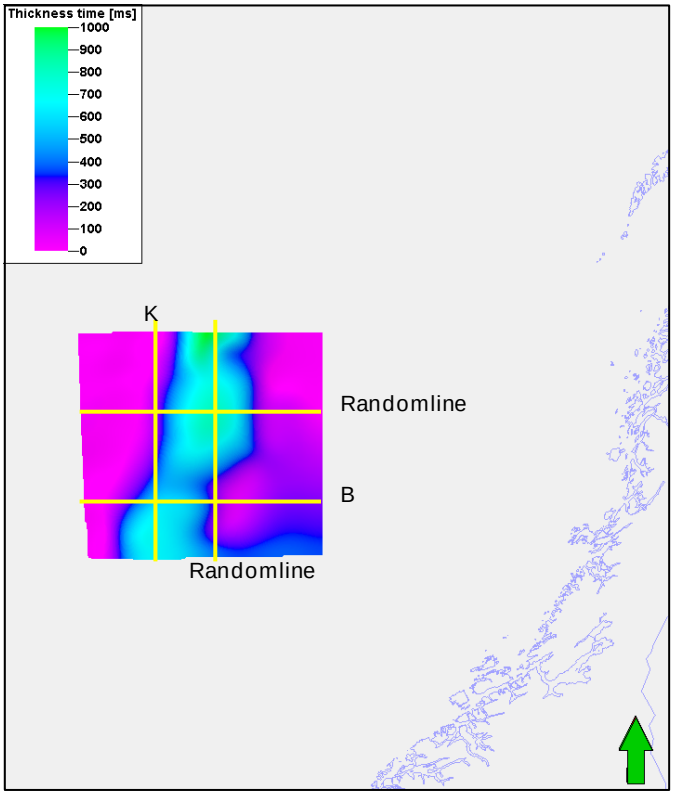

Figure 5.15 Time thickness map between SB 21 & SB 11 (megasequence-2). Map showing maximum thickness of megasequence-2 in north. Location of key seismic lines and random lines also shown.

The ice flowed southwest from the deep trough of Vestfjorden, across the outer Trænabanken and towards the Skjoldryggen area during third and second last glacial periods, Elsterian and Saalian, respectively (Fig. 5.21). The ice flow direction changed significantly after the Saalian and during last glaciation (Weichselian), the dominant ice flow passed through Vestfjorden before turning 90˚ into Trænedjupet and extending up to 100 km to shelf edge (Dowdeswell et al., 2006; Smelror et al., 2007) (Fig. 5.21).

The ice streams during the Saalian period were moving towards west of the study area (Fig. 5.21) and they eroded sediments from areas in the east and deposited them in the west. Whereas, the Weichselian ice streams moved NW and SE of study area (Fig. 5.21).

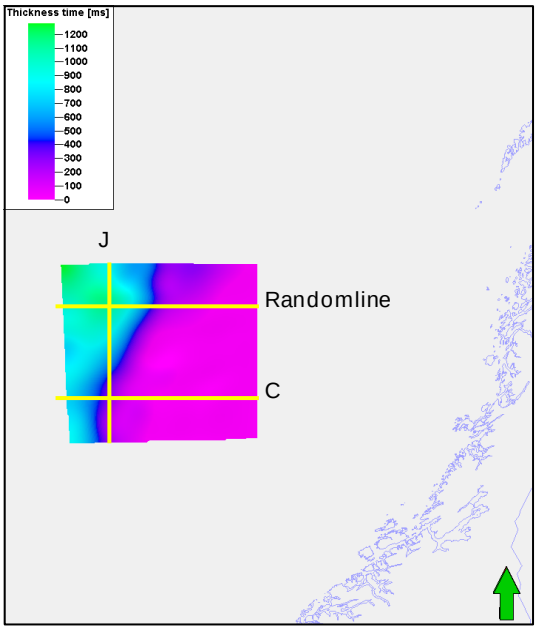

Figure 5.16 Time thickness map between SB 21 & URU (megasequence-3) with overlapped lines including line C and J. Map showing maximum thickness in the northwest revealing northwest progradation of megasequence-3. Location of key seismic lines and random lines also shown.

The ice streams eroded and transported sediments and eventually deposited those sediments in NW. The sedimentary lense is preserved in SS 30 along line J (Fig. 4.12) indicating floating ice sheet as well as relative sea level was dropped to a certain limit which did not cause removal of this lense during Elsterian glacial period.

5.5.6 Whole Naust Formation

The time-thickness map in Fig. 5.19 shows that thickness of the whole Naust Formation decreases from line A northwards to line F (Fig. 4.7) and then increased further north in line H (as illustrated in Fig. 4.9). The map shows that thickness is increased in NW. The thickness of the Naust Formation increases westwards due to development of prograding wedges and deposition by ice streams in northwest. North-south trending strike lines show progradation towards north e.g. in line J (Fig. 4.12) and east-west trending dip lines show progradation towards west. The map (Fig. 5.19) also shows increase in thickness NW.

The shelf was completely covered by ice sheets at the climax of glaciations during the last 0.5 m.y. (Butt et al., 2002; Bugge et al., 2004; Ottesen et al., 2005; Rise et al., 2005; Smelror et al., 2007). The Norwegian Channel ice stream played a key role during the last three glaciations while sediments were deposited beyond shelf edge forming thick succession of glacigenic debris on the North Sea Fan (Rise et al., 2005; Smelror et al., 2007).

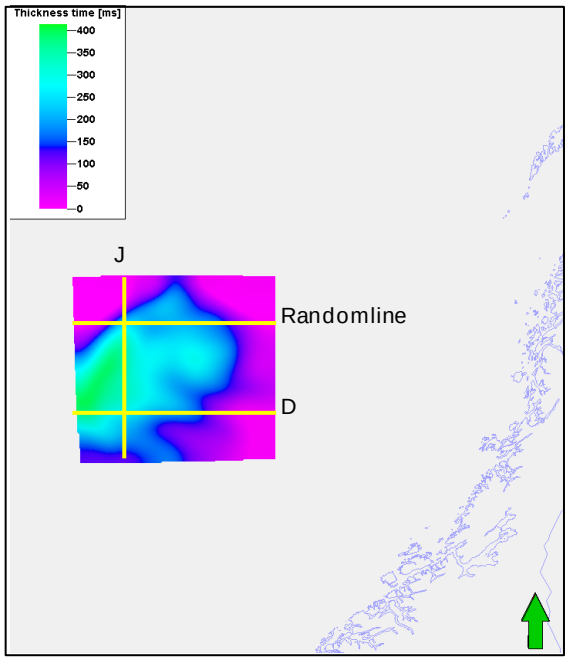

Figure 5.17 Time thickness map between URU & seabed (megasequence-4) with overlapped lines including line J and D. Location of key seismic lines and random lines also shown.

The Quaternary glaciation appears to have eroded approximately 520 m from bedrock in a large area of mid-Norway (Dowdeswell et al., 2010; Mangerud et al., 2011), and these

sediments have been deposited making progradational wedge during development of the Naust Formation.

5.6 Comparison with glaciations on Iceland and Svalbard

The biostratigraphic analysis suggests that the prograding wedge in the glaciomarine environment off Mid-Norway developed earlier than 2.3 Ma (Dahlgren et al., 2005; and references therein). Jansen et al. (2000) estimated the onset of first glaciation on the coastal areas of Norway to 2.74 Ma, based on the marked increase in the supply of ice rafted detritus (IRD) (Dahlgren et al., 2005). In north and mid-Norway, the development of glacigenic wedge growth was initiated at 2.74 Ma when there were small, mountain-centered ice sheets and during second phase, large scale Fennoscandian Ice Sheets developed during 1.1 to 0.9 Ma. However, the dating of the proximal parts of the sedimentary wedges offshore Norway is uncertain (Dahlgren et al., 2005). The high subsidence as well as the autocyclic sequence of glacial advances had variable magnitude (Dahlgren et al., 2002 a, b; Dahlgren et al., 2005).

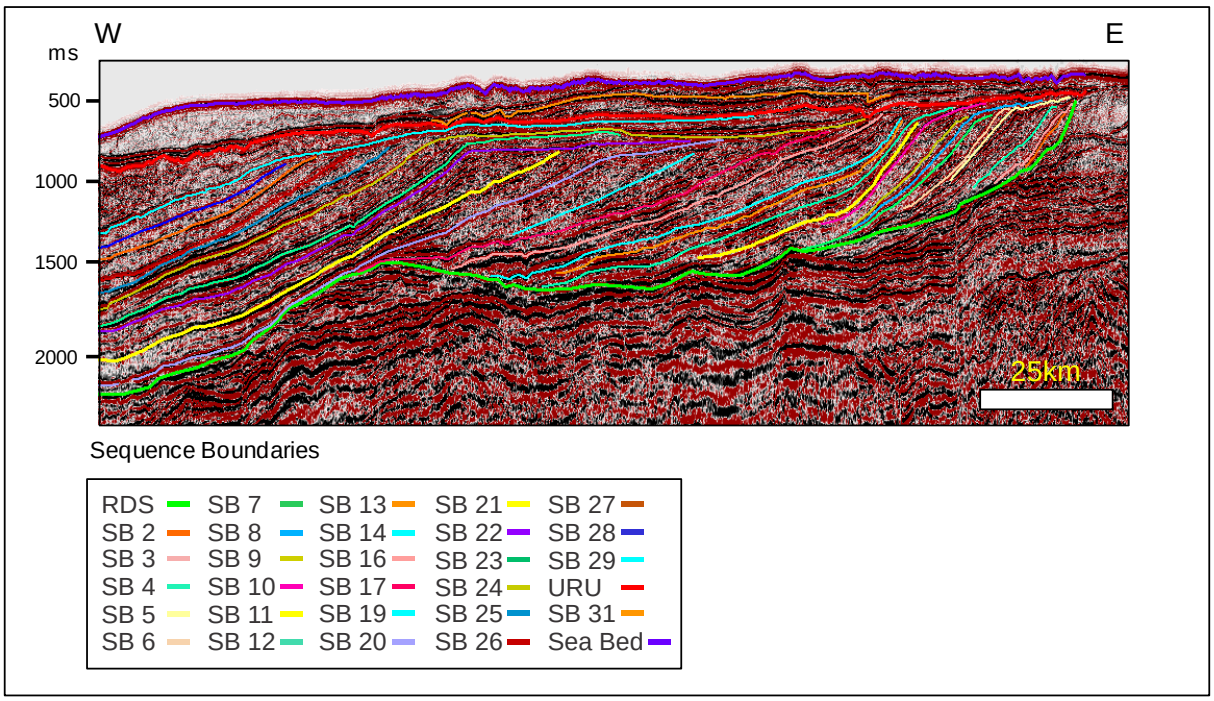

Figure 5.18 Random dip line (south of key line I) illustrating thickness of megasequence-4. See Fig. 4.2 for legends too.

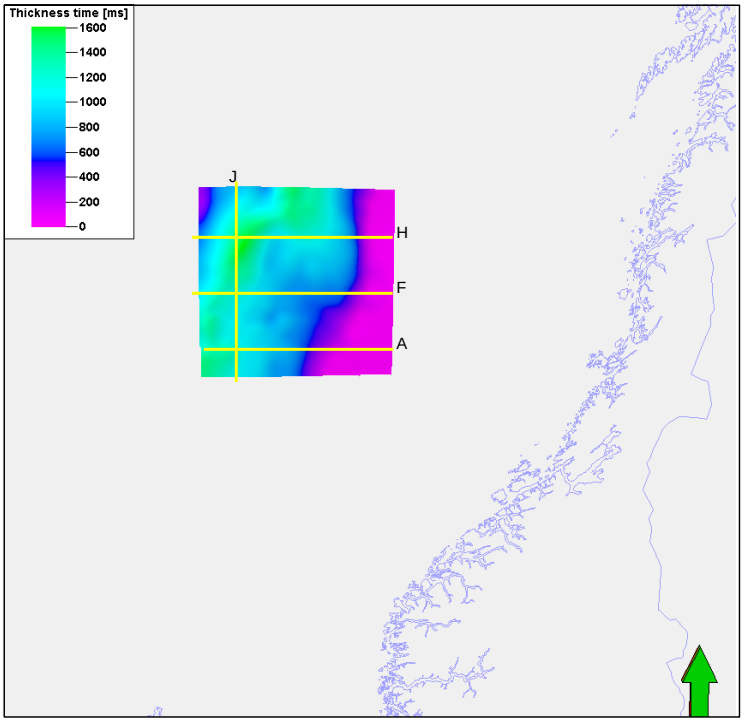

Figure 5.19 Time thickness map between RDS & seabed (whole Naust Formation). Thickness of the Naust Formation increased in northwest revealing ice stream deposition in northwest during the last glaciation as well as northwest progradation. Location of key seismic lines and random lines also shown.

Ages of glacial deposits in Iceland have been correlated with palaeomagnetic timescale of lava pile. K-Ar and fission-track ages of tephra associated with glacial deposits have been utilized and ages are estimated by Geirsdóttir and Eiríksson (1994). The recurrence frequency of the Iceland ice sheets were established comparable with deep-sea oxygen isotope amount from that of North Atlantic. The composite stratigraphy from east and north sections of Iceland demonstrated at least 22 glacial-interglacial cycles during last 3 Ma.

Three phases of ice growth have been envisioned, the initial phase was comprised of ice covering mountainous areas located in south-east from >4 to 3Ma, during the second phase (3-2.5 Ma) ice sheets covered most of Iceland, as documented from glacial deposits found across the country (Graham et al., 2011). It is proposed that extensive glaciation was initiated almost at about 2.9 Ma in Iceland. Valleys with 400 m depth were formed in the Tertiary basalts of eastern Iceland during 2.5-0.5 Ma. On the other hand, during the last 0.5 m.y. erosion rate was significantly increased from 50 to 175 cm/ka due to which 600 m deep valleys were incised. Therefore it is testified through very high rates of erosion, huge amount

of ice-rafted detritus as well as increased amount of ð ^{18}O in marine sediments that extensive glaciations occurred during 2.5 Ma and 0.5 Ma (Geirsdóttir et al., 2007).

Light ð ^{18}O values demonstrate interglacial periods as well as melt-water predominance. In addition, existence of light ð ^{18}O related with IRD peaks may indicate melt-water effect. Furthermore, more than 1% enrichment of ð ^{18}O indicates more than 4˚C increase in temperature. The ice-rafted debris peaks related to the Late Weichselian in the Fram Strait and Svalbard/Barents Sea were analyzed and hence found comparable (Mangerud et al., 1998).

IRD peaks are associated with lower values of ð ^{18}O and this association is established throughout the Norwegian Sea (Dokken and Hald, 1996; Mangerud et al., 1998). Similarly, IRD peaks are associated with break-up of the ice sheets of the great Isotope Stage 4, reflecting high iceberg production together with extensive melt-water runoff in Scandinavia (Baumann et al., 1995), Svalbard and Northern Barents Sea (Mangerud et al., 1998).

At c. 2.8 Ma glaciation occurred at large scale in Scandinavia, Svalbard and the Barents Sea; this is substantiated by ð ^{18}O curves (Fig. 5.20) together with IRD and palynological results. Whereas maximum erosion took place in the Svalbard and Barents Sea region between 2.8-0.9 Ma. Interglacial periods covered almost 6 to 8%, however the Late Weichselian covered < 5% of total time during last 2.6 Ma. Nevertheless, ice sheets covered Scandinavia through 90% of this time duration and they accessed western coast of Norway for much of this time period. It is noteworthy that great fluctuations held during last 900 k.y. due to the existence of the largest ice sheets and the most warm interglacials (Mangerud et al., 1996).
Elsterian glaciation has been revealed during this study through typical morphological element of subglacial tunnel valleys in SS 29 of lines A-I (see chapter 4). These tunnel valleys are related with unconformity formed during the Elsterian glacial stage found throughout the North Sea Basin (Huuse and Lykke-Andersen, 2000; Stoker et al., 2010; Graham et al., 2011). Episodic phases of valley incision took place due to meltwater (Lonergan et al 2006) as well as ice sheet was eroding and re-eroding its bed (Stewart and Lonergan 2011; Graham et al., 2011).

Durations of glacial-interglacial cycles were comparatively more fluctuating in megasequence-1 and 2 than megasequence-3 and 4. This is evident from increase in thickness

of individual sequences from megasequence-1 to 3 in seismic sections as well as ð ^{18}O curves in Iceland. ð ^{18}O curves reveal that interglacial periods have been warmer since c. 1 m.y. than previous interglacial periods. Rise in relative sea level due to warmer interglacial periods might have reasoned huge slides at almost 0.2 m.y.

The morphological features found in the seismic sections, i.e. iceberg plough marks on seabed (for instance Figs. 4.2 and 4.3), demonstrate that during the extensive Late Weichselian maximum, grounded ice was existing and was broken-up afterwards.

5.6.1 Ice Flow Model and Glacial Dynamics

Ice-flow models for the Scandinavian ice sheet during the Late Weichselian has been constructed through extensive bathymetric data analysis together with preceding research on the Norwegian continental shelf (Vorren and Laberg, 1997) and on basis of Antarctic Ice Sheet and ice streams (Ottesen et al., 2001). The first aspect to point out is that ice streams are considered to be foremost important in the dynamics of palaeo-ice sheets. The ice sheet mass balance may probably be re-organized through ice streams (Ottesen, 2006). Ice streams played undoubtedly most significant role in overall glacial dynamics; this fact is highlighted by Hubbard et al. (2009) and Graham et al. (2009; 2011). I infer that the glacial dynamics, including ice streams, were principally the same also during formation of all the glacial sequences reported here.

To assess the dynamic ice-flow pattern along the western margin of Barents Sea/Svalbard as well as the Scandinavian ice sheets, an analysis of regional morphology and extensive bathymetric data of Norwegian continental shelf extending from the North Sea (57˚N) to Svalbard (80˚N) were used (Ottesen et al., 2001, 2005 & Ottesen, 2006). The variations in ice sheet dimensions, dynamics, and intensity of particular glacial cycles as well as complex ice sheet dynamics in solitary deglaciations are of utmost importance (Dowdeswell et al., 2010).
It is worth stating at this point that ice sheet thickness, relative sea level as well as buoyancy are major factors for determining the ice margins. In addition, prograded shelf wedges are particularly controlled by ice margins (Miller, 1996). Glacial erosion and deposition are determined through buoyancy, whereas buoyancy establishes boundary at shelf where ice sheet may set up floating. With an increasing sea level, a grounded ice sheet becomes

buoyant, floats, breaks up and makes icebergs at its front. This process, in turn, releases sediments from the sole of the floating ice, as well as at the ice margin, and from melting ice bergs. The floating ice sheet does not erode earlier sediments. This mechanism of floating ice sheet is interpreted to explain the presence of the sedimentary lense that was recorded in SS-30, as shown in random seismic dip line illustrated in (Fig. 5.18) which is in north of line H.

Ice streams are parts of ice sheets that flow at faster rate as compared to adjacent parts of the ice sheets; moreover their direction may vary from that of the ice sheet as a whole (Swithinbank, 1954). Ice streams move with velocity of almost 100 m to several kms per year and may have widths of 10 to 100 km. Ice streams may have lengths up to several hundreds of kilometers. Ice streams are generally associated with the most extensive ice sheets, and ice streams drain a tangible part of the ice masses. For instance, above 90 % of the whole ice mass budget of the Antarctic Ice Sheet is drained through ice streams (Bamber et al., 2000; Ottesen, 2006).

Earlier pathways of fast moving ice streams related to almost 20 cross shelf troughs were interpreted through mega-scale glacial lineations (MSGL), along with elongate ridges and grooves having parallel orientation to trough long axes (Ottesen, 2006) (Fig. 5.21). Moreover, two leading ice streams, Norwegian Channel Ice Stream as well as Bear Island Trough Ice Stream were existing during Late Pliocene/Pleistocene, each having 150 to 200 km widths at their mouths (King et al., 1996; Nygård et al., 2004; Sejrup et al., 2003; Vorren and Laberg, 1997; Dowdeswell et al., 2006; Ottesen, 2006). The troughs in the mid-Norwegian continental shelf provided pathways to fast flowing ice streams during numerous glaciations (Ottesen et al., 2005; Rise et al., 2005; Dowdeswell et al., 2006; Ottesen et al., 2009). The Norwegian Channel is 800 km long, the largest ice-generated trough existing parallel to the coastline off southern Norway (Longva & Thorsnes 1997; Sejrup et al., 2003; Ottesen et al., 2005; Ottesen et al., 2009). The age of the Norwegian channel based upon study of sediments near channel base is dated to be at least 1.1 Ma by Sejrup et al. (1995) (Ottesen et al., 2009).

Besides these large ice streams, many large submarine fans at mouths of major cross-shelf troughs have been interpreted after analysis of large scale margin profile and seismic data (King et al., 1996; Nygård et al., 2004; Sejrup et al., 2003; Vorren and Laberg, 1997; Dowdeswell et al., 2006; Ottesen, 2006).

Maximum number of palaeo ice streams followed topographic lows on the Norwegian Shelf. Whilst crossing conjunction between crystalline and sedimentary rocks seawards, passing through coastline on inner shelf, ice streams or outlet glaciers were predicted to coalesce making broader corridors (c. 20 to 150 km width). It is worth stating that location of palaeo ice streams becomes significant for reorganizing palaeo-ice sheets since ice streams regulate mass balance together with stability of ice sheets (Ottesen, 2006).

In brief, seven controlling factors are significant for establishing the location of ice streams in ice sheets. These factors are topographic focusing, topographic steps, macro-scale bed roughness, calving margins, subglacial geology, geothermal heat flux as well as subglacial meltwater routing. Topographic focusing exhibits the foremost control when calving margin exists (Fig. 5.22). In spite of this, ice streams follow subglacial meltwater pathways and favourable subglacial geology. If earlier factors do not exist, then bed roughness, geothermal heat flux plus topographic steps may probably control ice streaming. Ice steams may behave variably when they are governed by meltwater routing and/or calving processes for the reason that these factors may vary comparatively on short time scales than others varying on long time scales. For instance, geothermal heat flux, subglacial roughness, geology and topography may vary long time scales, which seems to confirm the idea that controlling factors for ice stream location are of vital importance for ice stream permanence, past and future mobility (Winsborrow et al., 2010).

During the last glaciations the large cross shelf troughs and slides such as the Sklinnadjupet Slide (Fig. 5. 23) in study area and scars of gigantic submarine slides were developed by the palaeo-ice streams on the shelf edge (Smelror et al., 2007). The Sklinnadjupet Slide is clearly observable on various lines e.g. line D, E, F (Figs. 4.5, 4.6 & 4.7) and line given below (Fig. 5.23). Strike lines proved to be very helpful tool for tie with dip lines as well as for interpretation of some significant processes. For example, strike line L shown in chapter 4 (Fig. 4.14) demonstrates clinothems to be inter-fingered. SS 16, SS 17, SS 18, SS 21and SS 23 are inter-fingering in a trough which are inferred to be formed by the ice streams coming from north and south directions (Figs. 4.14 & 5.24).

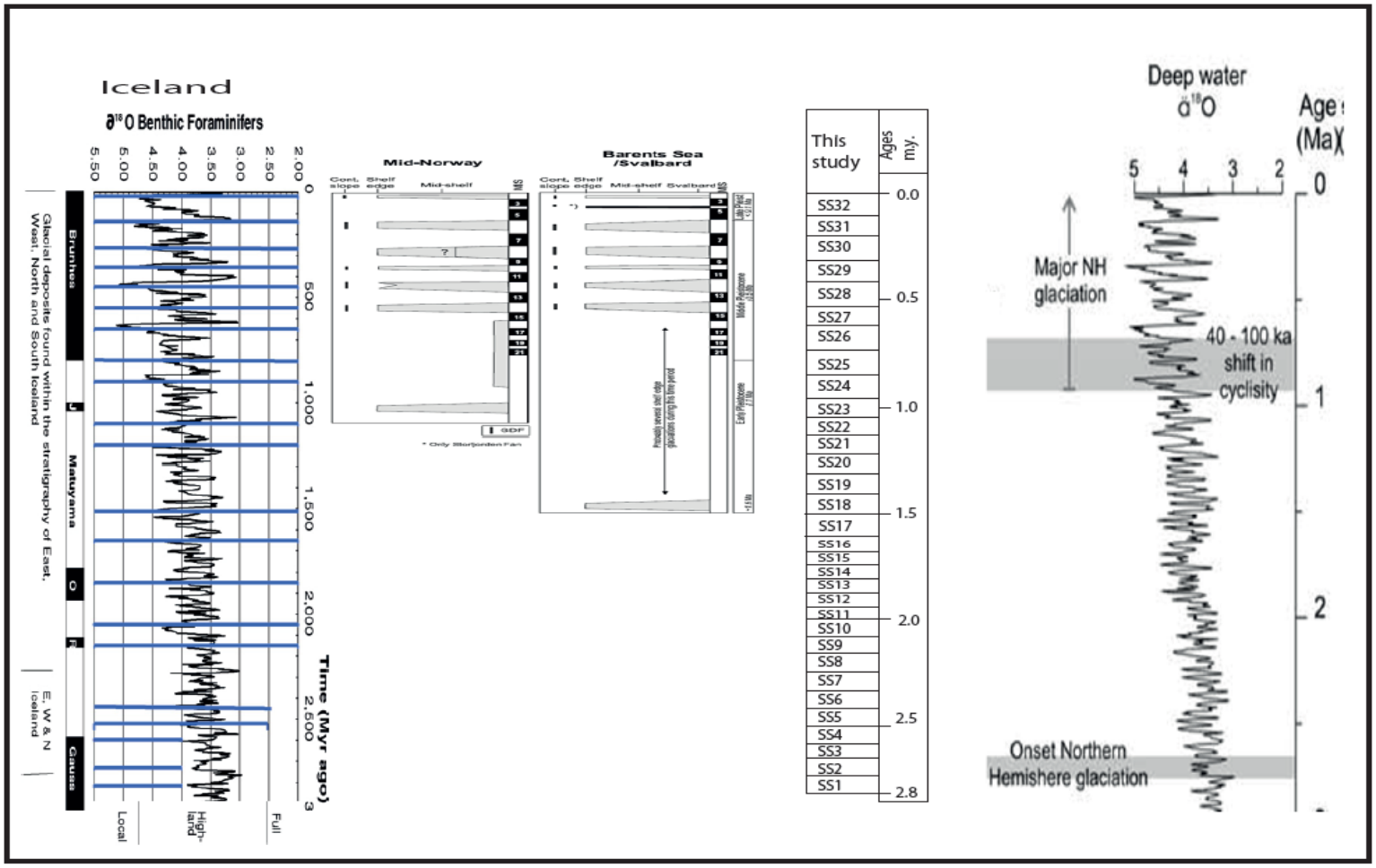

Figure 5.20 Correlation of seismic sequences along the mid-Norway, Barents Sea/Svalbard, Iceland together with sequences of this study showing comparison with $\delta^{18}O$ curve (modified from Sejrup et al., 2005, Dahlgren et al., 2005 and Geirsdóttir et al., 2006; Hafeez, 2011).

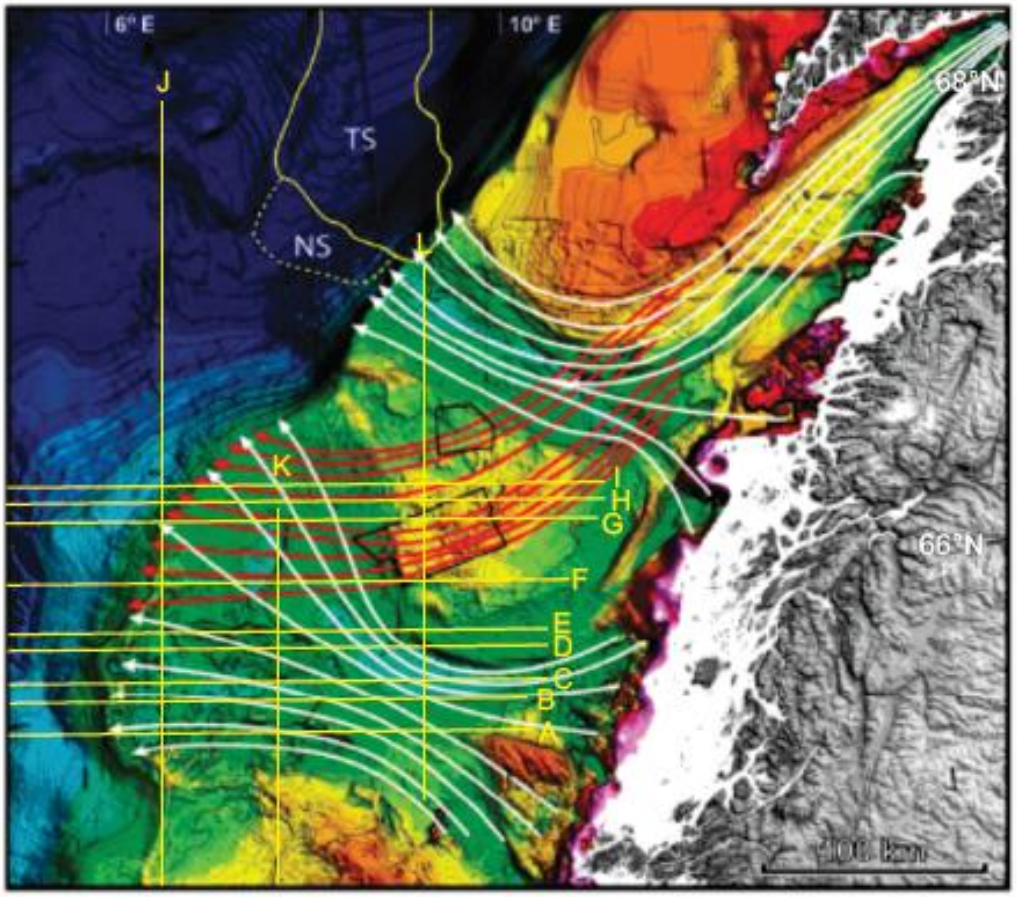

Figure 5.21 Map showing changing ice stream flow directions on the mid-Norwegian Shelf from the Elster/Saalian (red lines) to the Weichselian (white lines). TS-Trænadjupet Slide; NS-Nyk Slide (From Dowdeswell et al., 2006) from Smelror et al., 2007.

	Favourable →	Unfavourable
Strong	Topographic trough	Flat bed
	Calving margin	Land terminating
	Soft bed	Hard bed
	Abundant meltwater	Scarce meltwater
	Smooth bed	Rough bed
	High geothermal heat flux	Low geothermal heat flux
Weak	Topographic step	Flat bed

Figure 5.22 Generalized scheme of controlling factors for ice stream location. Primary controls are topographic focusing and existence of calving margin; secondary are suitable subglacial geology and meltwater pathways. While in nonexistence of above described primary and secondary factors, flat bed, high geothermal heat flux or topographic step may be influential (from Winsborrow et al., 2010).

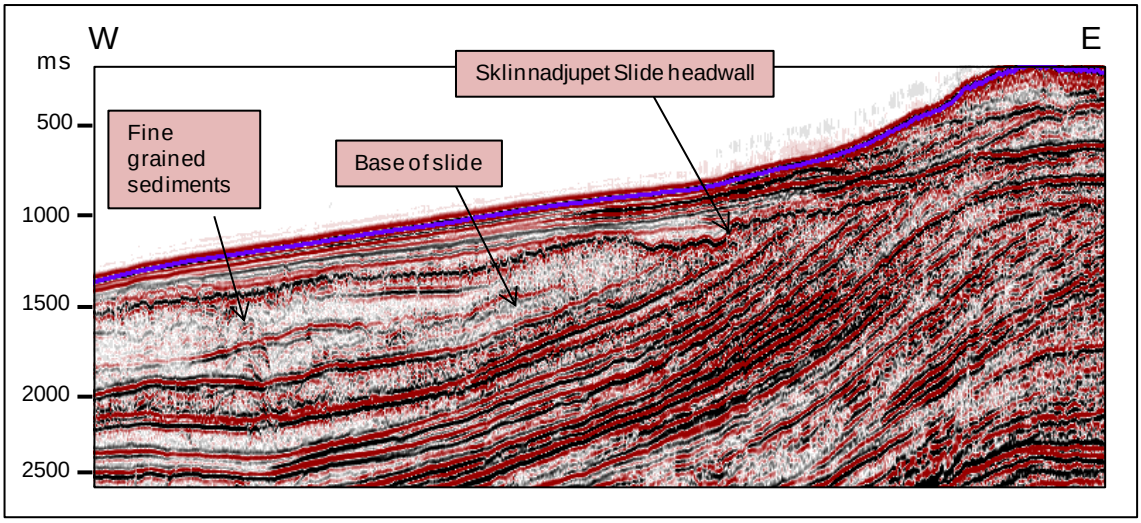

Figure 5.23 Seismic section illustrating the Sklinnadjupet Slide with its head wall and base. In addition, fine grained sediments illustrating chaotic to transparent reflections.

In addition, the URU is continuous above these sequences suggesting that trough was formed by ice streams but not by erosion at time of development of the URU. It is important to add that the Weichselian glacial ice streams eroded previously deposited sediments related to the Saalian glacial period and older sediments. While making comparison among lines from south to north, line A demonstrates preservation of lense of SS 30 in Dønna Terrace

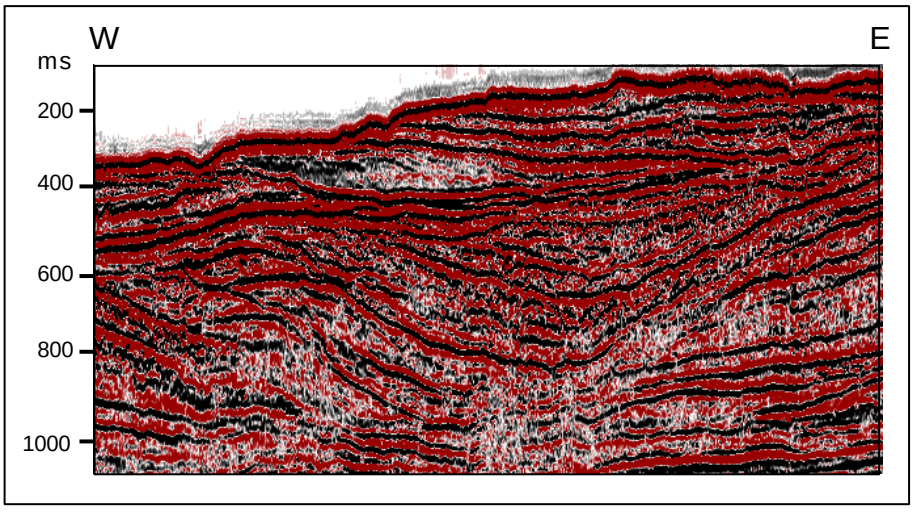

Figure 5.24 Random seismic section showing inter-fingering in trough while the URU is continuous above these sequences indicating ice streams heading from north and south directions.

while SB 31 was eroded further east showing that ice streams eroded SS 30 from east (Fig. 4.2). North of line A, line B and C show that the Weichselian ice streams were located in north as well represented by erosion of SB 31 (Figs. 4.3 & 4.4). The Weichselian ice streams eroded sediments deposited by Saalian, earlier interglacial and older sediments and eventually deposited these sediments as lateral moraine deposits (Figs. 4.3-4.7).

The ground moraine (Roksandic et al., 1978) situated within SS 32 is inferred to be formed by ice-push; in addition it seems to be superimposed on the palaeo-ice streams (Graham et al., 2009; 2011) as depicted in (Figs. 4.7 and 4.14). Moraines are thought to be generated by deglaciation phase rather than the Late Weichselian maximum (Graham et al., 2009; 2011).

The channels are considered to be incised during glacial maximum and melt-water channels have been filled by sediments during ice-recession (Graham et al., 2009; 2011). The channel found on the seabed in line B between SP 5412 and 7012 is interpreted to be formed through incision during the last glacial maximum (Fig. 4.3).

The remarkable features of iceberg plough marks remained preserved which were formed by scouring action of icebergs on seafloor during deglaciation (Graham et al., 2010; 2011). Ice-rafted debris (IRD) manifested continuous glacial records being deposited from icebergs. It is reasoned that ice sheets have been attaining tangible size before releasing icebergs (Mangerud et al., 2011).

5.7 Chronostratigraphic Chart

Chronostratigraphic chart is a graphic representation containing geological time scale along vertical axis and distance along horizontal axis. A chronostratigraphic chart illustrates relative ages and geographic extension of strata or stratigraphic units in a certain area; the type of chart is also termed a Wheeler diagram (Wheeler, 1958). Furthermore, a chronostratigraphic chart may briefly display sequence stratigraphic interpretations.

The chronostratigraphic chart in this study is constructed along line G and ages of these sequences have been assigned with those predicted by Rise et al., (2010). The chronostratigraphic chart clearly demonstrates development of sequences towards west during development of the Naust Formation (Fig. 5.25). Each of these 32 sequences has been

interpolated to have age of 0.1 Ma except SS 29 and SS 32. Each glacial cycle has been separated from the previous one through a sequence boundary having a high acoustic impedance contrast. Progradation was exhibited strongly before development of URU, however sequences deposited above URU show aggradation.

SS 30 and SS 31 cover comparatively extensive area from east to west (Fig. 5.25). Progradation of sequences below URU demonstrate relative sea level fall, enough sediment supply and subsidence due to glacial loading as well as through sediment loading. The aggrading sequences above URU were deposited during the last two glacial and interglacial cycles.

On the mid-Norwegian Shelf, the glaciers broadened to the shelf break both before and after the development of the URU (Dahlgren et al., 2005).

The ice sheets were floating during formation of SS 30 resulting in formation of a sedimentary lense. The aggradation refers to the relative sea level rise and hence increase in accommodation space. Extensive ice sheets were broken up due to retrogressive sea level and generated icebergs which released sediments. As mentioned in chapter 4, the iceberg plough marks indicated the break-up of the extensive ice sheets. In addition, lateral morainal ridge at the Skjoldryggen area represents the deposition through ice streams in northwest. Furthermore, currents have also influenced sediments as shown by contorted reflections.

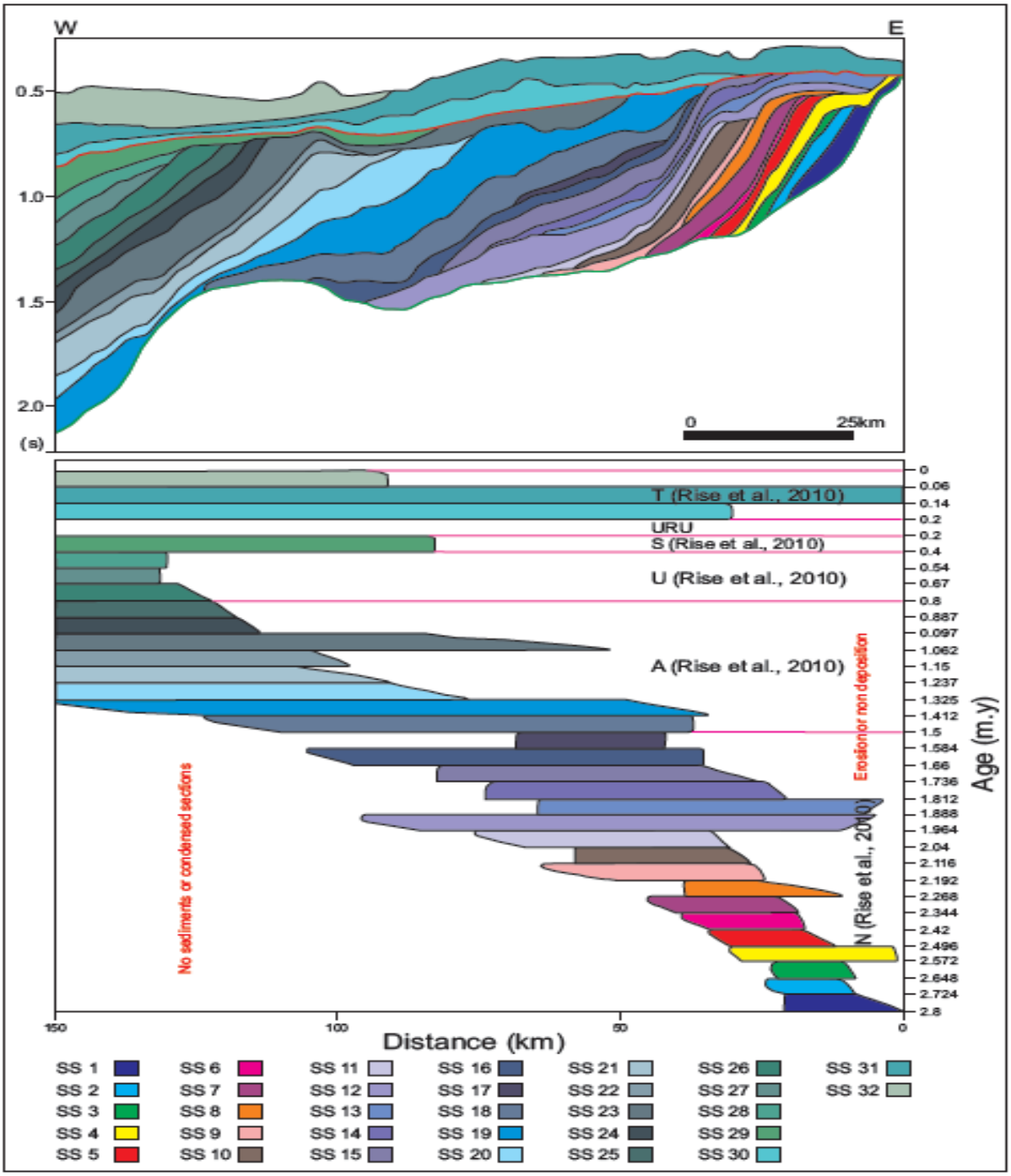

Figure 5.25 Chronostratigraphic chart (Wheeler diagram) of line G (illustrated in Fig. 4.8) along with integrated ages and distribution of sequences.

Conclusions

The mid-Norwegian continental shelf got its present configuration during the last 2.8 m.y. with deposition of the progradational Naust Formation. The Naust Formation developed during high sedimentation rate, triggered by uplift and repeated glaciations of mainland Norway. High rate of glacial erosion and transport of debris by ice sheets to a several hundred meters deep sea along the mid-Norwegian coast gave rise to the progradation of the Naust Formation with a maximum thickness of 1600 meters. The formation consists of 32 seismic stratigraphic sequences representing altogether 32 glacial-interglacial cycles. The sequences filled in an accommodation space above a Regional Downlap Surface (RDS) by successive progradation towards the NW of glaciomarine and interglacial sediments during the 32 glacial periods. Thick ice sheets and ice streams eroded, transported and deposited sediments by melting of glacial debris from below of grounded and floating glacial ice as well as at the calving front of the ice sheets at the shelf edge. Glacial till material, debris flows, slides and other gravity flow sediments produced clinothems that downlapped against the RDS and demonstrate that RDS was a maximum flooding surface. Ice berg erratics and suspended mud and clay were deposited as hemipelagic sediments further out in the marine basin. Reworking by marine currents as contourites took place episodically.

Fall and rise in relative sea level repetitively occurred after the formation of the RDS during successive glaciations-interglaciations, as a result of glacioeustacy and differential subsidence. RDS and glacial sequence clinothems were truncated by glacial erosion from grounded shelf ice sheets younger than glaciation No. 29. The Upper Regional Unconformity (URU, and sequence boundary 30) was formed. The unconformity represents a major fall in relative sea level.

Preservation of topset beds in glacial sequences represents rise in relative sea level. Moreover, geomorphological features like tunnel valleys and melt water channels are regarded as formed through incision by thick ice sheets and ice streams during fall in relative sea level. Ice-berg plough marks were as well likely produced on the shelf during all glacial periods. Mass wasting processes and mud diapirs prevailed during the depositional history of the Naust Formation as a result of high rate of sediment supply and rise in relative sea level.

The 32 glacial sequences of the Naust Formation are subdivided into four megasequences. Duration of megasequence-1 (SS 1-SS 10) is estimated to be 0.72 m.y. with average glacial periodicity of c. 70 000 years, megasequence-2 (SS 11-SS 20) 0.803 m.y. with average glacial periodicity of c. 80 000 years, megasequence-3 (SS 21-SS 29) 1.037 m.y. with average glacial periodicity of c. 115 000 years, and megasequence-4 as 0.2 m.y. with average glacial periodicity of c. 70 000 years. Average duration of megasequences and cyclicity of glacial periods were increased since onset of the Naust Formation (megasequence-1) to megasequence-3 which is confirmed by tunnel valleys in SS 29 and increased thickness of sequences. These tunnel valleys were formed by incision through thick ice sheets. After development of megasequence-3, average duration and cyclicity of glacial periods of megasequence-4 were reduced.

IRD peaks, ð ^{18}O curves, erosive power of ice sheets during glacial periods, periods when ice sheets reached shelf edge and thicknesses of sequences in four megasequences presented in this study represent that glaciations between Iceland, Barents Sea/Svalbard and mid-Norwegian continental shelf are correlatable.

References

ALLEY, R.B., BLANKENSHIP, D.D., ROONEY, S.T., BENTLEY, C.R., 1989. Sedimentation beneath ice shelves_the view from Ice Stream B. Marine Geology 85, 101-120.

BAMBER, J.L., VAUGHAN, D.G. and JOUGHIN, I., 2000: Widespread complex flow in the interior of the Antarctic Ice Sheet. Science, 287, 1248-1250.

BAUMANN, K. H., LACKSCHEWITZ, K.S., MANGERUD, J., SPIELHAGEN, R.F., WOLF-WELLING, T.C.W., HENRICH, R. and KASSENS, H. (1995) Reflection of Scandinavian Ice Sheet fluctuations in Norwegian Sea sediments during the last 150,000 years. Quaternary Research 43, 185-197.

BERG, K., SOLHEIM, A., BRYN, P., 2005. The Pleistocene to recent geological development of the Ormen Lange area. Marine and Petroleum Geology 22 (2005) 45-56.

BLYSTAD, P., BREKKE, H., FÆRSETH, R.B., SKOGSEID, J. & TØRUDBAKKEN, B. 1995. Structural elements of the Norwegian continental shelf. Part II: The Norwegian Sea Region. NPD-Bulletin No. 8, the Norwegian Petroleum Directorate, 45.

BREKKE, H., SJULSTAD, H.I., MAGNUS, C. & WILLIAMS, R.W. (2001). Sedimentary environments offshore Norway. In O.J. Martinsen and T. Dreyer (eds). Sedimentary Environments Offshore Norway – Paleozoic to Recent. Proceedings of the Norwegian Petroleum Society Conference, 3-5 May 1999, Bergen, Norway. NPF Special publication, no. 10, Amsterdam, Elsevier, 7-3.

BRITSURVEY, 1999. Seabed Project Geological and Geophysical Interpretation in Møre/Vøring Area, Phase III, Stage 1. Seabed Project Report No. Sp-26-BS-02-99. Final Report.

BRUHN, R., & PEGRUM, R.M., 2010. The `slump pump'_slumping and fluid flushing in the Møre Basin, Mid Norway. In: From Depositional Systems to Sedimentary Successions on the Norwegian Continental Shelf. Norwegian Petroleum Society 2010. pp. 75-77.

BRYN, P., SOLHEIM, A., BERG, K., LIEN, R., FORSBERG, C.F., HAFLIDASON, H., OTTESEN, D., RISE, L., 2003. The Storegga Slide complex: repeated sliding in response to climate cyclicity. In: LOCAT, J., MIENERT, J. (Eds.), Submarine Mass Movements and their Consequences. Kluwer Academic Publishers, Dordrecht, pp. 215-222.

BRYN, P., BERG, K., FORSBERG, C.F., SOLHEIM, A., LIEN, R., 2005. Explaining the Storegga Slide. Marine and Petroleum Geology, this issue, doi: 10.1016/j.marpetgeo. 2004.12.003.

BUTT, F.A., DRANGE, H., ELVERHØI, A., OTTERÅ, O.H. & SOLHEIM, A. 2002. Modelling late Cenozoic isostatic elevation changes in the Barents Sea and their implications for oceanic and climatic regimes; preliminary results. Quat. Sci. Rev. 21, 1643–1660.

BULAT, J., 2003. Imaging the Afen Slide from commercial 3D seismic_methodology and comparisons with high resolution data. In: Locat, J., Mienert, J. (Eds.), Submarine Mass Movements and their Consequences. Kluwer Academic Publishers, Dordrecht, pp. 205-213. 540 pp.

BUGGE, T., EIDVIN, T., SMELROR, M., AYERS, S., OTTESEN, D., RISE, L., ANDERSEN, E.S., DAHLGREN, T., EVANS, D. & HENRIKSEN, S., 2004. The Middle and Upper Cenozoic depositional systems on the Mid-Norwegian continental margin. NGF Abstr. Proc.Geol. Soc.Norway, vol. 3, 14–15.

BUGGE, T., BEFRING, S., BELDERSON, R. H., EIDVIN, T., JANSEN, E., KENYON, N. H., HOLTEDAHL, H., & SEJRUP, H. P. 1987. A giant three-stage submarine slide off Norway. Geo-Marine Letters, 7 191-198.

BUGGE, T., 1980. Shallow geology on the continental shelf off Møre and Trøndelag, continental Shelf Research Institute (IKU) Publication 104 1980. 44 pp. (In Norwegian with English summary).

BULLIMORE, S., HENRIKSEN, S., LIESTØL, F.M. & HELLAND-HANSEN, W. 2005. Clinoforms stacking patterns, shelf-edge trajectories and facies associations in Tertiary coastal deltas, offshore Norway: Implications for the prediction of lithology in prograding systems. Norwegian Journal of Geology, Vol. 85, pp. 169-187. Trondheim 2005. ISSN 029-196X.

BURGESS, P.M. & HOVIUS, N. 1998. Rates of delta progradation during highstands; consequences fo timing of deposition in deep-marine systems. Journal of the Geological Society of London 155, 217-222.

CATUNEANU, O., 2002. Sequence stratigraphy of clastic systems: concepts, merits, and pitfalls. Geological Society of Africa Presidential Review No. 1, Journal of African Earth Sciences 35 (2002) 1-43.

CATUNEANU, O., 2006. Principles of Sequence Stratigraphy. Elsevier, Amsterdam. 375 pp.

CATUNEANU, O., ABREU, V., BHATTACHARYA, J.P., BLUM, M.D., DALRYMPLE, R.W., ERIKSSON, P.G., FIELDING, C.R., FISHER, W.L., GALLOWAY, W.E., GIBLING, M.R., GILES, K.A., HOLBROOK, J.M., JORDAN, R., KENDALL, C.G.St.C., MACURDA, B., MARTINSEN, O.J., MIALL, A.D., NEAL, J.E., NUMMEDAL, D., POMAR, L., POSAMENTIER, H.W., PRATT, B.R., SARG, J.F., SHANLEY, K.W., STEEL, R.J., STRASSER, A., TUCKER, M.E., and WINKER, C. 2009. Towards the Standardization of sequence stratigraphy. Earth-Science Reviews 92 (2009) 1-33.

CERAMICOLA, S., STOKER, M.S., PRAEG, D., SHANNON, P.M., DE SANTIS, L., HOULT, R., HJELSTUEN, B.O., LABERG, J.S., MATHIESEN, A., 2005. Anomalous Cenozoic subsidence along the `passive` continental margin from Ireland to Norway. Marine and Petroelum Geology, this issue, doi: 10.1016/j.marpetgeo.2005.04.005.

DALLAND, A., WORSLEY, D. AND OFSTAD, K. 1988. A lithostratigraphic scheme for the Mesozoic and Cenozoic succession offshore mid- and northern Norway. NPD-Bulletin No. 4, (eds.), p.1-65.

DAHLGREN, K.I.T., VORREN,T.O., LABERG, J.S., 2002a. The role of grounding- line sediment supply in ice sheet advances and growth on continental shelves: an example from the Mid-Norwegian sector of the Fennoscandian Ice sheet during the Saalian and Weichselian. Quaternary International 95-96C, 25-33.

DAHLGREN, K.I.T., VORREN, T.O., LABERG, J.S., 2002b. Late Quaternary glacial development of the mid-Norwegian margin-65˚-68˚N. Marine and Petroleum Geology 19, 1089-1113.

DAHLGREN, K.I.T., VORREN, T.O., 2003. Sedimentary environment and glacial history during the last 40 Ka of the Vøring continental margin, mid-Norway. Marine Geology 193, 93-127.

DAHLGREN, K.I.T., VORREN, T.O., STOKER, M.S., NIELSEN, T., NYGÅRD, A., AND SEJRUP, H.P., 2005. Late Cenozoic prograding wedges on the NW Europe continental margin: their formation and relationship to tectonics and climate. Marine and Petroleum Geology 22, pp 1089-1110.

DOKKEN, T.M. and HALD, M. (1996) Rapid climatic shifts during isotope stages 2-4 in the Polar North Atlantic. Geology 24, 599-602.

DORÉ, A.G., LUNDIN, E.R., JENSEN, L.N., BIRKELAND, Ø., ELIASSEN, P.E., FICHLER, C. 1999. Principal tectonic events in the evolution of the northwest European Atlantic margin. In: Emery, D. and Myers, K., 1996. Sequence Stratigraphy. Blackwell Science Ltd., London, 297.

DORÉ, A.G., LUNDIN, E.R. 1996. Cenozoic compressional structures on the NE Atlantic margin: nature, origin and potential significance for hydrocarbon exploration. Pet. Geosci. 2, 299–311.

DOWDESWELL, J.A., OTTESEN, D., RISE, L., 2006. Flow-switching and large-scale deposition by ice streams draining former ice sheets. Geology 34, 313–316.

DOWDESWELL, J.A., OTTESEN, D. AND RISE, L., 2010. Rates of sediment delivery from the Fennoscandian Ice Sheet through an ice age. Geology vol. 38; no. 1; 3–6.

DORÉ, A.G., LUNDIN, E.R., KUSZNIR, N.J., AND PASCAL, C., 2008. Potential mechanisms for the genesis of Cenozoic domal structures on the NE Atlantic margin: pros, cons and some new ideas. The Geological Society of London, Special Publications, 306, 1-26.

EIDVIN, T. AND RIIS, F., 1989: Nye dateringer av de tre vestligste borehullene i Barentshavet. Resultater og konsekvenser for den Tertiære hevningen. NPD-Contribution 27, 44 pp.

EIDVIN, T., JANSEN, E. AND RIIS, F., 1993: Chronology of Tertiary fan deposits of the western Barents Sea: implications for the uplift and erosional history of the Barents Shelf. Marine Geology 112, 109-131.

EIDVIN, T., JANSEN, E., RUNDBERG, Y., BREKKE, H., GROGAN, P., 2000. The upper Cainozoic of the Norwegian continental shelf correlated with the deep sea record of the Norwegian Sea and the North Atlantic. Marine and Petroleum Geology 17, 579–600.

EIDVIN, T. AND RUNDBERG, Y. 2001. Late Cainozoic stratigraphy of the Tampen area (Snorre and Visund fields) in the northern North Sea, with emphasis on the chronology of early Neogene sands. Norsk Geologisk Tidsskrift, 81, 119–160.

EIDVIN, T., BUGGE, T. & SMELROR, M., 2007. The Molo Formation, deposited by coastal progradation on the inner Mid-Norwegian continental shelf, coeval with the Kai Formation to the west and the Utsira Formation in the North Sea. Norwegian Journal of Geology, Vol. 87, pp. 35-102.

ELDHOLM, O., THIEDE, J., TAYLOR, E. et al. 1987. Summary and preliminary conclusions, ODP Leg 104. *In:* Eldholm, O., Thiede, J., Taylor, E. et al. (eds), Proceedings, Initial Reports of the Ocean Drilling Program, 104: College Station, Tx (Ocean Drilling Program),751-771.

ELVERHØI, A., NOREM, H., ANDERSEN, E.S., DOWDESWELL, J.A., FOSSEN, I., HAFLIDASON, H., KENYON, N.H., LABERG, J.S., KING, E.L., SEJRUP, H.P., SOLHEIM, A., VORREN, T.O., 1997. On the origin and flow behaviour of submarine slides on deep-sea fans along the Norwegian-Barents Sea continental margin. Geo-Marine Letters 17, 119-125.

EMERY, K.O., 1981. Geological limits of the "continental shelf". Ocean Div. Int. Law, 10, 1-11.

EMERY, D., 1996. Historical Perspective. In: EMERY, D., & MYERS, K., Sequence Stratigraphy. BP Exploration, Stockley Park Uxbeidge, London. pp. 3-7.

EVANS, D., KING, E.L., KENYON, N.H., BRETT, C., WALLIS, D., 1996. Evidence for long-term instability in the Storegga slide region off western Norway. Marine Geology 130, 281-292.

FARMER, L.G., BARBER, D., ANDREWS, J., 2003. Provenance of late Quaternary ice-proximal sediments in the North Atlantic: Nd, Sr and Pb isotopic evidence. Earth and Planetary Science Letters 209, 227-243.

FALEIDE, J. I., BJØRLYKKE, K., GABRIELSEN, R.H 2010. "Geology of the Norwegian Continenetal Shelf" in book Petroleum Geoscience: From Sedimentary Environment to Rock Physics, 2010. pp. 467-499.

FALEIDE, J.I., NYSTUEN, J.P. and HAFEEZ, A., 2012. The Late Plio-Pleistocene outbuilding of the mid-Norwegian continental shelf: sesimic sequence stratigraphy reflecting

~ 30 glaciations. In: Sæmundsson, Þ. and Benediktsson, Í.Ö., 30th Nordic Geological Winter Meeting, Programme and Abstracts, Reykjvík, Iceland 9-12 January 2012, 58-59.

FRAZIER, D.E., 1974. Depositional episodes: their relationship to the Quaternary stratigraphic framework in the northwestern portion of the Gulf Basin. University of Texas at Austin, Bureau of Economic Geology. Geological Circular, vol. 4, 1. 28 pp.

FRONVAL, T., JANSEN, E., 1996. Late Neogene paleoclimates and paleocenography in the Iceland–Norwegian Sea: evidence from the Iceland and Vøring Plateaus. In: Thiede, J., et al. (Eds.), Proc. ODP, Sci. Res., vol. 151, pp. 455–468.

GALLOWAY, W.E., 1989. GENETIC STRATIGRAPHIC SEQUENCES IN BASIN ANALYSIS, 1. Architecture and genesis of flooding-surface bounded depositional units. American Association of Petroleum Geologists Bulletin 73, 125-142.

GEIRSDO´TTIR, A´ ., EIRE´ıKSSON, J., 1994. Growth of an intermittent ice sheet in Iceland during the late Pliocene and early Pleistocene. Quaternary Res. 42, 115–130.

GEIRSDO´TTIR, A´ ., MILLER, G.H., & ANDREWS, J.T., 2007. Glaciation, erosion, and landscape evolution of Iceland. Journal of Geodynamics 43 (2007) 170-186.

GIBBARD P.L., HEAD M.J., WALKER M.J.C. & the SUBCOMMISSION ON QUATERNARY STRATIGRAPHY., 2009. Formal ratification of the Quaternary System/Period and the Pleistocene Series/Epoch with a base at 2.58 Ma. Journal of Quaternary Science, 24: DOI: 10.1002/jqs. 1338.

GLØRSTAD-CLARK, E., FALEIDE, J.I., LUNDSCHIEN, B.A., and NYSTUEN, J.P., 2010. Triassic seismic sequence stratigraphy and paleogeography of the western Barents Sea area. Marine and Petroleum Geology 27 (2010) 1448-1475.

GLØRSTAD-CLARK, E., BIRKELAND, E.P., NYSTUEN, J.P., FALEIDE, J.I., and MIDTKANDAL, 2011. Triassic platform-margin deltas in the western Barents Sea. Marine and Petroleum Geology 28 (2011) 1294-1314.

GRAHAM, A.G.C., LONERGAN, L. & STOKER, M.S., 2007. Evidence for Late Pleistocene ice stream activity in the Witch Ground Basin, central North Sea, from 3D seismic reflection data. Vol. 26, Issues 5-6, March 2007, pp. 627-643.

GRAHAM, A.G.C., LONERGAN, L., STOKER, M.S., 2009. Seafloor glacial features reveal the extent and decay of the last British Ice Sheet, east of Scotland. J. Quatern. Sci. 24, 117-138.

GRAHAM, A.G.C., LONERGAN, L., & STOKER, M.S., 2010. Depositional environments and chronology of Late Weichselain glaciation and deglaciation in the central North Sea. Boreas 39, 471-491.

GRAHAM, A.G.C., STOKER, M.S., LONERGAN, L., BRADWELL, T. & STEWART, M.A., 2011. The Pleistocene Glaciations of the North Sea Basin, in EHLERS, J., Quaternary

Glaciations-Extent and Chronology. A closer look. Developments in Quaternary Science. 1ST Edition, Vol. 15, pp. 261-278.

HAFEEZ, A., 2011. Late Cenozoic Sedimentary Outbuilding Offshore Mid-Norway: A Sequence Stratigraphic Analysis. Master Thesis in Geosciences, Petroleum Geology and Geophysics, Department of Geosciences, University of Oslo, 91.

HAMPSON, G.J., DAVIES, S.J., ELLIOTT, T., FLINT, S.S., & STOLLHOFEN, H., 1999. Incised valley fill sandstone bodies in Upper Carboniferous Fluvio-deltaic strata: recognition and reservoir characterisation of Southern North Sea analogues. In: Petroleum Geology of NW Europe: Poceedings of the 5th Conference. (Edited by FLEET, A.J., & BOLDY, S.A.R.). The Geological Society, London. 771-788.

HELLAND-HANSEN, W. & GJELBERG, J.G. 1994. Conceptual basis and variability in sequence stratigraphy; a different perspective. Sedimentary Geology 92, 31-52.

HELLAND-HANSEN,W. & MARTINSEN, O.J. 1996. Shoreline trajectories and sequences; description of variable depositional-dip scenarios. Journal of Sedimentary Research 66, 670-688.

HELLAND-HANSEN, W., and HAMPSON, G.J., 2009. Trajectory analysis: concepts and applications. Basin Research (2009) 21, pp. 454-483.

HELLAND-HANSEN, W., STEEL, R.J., and SØMME, T.O., 2012. Shelf genesis revisited. Journal of Sedimentary Research, v. 82, 133-148.

HENRIKSEN, S., FICHLER, C., GRØNLIE, A., HENNINGSEN, T., LAURSEN, I., LØSETH, H., OTTESEN, D. & PRINCE, I., 2005. The Norwegian Sea during the Cenozoic. In: WANDÅS. et al. (eds) Onshore-Offshore Relationships on the North Atlantic Margin. NPF Special Publication, 12, 111-133, Elsevier.

HENRIKSEN, S. & VORREN, T.O. 1996. Late Cenozoic sedimentation and uplift history on the mid-Norwegian continental. Global and Planetary Change, 12, 171-199.

HJELSTUEN, B.O., SEJRUP, H.P., HAFLIDASON, H., BERG, K., BRYN, P., 2004a. Neogene and Quaternary depositional environments on the Norwegian continental margin, 62_Ne68_ N. Marine Geology 213, 257e276.

HJELSTUEN, B.O., SEJRUP, H.P., HAFLIDASON, H., NYGÅRD, A., BERSTAD, I.M., KNORR, G., 2004b. Late Quaternary seismic stratigraphy and geological development of the south Vøring margin, Norwegian Sea. Quaternary Science Reviews 23, 1847-1865.

HJELSTUEN, B.O., SEJRUP, HP., HAFLIDASON, H., NYGÅRD, A, CERAMICOLA, S. & BRYN P 2005. Late Cenozoic glacial history and evolution of the Storegga Slide area and adjacent slide flank regions, Norwegian continental margin. Mar. Pet. Geol. 22: 57–69.

HOOKE, R., ELVERHØI, A., 1996. Sediment flux from a fjord during glacial periods, Isfjorden, Spitsbergen. Global and Planetary Change 12, 237-249.

HOLMES, R., LONG, D., DODD, L.R., 1998. Large-scale debrites and submarine landslides on the Barra fan, west of Britian. In: Stoker, M. S., Evans, D., Cramp, A. (Eds.), Geological Processes on Continental Margins: Sedimentation, Mass-Wasting and Stability. Geological Society, London, Special Publication 129, 67-79.

HUBBARD, A.L., BRADWELL, T., GOLLEDGE, N.R., HALL, A., PATTON, H., SUGDEN, D., et al., 2009. Dynamic cycles, ice streams and their impact on the extent, chronology and deglaciation of the British-Irish ice sheet. Quatern. Sci. Rev. 28, 758-776.

HUUSE, M., & LYKKE-ANDERSEN, H., 2000. Overdeepened quaternary valleys in the eastern Danish north sea: morphology and origin. Quatern. Sci. Rev. 19, 1233-1253.

HUNT, D. & TUCKER, M.E. 1992. Stranded parasequences and the forced regressive wedge systems tract; deposition during base-level fall. Sedimentary Geology 81, 1-9.

ISAKSEN, D. AND TONSTAD, K. (eds.) 1989: A revised Cretaceous and Tertiary lithostratigraphic nomenclature for the Norwegian North Sea. NPD-Bulletin No. 5, 59 pp.

JANSEN, E., FRONVAL, T., RACK, F., CHANNEL, J.E.T., 2000. Pliocene–Pleistocene ice rafting history and cyclicity in the Nordic Seas during the last 3.5 My. Palaeoceanography 15, 709–721.

JARSVE, E.M., GABRIELSEN, R.H., FALEIDE, J.I., & NYSTUEN, J.P., 2010. Mesozoic and Cenozoic asymmetrical depositional systems in the North Sea inrelation to uplift of southern Norway ("source-to-sink"). In: From Depositional Systems to Sedimentary Successions on the Norwegian Continental Shelf. Norwegian Petroleum Society 2010. pp. 78-82.

KING, E.L., SEJRUP, H.P., HAFLIDASON, H., ELVERHØI, A., AARSETH, I., 1996. Quaternary sesimic stratigraphy of the north Sea Fan: glacially-fed flow aprons, hemipelagic sediments, and large scale submarine slides. Marine Geology 130, 293-315.

KING, E.L., 1996. Quaternary stratigraphy and processes on the Norwegian North Sea margin: Ice stream products and gravity mass movements. Dr Scient. thesis, Department of Geology, University of Bergen, Norway.

LABERG, J.S., VORREN, T.O., 1995. Late Weichselian submarine debris flow deposits on the Bear Island Trough Mouth Fan. Marine Geology 127, 45-72.

LEBESBYE, E., VORREN, T.O., 1996. Submerged terraces in the southwestern Barents Sea: origin and implications for the late Cenozoic geological history. Marine geology 130, 265-280.

LABERG, J.S., DAHLGREN, T., VORREN, T.O., HAFLIDASON, H., BRYN, P., 2001. Seismic analysis of Cenozoic contourite drift development in the Northern Norwegian Sea. Marine Geophysical Researches 22, 401-416.

LABERG, J.S., VORREN.T.O., 2000. The Trænedjupet Slide, Offshore Norway-morphology, evacuation and triggering mechanisms. Marine Geology 171, 95-114.

LONGVA, O. & THORSNES, T. (eds.) 1997. Skagerrak in the past and at the present – an integrated study of geology, chemistry, hydrography and microfossil ecology. Norges geologiske undersøkelse Special Publication 8, 100 pp.

LONERGAN, L., MAIDMENT, S., COLLIER, J., 2006. Pleistocene sub-glacial tunnel valleys in the central North Sea: 3D morphology and evolution. J. Quatern. Sci. 21, 891-903.

LUNDIN, E.R. & DORÉ, A.G., 2002. Mid-Cenozoic post-breakup deformation in the passive margins bordering the Norwegian–Greenland Sea. Mar. Pet. Geol. 19, 79–93.

LØSETH, H. & HENRIKSEN, S. 2005. A Middle to Late Miocene compressional phase along the Norwegian passive margin. In: A.G. Doré & B.A. Vining (eds). Petroleum Geology: North-West Europe and Global Perspectives. Proceedings of the 6th Petroleum Geology Conference, 845-859.

MANGERUD, J., JANSEN, E., & LANDVIK, J.Y., 1996. Late Cenozoic history of the Scandinavian and Barents Sea ice sheets. Global and Planetary Change 12 (1996) 11-26.

MANGERUD, J., DOKKEN, T., HEBBELN, D., HEGGEN, B., INGÓLFSSON, Ó., LANDVIK, J.Y., MEJDAHL, V., SVENDSEN, J.I., & VORREN, T.O., 1998. Fluctauations of the Svalbard-Barents Sea Ice Sheet during the last 150 000 years. Quaternary Science Reviews, vol. 17, pp. 11-42.

MANGERUD, J., GYLLENCREUTZ, R., LOHNE, Ø., & SVENDSEN, J.I., 2011. Glacial History of Norway, in EHLERS, J., Quaternary Glaciations-Extent and Chronology. A closer look. Developments in Quaternary Science. 1st Edition, Vol. 15, pp. 279-298.

MARTINSEN, O.J., BØEN, F., CHARNOCK, M.A., MANGERUD, G. & NØTTVEDT, A. 1999. Cenozoic development of the Norwegian margin 60-64º N, sequences and sedimentary response to variable basin physiography and tectonic setting. In A.J. Fleet & S.A.R. Boldy (eds), Petroleum Geology of NW Europe, Proceedings of the 5th Conference. Geological Society, London, 293-304.

MARTINS-NETO, M.A., & CATUNEANU, O., 2010. Rift sequence stratigraphy. Marine and Petroleum Geology 27, 247-253.

MILLER, J.MG., 1996. Glacial sediments. In Reading, H.D. (ed.). Sedimentary Environments: Processes, Facies and Stratigraphy. 3rd ed. Oxford: Blackwell Science, 454-483.

MITCHUM, Jr., R.M., 1977. Seismic stratigraphy and global changes of sea level, part 11: glossary of terms used in seismic stratigraphy. In: PAYTON, C.E. (Ed.), Seismic Stratigraphy_ Applications to Hydrocarbon Exploration. Memoirs, vol. 26. American Association of Petroleum Geologists, pp. 205-212.

MUTO, T. & STEEL, R.J. 2002. In defense of shelf-edge delta development during falling and lowstand of relative sea level. Journal of Geology 110, 421-436.

MYERS, K.J., & MILTON, N.J., 1996. Concepts and Principles of Sequence Stratigraphy. In: EMERY, D., & MYERS, K., Sequence Stratigraphy. BP Exploration, Stockley Park Uxbeidge, London. pp. 11-41.

NESJE, A., ANDA, E., RYE, N., LIEN, R., HOLE, P.A., BLIKRA, L.H., 1987. The vertical extent of the Late Weichselian ice sheet in the Nordfjord-Møre area, western Norway. Norsk Geologisk Tidsskrift 67, 125-141.

NESJE, A., DAHL, S.O., 1992. Geometry, thickness and isostatic loading of the Late Weichselian Scandinavian ice sheet. Norsk Geologisk Tidsskrift 72, 271-273.

NUMMEDAL, D., RILEY, G.W., COLE, R.D. & TREVENA, A.S. 1992. The distribution of depositional systems within falling sea level and lowstand systems tracts; examples from the Gallup Sandstone. In Ethridge, F.G. (ed.), SEPM 1992 theme meeting; Mesozoic of the Western Interior; abstracts, 50. Society of Economic Paleontologists and Mineralogists, Tulsa, OK, United States.

NYGÅRD, A., SEJRUP, H.P., HAFLIDASON, H., CECCHI, M., OTTESEN, D., 2004. The deglaciation history of the southwestern Fennoscandian Ice Sheet between 15 and 13 ^{14}C ka. Boreas 33, 1-17.

NYGÅRD, A., SEJRUP, H.P., HAFLIDASON, H., BRYN, P., 2005. The glacial North Sea Fan, southern Norwegian Margin: architecture and evolution from the upper continental slope to the deep-sea basin. Marine and Petroleum Geology 22, 71-84.

NYSTUEN, J.P. 1998. History and development of sequence stratigraphy. In: Sequence Stratigraphy, Concepts and Applications (Ed. by Gradstein, F.M., SANDVIK, K.O., & MILTON, N.J.), Norw. Petrol. Soc. (NPF) Spec. Publ., 8, 31-116.

ÓGRADY, D.B., SYVITSKI, J.P.M., 2002. Large-scale morphology of arctic continental slopes: the influence of sediment delivery on slope form. In: Dowdeswell, J.A., O`Cofaigh, C. (Eds.), Galcier Influenced Sedimentation on High-Latitude Continental Margins. Geological Society, London, Special Publications 203, 11-31.

OTTESEN, D., RISE, L., ROKOENGEN, K., & SÆTTEM, J., 2001. Glacial processes and large-scale morphology on the mid-Norwegian continental shelf. Sediementary Environments Offshore Norway_Paleozoic to Recent edited by MARTINSEN, O.J., & DREYER, T., NPF Special Publication 10. pp. 441-449, Published by Elsevier Science B.V., Amsterdam. Norwegian Petroleum Society (NPF), 2001.

OTTESEN, D., DOWDESWELL, J.A. & RISE, L., 2005. Submarine landforms and reconstruction of fast-flowing ice streams within a large Quaternary ice sheet: The 2500-km-long Norwegian–Svalbard Margin (57°–80° N). GSA Bull. 117, 1033–1050.

OTTESEN, D., 2006. Ice-sheet dynamics and glacial development of the Norwegian continental margin during the last 3 million years. Dr. philos Thesis in Earth Science, Department of Earth Science, University of Bergen, 40.

OTTESEN, D., RISE, L., ANDERSEN, E.S., BUGGE, T. & EIDVIN, T., 2009. Geological evolution of the Norwegian continental shelf between 61˚N and 68˚N during the last 3 million years. Norwegian Journal of Geology Vol. 89, pp. 251-256. Trondheim 2009. ISSN 029-196x.

PIRMEZ, C., PRATSON, L.F. & STECKLER, M.S., 1998. Clinoform development by advection-diffusion of suspended sediment; modeling and comparison to natural systems. Jounal of Geophysical Research, B, Solid Earth and Planets 103/B10.24, 141-24, 157.

PLINT, A.G. & NUMMEDAL, D. 2000. The falling stage systems tract; recognition and importance in sequence stratigraphic analysis. In Hunt, D. & Gawthorpe, R.L. (eds.), Sedimentary responses to forced regressions. Geological Society of London Special Publication 172, 1-17.

POSAMENTIER, H.W. & VAIL, P.R. 1988. Eustatic controls on clastic deposition; II, Sequence and systems tract models. *In*Wilgus, C.K., Hastings, B.S., Ross, C.A., Posamentier, H., Van Wagoner, J. & Kendall, C.G.St C. (eds.), Sea-level changes; an integrated approach. Society of Economic Paleontologists and Mineralogists Special Publication 42, 125-154.

POSAMENTIER, H.W., JERVEY, M.T. & VAIL, P.R. 1988. Eustatic controls on clastic deposition; I, Conceptual framework. *In* Wilgus, C.K., Hastings, B.S., Ross, C.A., Posamentier, H., Van Wagoner, J. & Kendall, C.G.St C. (eds.), Sea-level changes; an integrated approach. Society of Economic Paleontologists and Mineralogists Special Publication 42, 109-124.

POSAMENTIER, H.W., & MORRIS, W.R., 2000. Aspects of the stratal architecture of forced regressive deposits. In: HUNT, D., GAWTHORPE, R.L. (Eds.), Sedimentary Responses to Forced Regressions. Special Publication, vol. 172. Geological Society of London, pp. 19-46.

POROBSKI, S.J. & STEEL, R.J. 2003. Shelf-margin deltas: their stratigraphic significance and relation to deepwater sands. Earth-Science Reviews 62, 283-326.

PRAEG, D., STOKER, M.S., SHANNON, P.M., CERAMICOLA, S., HJELSTUEN, B., LABERG, J.S., & MATHIESEN, A., 2005. Episodic Cenozoic tectonism and the development of the NW European ‘passive’ continental margin. Marine and Petroleum Geology, 22: 1007-1030.

Redfield T.F., Osmundsen P.T. & Hendriks , B.W.H, 2005.The role of fault reactivation and growth in the uplift of western Fennoscandia. J. Geol. Soc. (Lond.), 162 (2005), pp. 1013–1030.

REEMST, P., SKOGSEID, P. & LARSEN, B.T., 1996. Base Pliocene velocity inversion on the eastern Vøring Margin-causes and implications. Global and Planetary Change 12, 201-211.

RICH, J.L., 1951. Three critical environments of deposition and criteria for recognition of rocks deposited in each of them. GSA Bull., 62, 1-20.

RISE, L., OTTESEN, D., LARSEN, E., LUNDIN, E., OLSEN, L., THORSNES, T., 2002. Large scale development of the mid-Norwegian shelf and margin with emphasis on the last 3 million years. Norges Geologiske Undersøkelse, Report 2002.015.200 pp.

RISE, L., OTTESEN, D., BERG, K., & LUNDIN, E., 2005. Large-scale development of the mid-Norwegian shelf and margin during the last 3 million years. Mar. Pet. Geol. 22, 33–44.

RISE, L., OTTESEN, D., LONGVA, O., SOLHEIM, A., ANDERSEN, E.S., AYERS, S., 2006. The Sklinnadjupet Slide and it relation to the Elsterian glaciation on the mid-Norwegian margin. Marine and Petroleum Geology 23, 569-583.

RISE, L., CHAND, N., HJELSTUEN, B.O., HAFLIDASON, H. & BØE, R., 2010. Late Cenozoic geological development of the south Vøring margin, mid Norway. Marine and Petroleum Geology 27, 1789-1803.

ROKOENGEN, K., RISE, L., BRYN, P., FRENGSTAD, B., GUSTAVSEN, B., NYGAARD, E., SÆTTEM, J., 1995. Upper Cenozoic stratigraphy on the mid-Norwegian continental shelf. Norsk geologisk Tidsskrift 75, 88-104.

ROKSANDIC, M.M., 1978. Seismic facies analysis concepts. Geophysical prospecting 26, 383-398.

RUNDBERG, Y. AND EIDVIN, T., 2005: Controls on depositional history and architecture of the Oligocene-Miocene succession, northern North Sea Basin. In B.T.G. Wandaas et al. (eds.): Onshore-Offshore Relationships on the North Atlantic Margin. NPF Special Publication 12, 207-239.

SÆTTEM, J., POOLE, D.A.R., ELLINGSEN, L., SEJRUP, H.P., 1992. Glacial geology of outer Bjørnøyrenna, southwestern Barents Sea. Marine Geology 103, 15-51.

SEJRUP, H. P., AARSETH, I., HAFLIDASON, H., LOVLIE, R., BRATTEN, A., TJOSTHEIM, G., FORSBERG, C. F. & ELLINGSEN, K. L. 1995. Quaternary of the Norwegian Channel: glaciation history and palaeocenography. Norsk Geologisk Tidsskrift, 75**,** 65-87.

SEJRUP, KING, E. L., AARSETH, I., HAFLIDASON, H. & ELVERHOI, A. 1996. Quaternary erosion and depositional processes, western Norwegian fjords, Norwegian channel and North Sea Fan. In: DE BATIST, M. & JACOBS, P. (eds) Geology of Siliciclastic Shelf Seas. Geological Society, London, Special Publications, 117, 187-202.

SEJRUP, H.P., LARSEN, E., HAFLIDASON, H., BERSTAD, I.M., HJELSTUEN, B.O., JONSDOTTIR, H., KING, ELLER LIGNENDE, LANDVIK, J.Y., LONGVA, O., NYGÅRD, A., OTTESEN, D., RAUNHOLM, S., RISE, L. & STALSBERG, K. 2003. Configuration, history and impact of the Norwegian Channel Ice Stream. Boreas 32, 18-36.

SKOGSEID, J., PEDERSEN, T. & LARSEN, V.B., 1992. Vøring basin: subsidence and tectonic evolution. Structural and Tectonic Modelling and its Application to Petroleum Geology. NPF Special Publication, 1. Norsk Petroleumsforening (NPF) 55-82.

SMELROR, M., DEHLS, J., EBBING, J., LARSEN, E., LUNDIN, E.R., NORDGULEN, Ø., OSMUNDSEN, P.T., OLESEN, O., OTTESEN, D., PASCAL, C., REDFIELD, T.F., RISE, L, 2007: "Towards a 4D topographic view of the Norwegian sea margin". Global and Planetary Change, 58, pp. 382-410.

SOLHEIM, A., ANDERSEN, E.S., ELVERHØI, A., FIEDLER, A., 1996. Late Cenozoic depositional history of the western Svalbard continental shelf, controlled by subsidence and climate. Global and Planetary Change 12, 135-148.

SOLHEIM, A., BERG, K., FORSBERG, C.F., BRYN, P., 2005. The Storegga Slide Complex: repetitive large scale sliding with similar cause and development. Marine and Petroleum Geology, this issue, doi: 10.1016/j.marpetgeo.2004.10.013.

STEEL, R. & OLSEN, T., 2002. Clinoforms, Clinoform Trajectories and Deepwater Sands. In Armentrout, J.M. & Rosen, N.C. (eds.), Sequence Startigraphic models for exploration and production: Evolving Models and Application Histories. 367-381. Special Publication GCS-Society of Economic Paleontologists and Mineralogists.

STEWART, M.A., & LONERGAN, L., 2011. Direct evidence for seven glacial cycles in the Middle-Late Pleistocene of NW Europe. Geology 39, 283-286.

STOKER, M.S., PRAEG, D., HJELSTUEN, B.O., LABERG, J.S., NIELSEN, T., SHANNON, P.M., 2005. Neogene stratigraphy and the sedimentary and oceanographic development of the NW European Atlantic margin. Marine and Petroleum Geology 22, 977e1005.

STOKER, M.S., LESLIE, A.B., SCOTT, W.D., BRIDEN, J.C., HINE, N.M., HARLAND, R., WIKINSON, I.P., EVANS, D., ARDUS, D.A., 1994. A record of late Cenozoic stratigraphy, sedimentation and climate change from the Hebridies Slope, NE Atlantic Ocean. Journal of the Geological Society, London 151, 235-249.

STOKER, M.S., BALSON, P.S., LONG, D., TAPPIN, D.R., 2010. An overview of the lithostratigraphical framework for the Quaternary deposits in the United Kingdom continental shelf. British geological Survey Research Report, RR/00/00. 48pp. http://nora.nerc.ac.uk/3241/1/RR04004.pdf.

STORVOLL, V., BJØRLYKKE, K., MONDOL, N.M., 2005. Velocity-depth trends in Mesozoic and Cenozoic sediments from the Norwegian shelf. American Association of Petroleum Geologists Bulletin 89, 359-381.

STUEVOLD, L.M., ELDHOLM, O., 1996. Cenozoic uplift of Fennoscandia inferred from a study of the mid Norwegian margin. Global and Planetary Change 12, 359-386.

STRATAGEM PARTNERS, 2002. Stoker, M.S. (Compiler). The Neogene stratigraphy of the glaciated European margin from Lofoten to Porcupine, Atlas. A Product of the EC-supported STRATAGEM Project 2002.

SWITHINBANK, C.W.M., 1954: Ice streams. Polar Record, 7, 185-186.

VAN WAGONER, J.C., POSAMENTIER, H.W., MITCHUM, R.M., VAIL, P.R., SARG, J.F., LOUTIT, T.S., HARDENBOL, J., 1988a. An overview of sequence stratigraphy and key definitions. In: WILGUS, C.K., HASTINGS, B.S., KENDALL, C.G. St. C., POSAMENTIER, H.W., ROSS, C.A., VAN WAGONER, J.C. (Eds.), Sea Level Changes – An Integrated Approach. Special Publication, vol. 42. Society of Economic Paleontologists and Mineralogists (SEPM), pp. 39-45.

VORREN, T.O., LEBESBYE, E., ANDREASSEN, K., LARSEN, K.B., 1989. Glacigenic sediments on a passive continental margin as exemplified by the Barents Sea. Marine Geology 85, 251-271.

VORREN, T.O., ROKOENGEN, K., BUGGE, T. & LARSEN, O.A., 1992. Kontinentalsokkelen, Tykkelsen pgt kvart~ere sedimenter, 1:3 mill. Nasjonalatlas for Norge, kartblad 2.3.9. Statens kartverk.

VORREN, T.O., & LABERG, J.S., 1997. Trough mouth fans-paleoclimate and ice-sheet monitors. Quat. Sci. Rev., 16(8): 865-881.

Vorren, T.O. & Mangerud, J., 2006, Istider kommer og går, *in* Ramberg, I., Bryhni, I., and Nøttvedt, A., eds, Landet blir til. Norges Geologi. pp. 478–531: Norsk Geologisk Forening.

VORREN, T. & MANGERUD, J., 2008. Glaciations come and go. In: Ramberg, I.B., Bryhni, I., Nøttvedt, A. and Rangnes, K., The Making of a Land – Geology of Norway. Chapter 15, 480-533. Norsk geologisk forening (The Norwegian Geological Association).

WAGONER, J.C.V., POSAMENTIER, H.W., MITCHUM, R.M., VAIL, P.R., SARG, J.F., LOUTIT, T.S., & HARDENBOL, J., 1988b. An overview of the fundamentals of sequence stratigraphy and key definitions. Sea-Level Changes—An Integrated Approach, SEPM Special Publication No. 42. The Society of Economic Paleontologists and Mineralogists, ISBN 0-918985-74-9

WINSBORROW, M.C.M., CLARK, C.D., & STOKES, C.R., 2010. What controls the location of ice streams? Earth-Science Reviews 103 (2010) 45-59.

WHEELER, H.E., 1958. Time stratigraphy. American Association of Petroleum Geologists, Bulletin, v. 42, p. 1047-1063.

WOHLFARTH, B., BJÖRCK, S., FUNDER, S., HOUMARK-NIELSEN, M., INGÓLFSSON, Ó., LUNKKA, J.P., MANGERUD, J., SAARNISTO, M. and VORREN, T. 2008. Quaternary of Norden. Episodes, Vol. 31, No.1, pp 73-81.